Landsvirkjun

LV-2022-054

Vatnajökull

Mass balance, meltwater drainage and surface velocity of the glacial year 2021-22

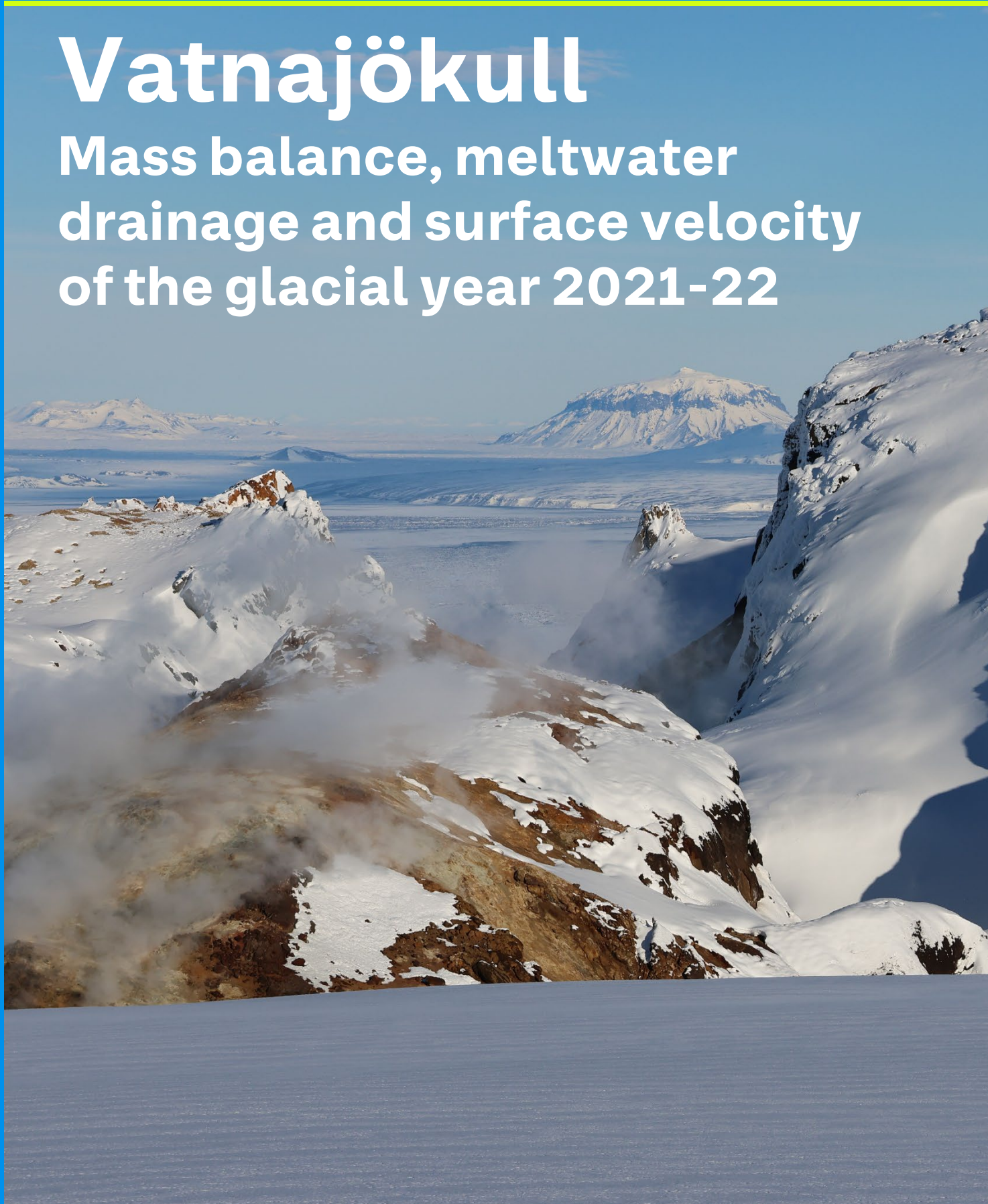

Vatnajökull

Mass balance, meltwater drainage and surface velocity of the glacial year 2021-22

Höfundar
Finnur Pálsson, Andri Gunnarsson, Eyjólfur Magnússon, Guðfinna Aðalgeirsdóttir, Sveinbjörn Steinþórsson, Karl Eiríksson og Andri Björnsson

Dagsetning
Desember 2022

Lykilsíða

Skýrsla LV nr	LV-2022-054	**Dagsetning**	Desember 2022
Fjöldi Síðna	55	**Upplag**	1
Dreifing	[X] Birt á vef LV	[ ] Opin	[ ] Takmörkuð til [Dags.]
Titill	Vatnajökull: Mass balance, meltwater drainage and surface velocity of the glacial year 2021-22		
Höfundar/fyrirtæki	Finnur Pálsson, Andri Gunnarsson, Eyjólfur Magnússon, Guðfinna Aðalgeirsdóttir, Sveinbjörn Steinþórsson, Karl Eiríksson og Andri Björnsson		
Verkefnisstjóri	Andri Gunnarsson		
Unnið fyrir			
Samvinnuaðilar	Jarðvísindastofnun Háskólans, RH-8-22		
Útdráttur	Mass balance measurements were done at 67 sites in spring and fall 2022. For the glaciological year 2021-22 the winter balance for Vatnajökull was 27% more than average, over the observation period from 1991-92. The total summer surface mass loss was 97% of average since 1995. An extensive dust event over the SW outlets in early July greatly enhanced melt in SW Vatnajökull, especially in the accumulation areas. The glaciological year 2021-22 results in a slightly negative net balance.		
Lykilorð	Mass balance, Vatnajökull		

Samþykki verkefnisstjóra
Landsvirkjunar

Contents:

Figures:

1. **INTRODUCTION**

In 1992 (glacial year 1991_92) a program of surface mass balance measurements was started for Vatnajökull by the Science Institute University of Iceland (now Institute of Earth Sciences, IES) in collaboration with the National Power Company (NPC). For the first year the program was limited to the western part of the glacier, but then expanded to include the northern outlets as well. In 1996 this study was further expanded to include southern outlets, with support from The European Union (Framework IV - Environment and Climate, TEMBA project 1996-1997). This program was extended 1998–2000 with further support from EU (Framework IV - Environment and Climate, ICEMASS project, 1998-2000). In 2000-2002 NPC and IES continued the program. In 2003-2005 IES participated in a multinational research project, which was financially supported by The European Union (EVK2-CT-2002-00152 SPICE). IES was responsible for obtaining data sets for calibration of models of the mass balance and dynamics of Vatnajökull. This work was also supported by The National Power Company of Iceland and The National Road Authority and was a continuation of the TEMBA-project of 1996-97 and ICEMASS project 1998-2001.
Since then IES and NPC have continued a similar program. Mass balance measurements on the southeast outlet Breiðamerkurjökull is financially supported by the National Road Authority.
The aim of the collaborative work of NPC and IES is to improve understanding of the mass balance and melt water runoff from glaciers. This work in combination with energy balance measurements by NPC and IES on Vatnajökull will is used for calibration of models of the surface energy and mass balance of Vatnajökull.
This report describes the field measurements, mass balance, melt water runoff and GPS survey, for the glaciological year 2021_22.

2. DIARY

March 30: installation of melt wires and maintenance of the lower AWS on Breiðamerkurjökull.
May 2-8, 27, June 4: measurements of the winter balance, setup of AWSs.
August 4-5: maintenance of the AWSs on Vatnajökull
August 6: maintenance of the lower AWS on Breiðamerkurjökull
October 17-20, 27: summer balance measurements, take down of AWSs;

In all expeditions the locations of mass balance stakes were measured with Kinematic GPS (or fast static GPS) for surface velocity calculation.

The following members of staff of the Institute of Earth Sciences, University of Iceland, carried out the fieldwork on Vatnajökull: Finnur Pálsson, Sveinbjörn Steinþórsson, Eyjólfur Magnússon, Guðfinna Aðalgeirsdóttir with Andri Gunnarsson (National Power Company), Karl Eiríksson (Reykjavík Rescue Team) and Andri Björnsson.
Volunteers in the Iceland Glaciological Society Spring expedition to Vatnajökull helped in the field work in June.

3. MASS BALANCE MEASUREMENTS

The purpose of the mass balance measurements is to describe the temporal and spatial distribution of the components of the mass balance. The mean annual values of the components and their variation from year to year are analyzed and related to meteorological conditions and climatic variability. The results are used in studies of changes in the glacier volume, estimates of meltwater contribution to glacial rivers, mass balance modeling, evaluation of altitudinal and regional variations of mass balance in response to climatic variations, and to assess the hydrometeorological and dynamic response of the ice cap to climate change.

The mass balance was determined by a stratigraphic method, measuring changes in thickness and density relative to the summer surface. The winter balance was estimated by drilling ice cores through the winter layer in the spring. Ablation was monitored from markers; snow stakes were put up on the glacier and wires were drilled down in the ablation area. The summer balance was measured in the autumn.

3.1 Methods

Measurements of the surface mass balance on a large ice cap like Vatnajökull are impractical in terms of cost with conventional techniques and sampling density that are typically used on small glaciers. The spatial variability of the mass balance may, however, be predictable on the flat large outlets of such an ice cap given data on several profiles extending over the elevation range of the glacier. The precipitation generally increases with elevation and decreases with the distance from the coast, but both the distribution of snowfall and redistribution of snow by drift depend on the prevailing wind direction during the winter. The summer melting depends mainly on the altitude and the albedo of the glacier surface. Therefore, we have used observations along a limited number of flowlines, which span the elevation ranges of the outlets to assess aerial estimates of surface mass balance. Each profile describes the variation with elevation, but together they also describe the lateral variation of the mass balance. Recently, modern over-snow vehicles and helicopters have allowed fast traverses to ensure successful fieldwork despite frequently poor weather conditions. The error for individual point measurement is estimated ~30 cm_{we} for both summer and winter balance. The error for the glacier wide specific mass balance, based on area integral of mass balance, is however considered smaller, since the error for individual survey sites is independent.

The winter mass balance (b_w) is defined as the mass of snow accumulated during the winter months, the summer balance (b_s) is the mass balance during the summer, and the net balance (b_n) is defined as their sum. The specific mass balance is expressed in terms of the equivalent thickness of water. All mass balance components apply to a time interval between given measurement dates, which are not fixed from one year to another. The dates in the autumn are separated by approximately one calendar year, which roughly coincides with the glaciological year defined as October 1st to September 30th. Snow cores are drilled in April-May through the winter layer and profiles of the density are measured. The summer balance is derived in the autumn from measurements of the changes in the snow core density during the summer in the accumulation area and from

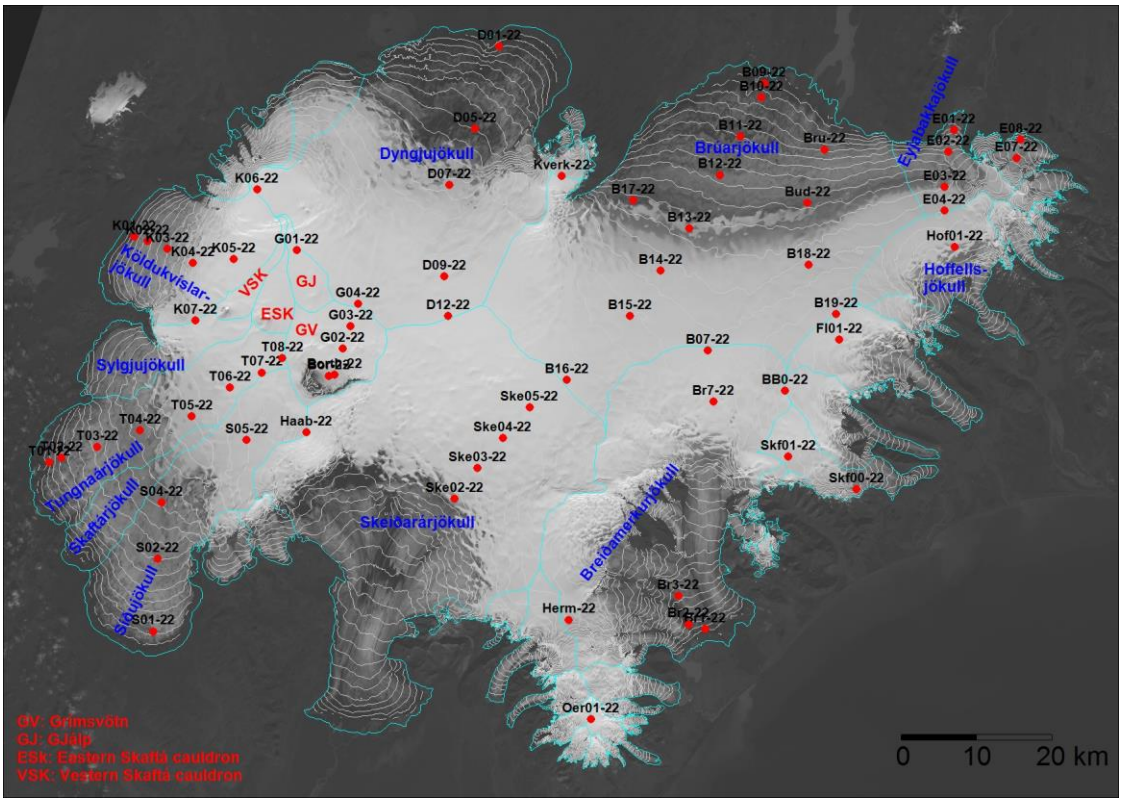

Figure 1. Outlets of Vatnajökull and location of mass balance survey sites 2021_22.

readings at stakes and wires drilled into the ice in the ablation areas.

Digital maps are created for winter, summer and net balance for the whole ice cap based on the in-situ measurements. The mass balance is calculated over both the ice and water drainage basins. The summer balance over the water basin is an estimate of meltwater contribution to rivers and groundwater storage. This estimate, however, does not include precipitation that falls as rain on the glacier or snow, which falls and melts during the summer. As conventional for the north hemisphere we define the glaciological year from the start of October to the end of September next year and the period draining meltwater from the glacier during the summer from start of June through September. It would be misleading to include May in the summer period because runoff from the glacier melt in May is delayed due to refreezing during the elimination of the frost in the surface layer.

3.2 Results of mass balance measurements.

Winter mass balance measurements were done at 67 sites in spring 2022 (Fig. 1). The specific mass balance at individual sites is shown in Fig. 2. Most survey sites are on approximate central flow lines at individual outlets. The specific mass balance along the flow lines is given in Fig 3. for the glacier outlets: Síðujökull, Tungnaárjökull, Köldukvíslarjökull, Dyngjujökull, Brúarjökull (west and east), Eyjabakkajökull, Breiðamerkurjökull, SE-Vatnajökull, Skeiðarárjökull accumulation zone and the ice catchment of Grímsvötn.

Digital maps for winter, summer and net balance are shown in Figure 4. The mass balance of individual outlet is discussed in the following subsections.

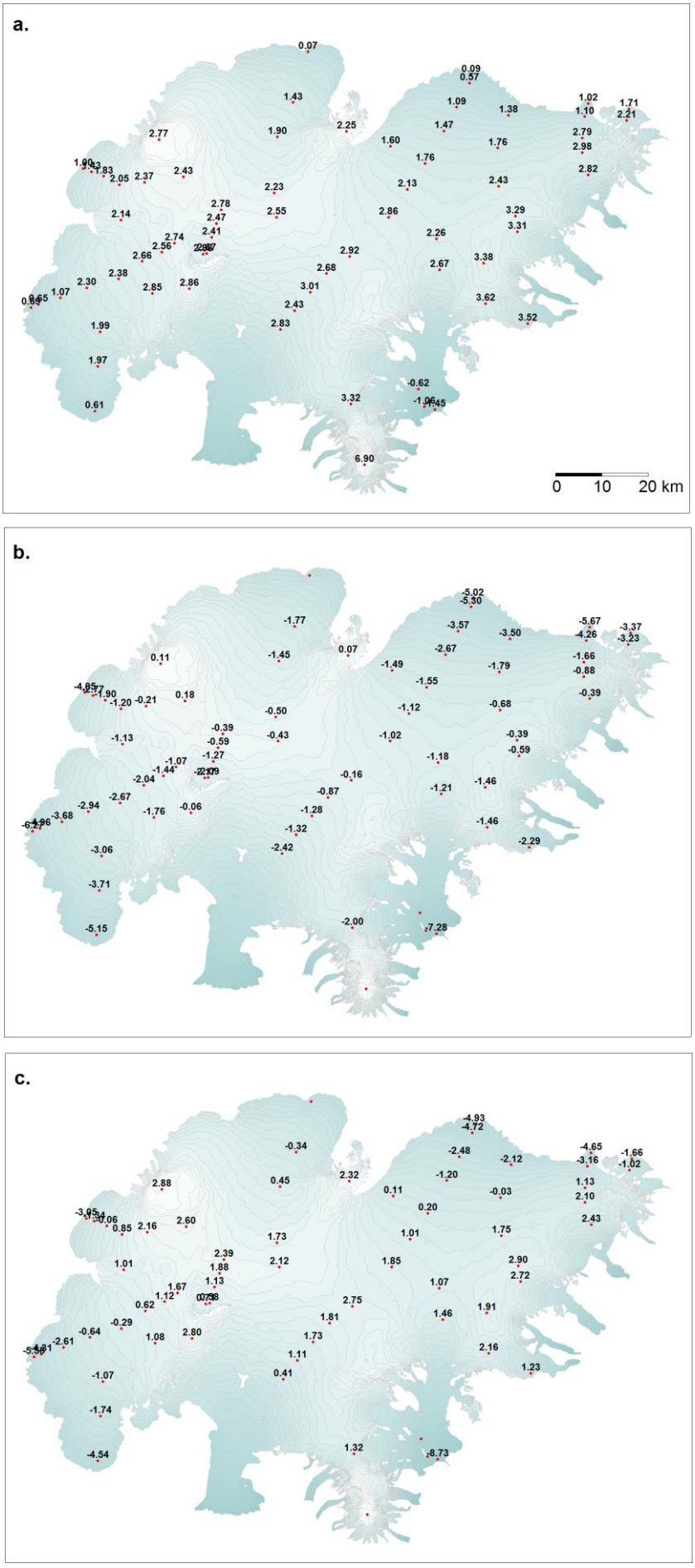

Figure 2. Maps showing point values of specific surface mass balance in m water equivalent (m_{we}), 2021_22. a. winter, b. summer, c. net balance.

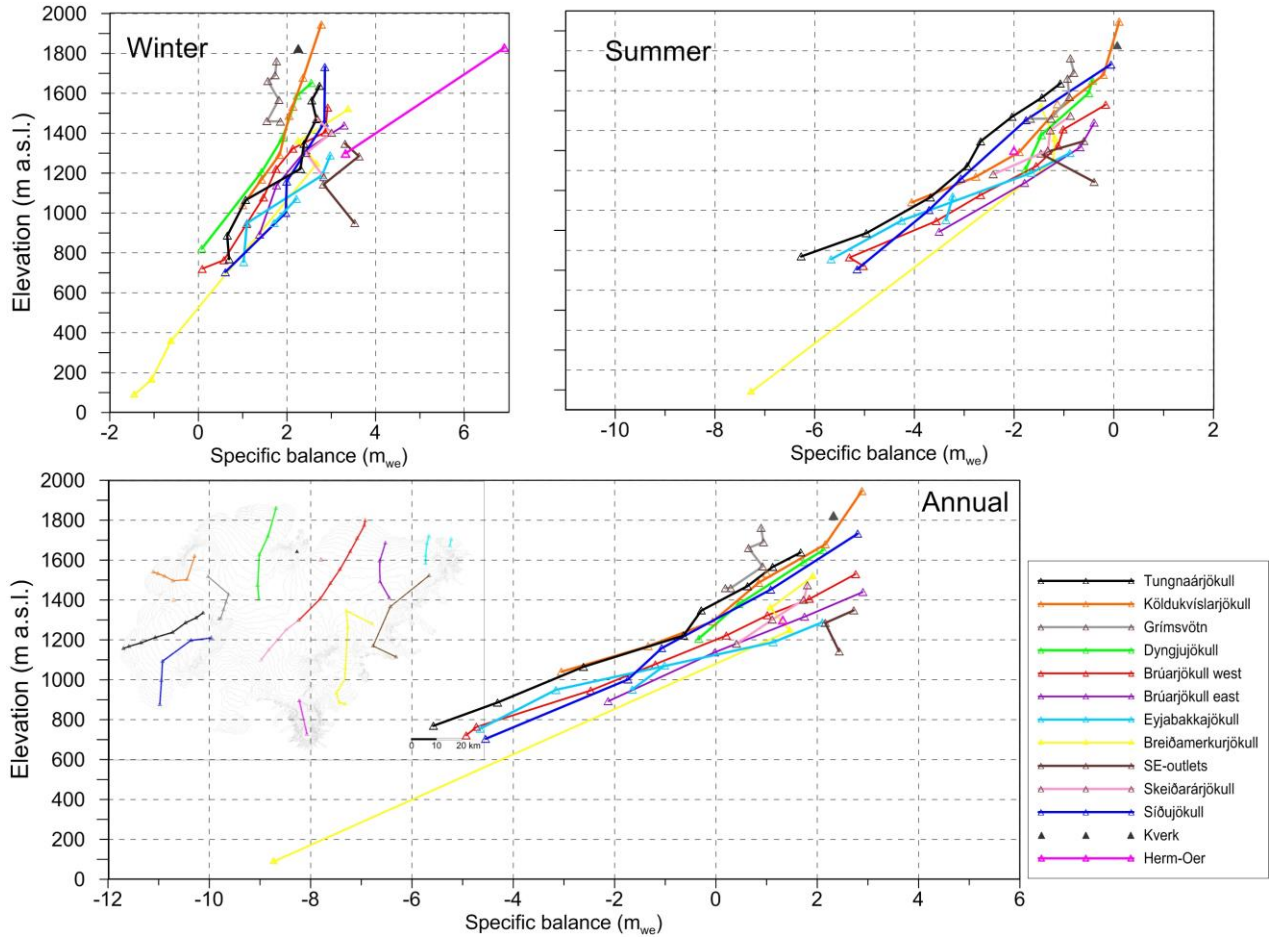

Figure 3. a. Specific mass balance (m_{we}), at survey sites along all mass balance profiles 2021_22.

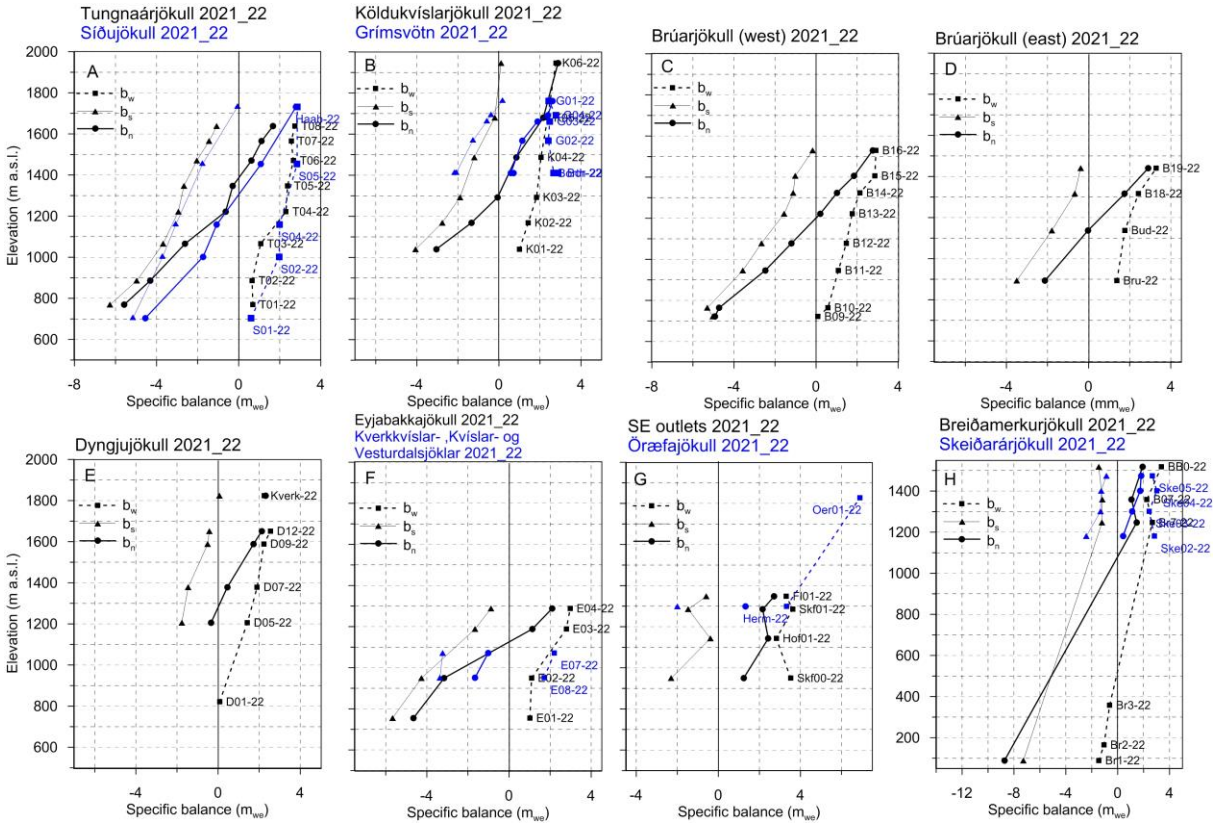

Figure 3. b. Specific point mass balance (m_{we}) 2021_22 as a function of elevation on central flow lines on Vatnajökull outlets.

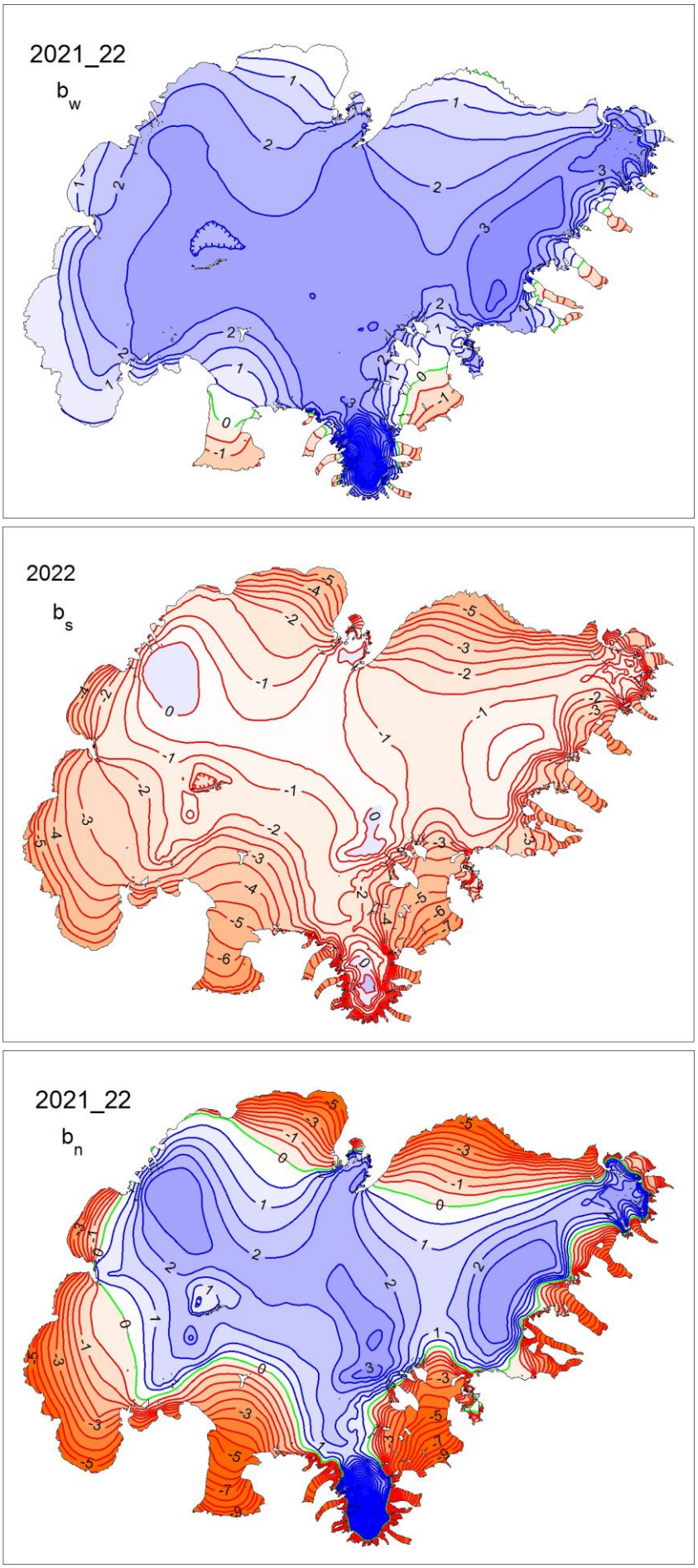

Figure 4. Specific mass balance (m_{we}) maps of Vatnajökull 2021_22. Top: winter, Centre: summer, Bottom: net balance.

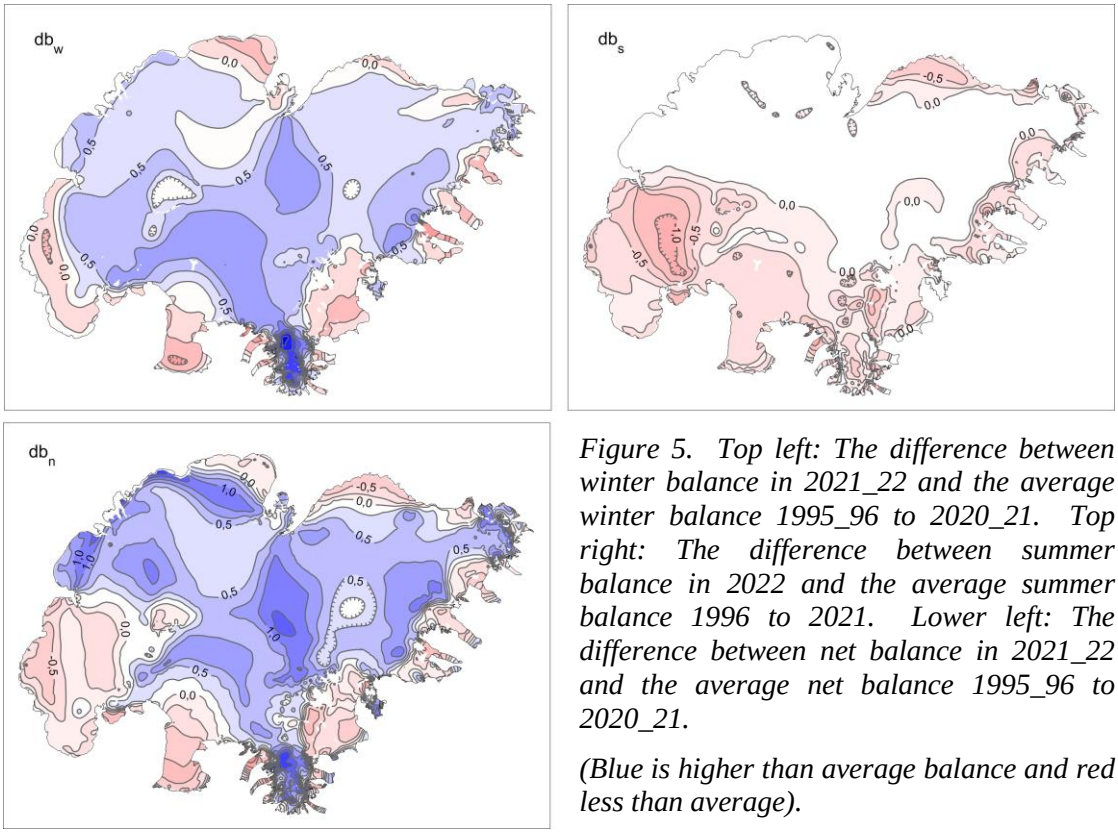

Figure 5. Top left: The difference between winter balance in 2021_22 and the average winter balance 1995_96 to 2020_21. Top right: The difference between summer balance in 2022 and the average summer balance 1996 to 2021. Lower left: The difference between net balance in 2021_22 and the average net balance 1995_96 to 2020_21.

(Blue is higher than average balance and red less than average).

A surface DEM is needed for surface area distribution and delineation of ice divides for individual outlets and catchments. The currently used surface DEM is mostly based on SPOT5 satellite images in 2010*, and partly from LiDAR survey 2010 -11 and -12 (**Jóhannesson et al. 2013), but the large set of GPS profiles measured in spring 2020 was used to locally shift the older DEMs. This DEM represents the surface of 2020 but cut to the glacier terminus of autumn 2021, was used in all area distributions; ice and water divides were not reworked.

The weather in the autumn 2021 was wet and rather warm but December to first days of January 2022 extremely dry. From mid-February to late-April snow gradually collected, followed by a cold dry period till late May.

Distribution of the winter snow was not typical (see fig. 5). In general, there was less snow than average in the lower ablation zones of the icecap, by far less in the west and south, but more than average in the mid elevation and upper ranges. Winter melting at the low-lying S-outlets slightly less than average. The summer months were cloudy and relatively cold in East Iceland, resulting in under average summer melt. However, the warm autumn contributed markedly to the total melt. An event of dust blown from south over the SW outlets in early July greatly enhanced melt there, especially in the accumulation areas of those outlets (see fig. 5)

**Jóhannesson, T., Björnsson, H., Magnússon, E., Guðmundsson, S.,Pálsson, F., Sigurðsson, O., Thorsteinsson, T., and Berthier, E.: Ice-volume changes, bias estimation of mass-balance measurements and changes in subglacial lakes derived by lidar mapping of the surface Icelandic glaciers, Ann. Glaciol., 54, 63–74, doi:10.3189/2013AoG63A422,2013.

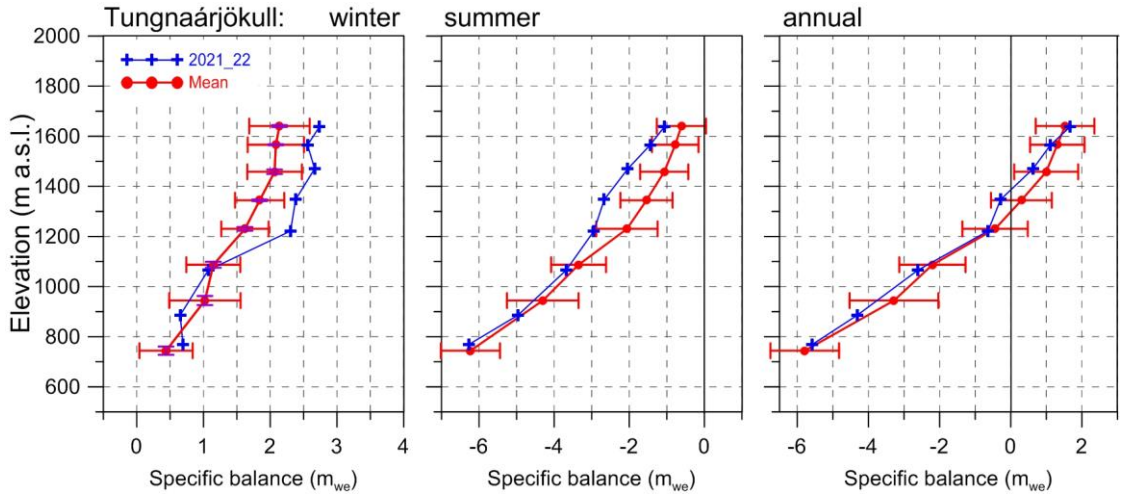

Figure 6. Mass balance at a central flow line of Tungnaárjökull 2021_22 and average mass balance 1991_92 to 2020_20 (the horizontal red lines indicate std. dev of the variability at the survey site during the survey period).

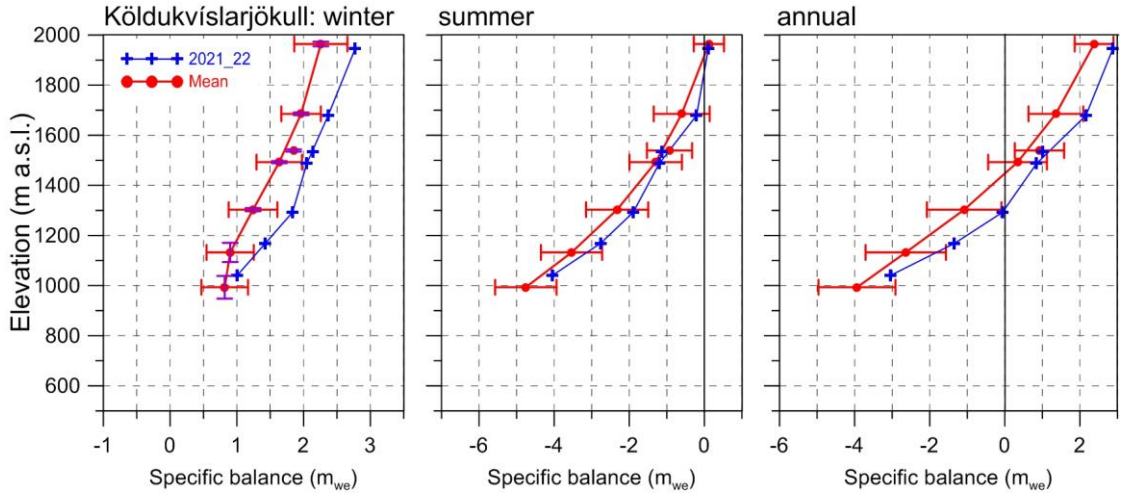

Figure 7. Mass balance at a central flow line of Köldukvíslarjökull 2021_22 and average mass balance 1991_92 to 2020_21.

3.2.1 Tungnaárjökull.

Area = 327 km^2
B_w= 0.60 km^3_{we} ; b_w = 1.51 m_{we}
B_s = -1.04 km^3_{we} ; b_s = -2.61 m_{we}
B_n = -0.44 km^3_{we} ; b_n = -1.11 m_{we}
ELA = 1385 m a.s.l. (at profile)
AAR = 29 %
(The terms are defined at the foot of this page)

Variation of mass balance along a central flow line on Tungnaárjökull is shown in Fig. 6. The winter accumulation was over 1std. (~0.75 m) more than average at all survey sites except the lowest. The total winter balance was 21% over the average. Summer mass loss was also more than 1 std. over average in the accumulation zone due to dust blown over from the south in 1st week of July, but at average below the equilibrium line. In total summer mass loss was almost at average of the survey period. This is the 27th year out of the 31 surveyed with negative net balance on Tungnaárjökull catchment.

3.2.2 Köldukvíslarjökull

Area = 286 km^2
B_w = 0.55 km^3_{we}; b_w = 1.92 m_{we}
B_s = -0.44 km^3_{we}; b_s = -1.53 m_{we}
B_n = 0.39 km^3_{we}; b_n = 0.39 m_{we}
ELA = 1300 m a.s.l. (at profile)
AAR = 66 %
Variation of mass balance along a central flow line on Köldukvíslarjökull

For each ice catchment basin, B_w, B_s and B_n are water equivalent volumes of winter, summer and net balance, ELA the equilibrium line altitude, and AAR is the accumulation area ratio.

is shown in Fig. 7. The winter accumulation was over 1std. (~0.75 m) more than average at all sites in the accumulation zone. The total winter accumulation was 30% over the average. Summer mass loss was 0-20 cm less than average at all survey sites. In total summer mass loss only 79% of the average during the survey period. This year Köldukvíslarjökull gained mass, this is the 6th year out of the 30 surveyed with positive net balance, now similar to 2017_18, but only 1/3 of the mass gain in 2014_15 (the highest in the survey period).

3.2.3 Dyngjujökull

Area = 1034 km^2
B_w = 1.89 km^3_{we} ; b_w= 1.83 m_{we}
B_s = -1.45 km^3_{we} ; b_s = -1.41 m_{we}
B_n = 0.44 km^3_{we} ; b_n = 0.42 m_{we}
ELA = 1353 m a.s.l. (at profile)
AAR = 60 %

Variation of mass balance along a flow line on Dyngjujökull is shown on Fig. 8. At the measurements sites snow accumulation was ~l std. over average except the lowest, where it was ~1 std under. The total winter accumulation is estimated 14% over the average of the survey period.
Summer mass loss was almost at average over the survey period at the upper survey sites but less than average at 1200 m (probably due to the thick snow cover). The lowest site has not been visited yet when the report is written. The net balance was positive by 0.42 m_{we} while the average for Dyngjujökull is slightly negative (-0.03 m_{we}).
Dyngjujökull has often had mass balance close to zero, and the net balance has been estimated positive in at least 12 years of the three-decade period of almost continuous mass loss for Vatnajökull as a whole. The inland Dyngjujökull, is the outlet of Vatnajökull closest to mass equilibrium during the survey period.

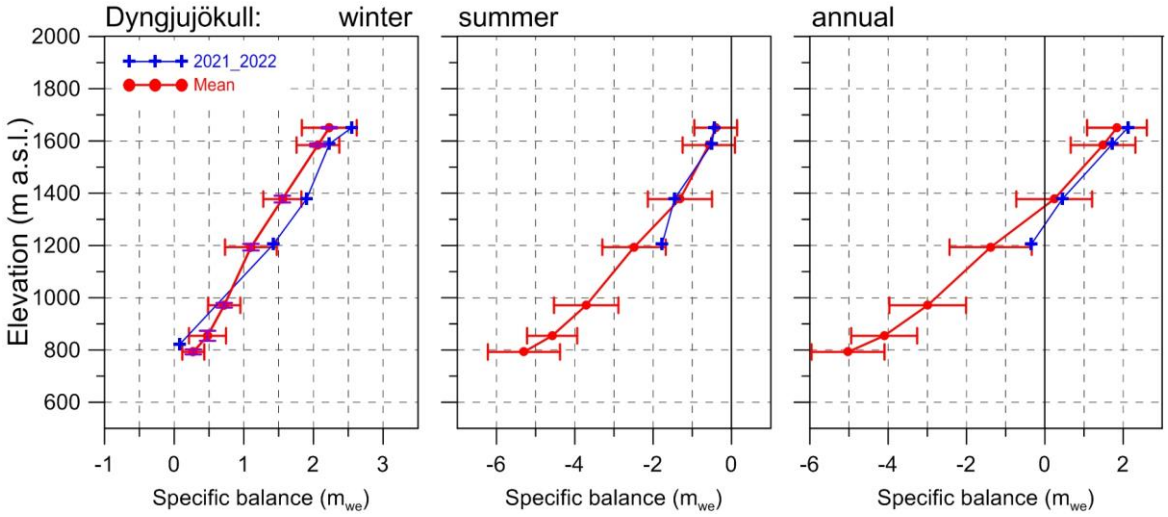

Figure 8. Mass balance at a central flow line on Dyngjujökull 2021_22 and average mass balance 1991_92 to 2020_21 (except 1998_99 – 2003_04 at all but the top elevation).

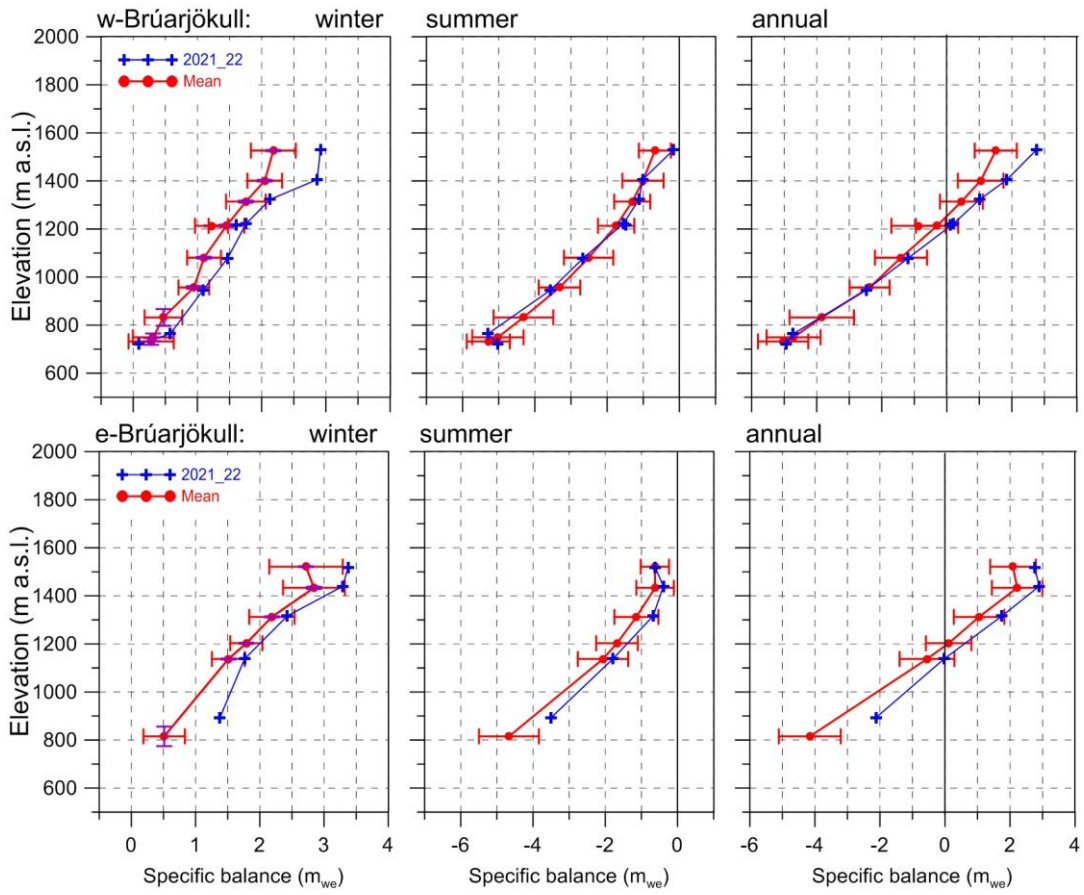

Figure 9. Mass balance at two flow lines on Brúarjökull 2021_22 and average mass balance 1992_93 to 2020_21.

3.2.4 Brúarjökull

Area = 1491 km^2
B_w = 3,09 km^3_{we} ; b_w = 2.07 m_{we}
B_s = -2,57 km^3_{we}; b_s = -1.73 m_{we}
B_n = 0,52 km^3_{we}; b_n = 0.34 m_{we}
ELA = 1200 m a.s.l. (western flow line)
ELA = 1140 m a.s.l. (eastern flow line)
AAR = 67 %

Variation of mass balance along the flow lines on Brúarjökull is shown in Fig. 9. At the western flow line accumulation was well over average (1 std.) for much of the elevation range, and far over at two highest sites (almost 2 std.). At the lowest site almost no snow had accumulated. At the eastern survey line accumulation was 1. more Std. more than average at all sites. The distribution of the snow accumulation reflects prevailing path of the Atlantic low-pressure systems south and east of Iceland, for long periods of the winter, resulting in precipitation in eastern and northern winds. The winter accumulation was in total ~29% over average. Summer mass loss was close to average at most of the western survey sites, but less than average at all the eastern, probably due to snowfall in summer. In total the mass loss in summer was 91% of the average.

The net balance was about 1 std. above the average at almost all the eastern survey sites but varied from average at the lowest to almost 2 std. over at the highest site at the western survey line. In total the net balance was positive by 0.34 m_{we}. During the survey period, there have been 9 years of positive balance and 21 years with negative net balance.

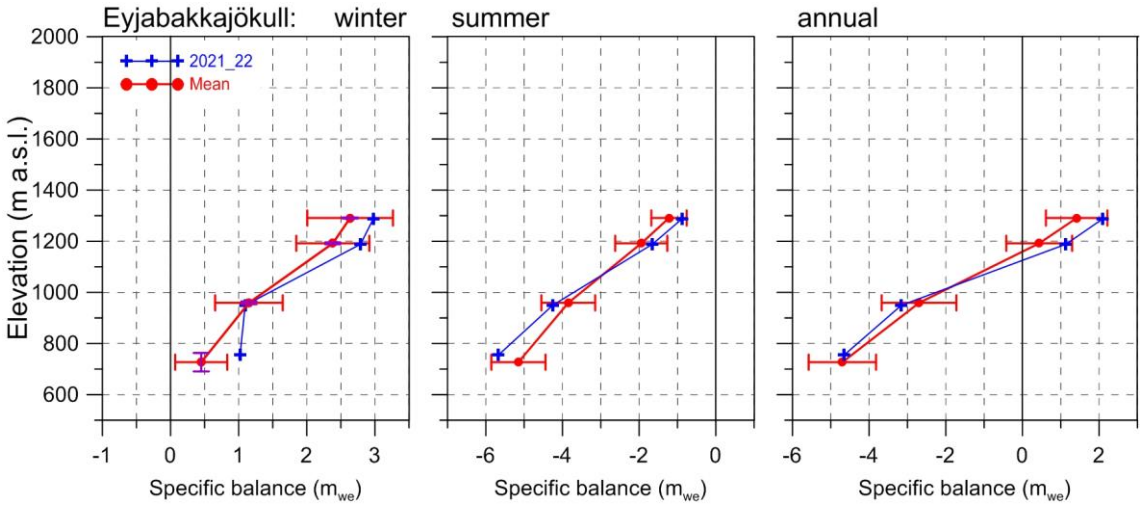

Figure 10. Mass balance at a central flow line of Eyjabakkajökull 2021_22 and average mass balance 1995_96 to 2020_21.

3.2.5 Eyjabakkajökull

Area = 105 km^2
B_w= 0.22 km^3 we; b_w = 2.15 m_{we}
B_s = -0.26 km^3 we; b_s = -2.51 m_{we}
B_n = -0.04 km^3 we; b_n = -0.36 m_{we}
ELA = 1126 m a.s.l. (at profile)
AAR = 50 %

Variation of mass balance along a central flow line on Eyjabakkajökull is shown in Fig. 10. As at the neighboring E-Brúarjökull accumulation was over average at all sites except, at 950 m. The total winter accumulation 18% more than average of the survey period. Summer mass loss was more than average at the lowest survey site, but much less than average above ELA (probably partly due to summer snowfall). The total summer mass loss was about 95% of the average. The net balance was negative by about half that of the average of the survey period and has been negative for all but 3 years of the 27 years of survey. It is of interest that the neighboring Brúarjökull had positive balance.

3.2.6 Breiðamerkurjökull

Area = 878 km^2
B_w = 1.69 km^3we; b_w = 1.92 m_{we}
B_s = -2.17 km^3 we; b_s = -2.46 m_{we}
B_n = -0.48 km^3we; b_n= -0.54 m_{we}
ELA = 1075 m a.s.l. (at profile)
AAR = 60
Variation of mass balance along a

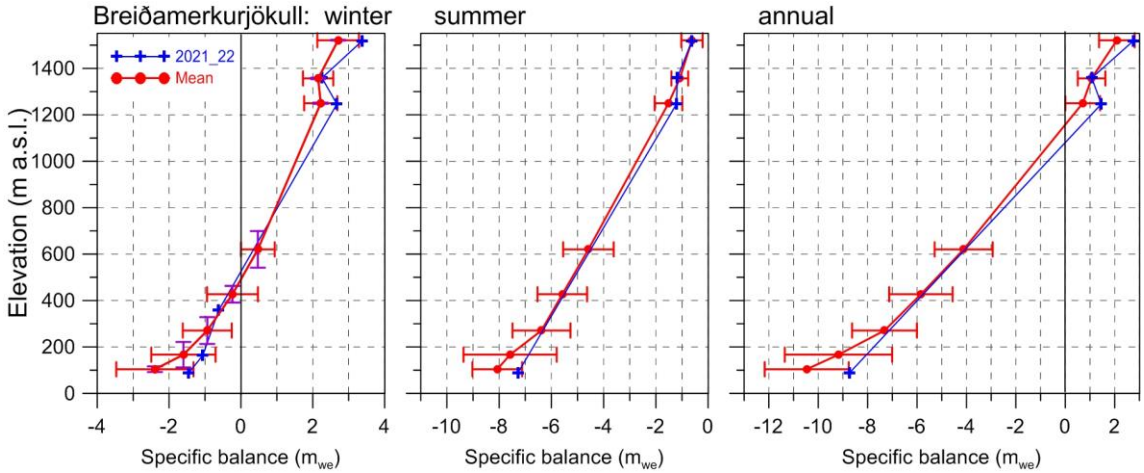

Figure 11. Mass balance at a central flow line of Breiðamerkurjökull 2021_22 and average mass balance 1995_96 to 2020_21.

central flow line on Breiðamerkurjökull is shown in Fig. 11.
Winter accumulation was over average at the survey sites in the accumulation zone, but at the lower sites in the ablation zone mass loss in winter was much less than average. The total winter balance was 29% over the average of the survey period.
Summer mass loss was not far from to average in the accumulation zone), but more than 1 std. over average in the lower ablation zone. As this is written the two upper sites of the ablation zone have not been visited for autumn read off, so the results presented here are preliminary. The total summer mass loss is estimated 95% of the average during the survey period. The net mass loss was only 50% of an average year.
In addition to mass loss due to surface melt Breiðamerkurjökull loses in the order of 0.5 km^3 annually via calving into the marginal lake Jökulsárlón; this mass loss is not accounted for here.

3.2.7 Síðujökull

Area = 407 km^2
B_w= 0.76 km^3_{we}; b_w = 1.87 m_{we}
B_s = -1.31 km^3_{we}; b_s = -3.24 m_{we}
B_n = -0.55 km^3_{we}; b_n= -1.37 m_{we}
ELA = 1300 m a.s.l. (at profile)
AAR = 34 %

Variation of mass balance along a central flow line on Síðujökull is shown in Fig. 12.
The winter snow accumulation was over average at mid elevation range survey sites, but less than average at the highest and lowest. The total winter balance was 16% over the average (since 2004_05). Summer mass loss was more than average at all sites except the highest, where it was far less than average (probably due to summer snowfall). Ablation was greatly enhanced by dust blown over from the south, and precipitating to the snow surface, in 1st week of July. The total summer mass loss was 12% over the average of the survey period. Net mass loss was ~6% more than average during the 17-year survey period. Here the only year of surveyed positive net balance was 2014_2015.

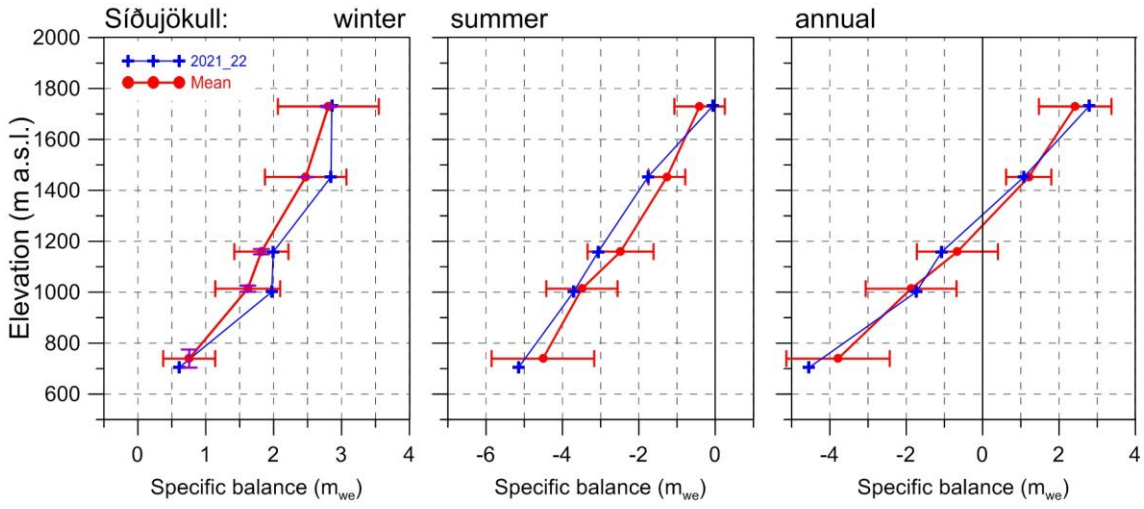

Figure 12. Mass balance at a central flow line of Síðujökull 2021_22 and average mass balance 2004_05 to 2020_21.

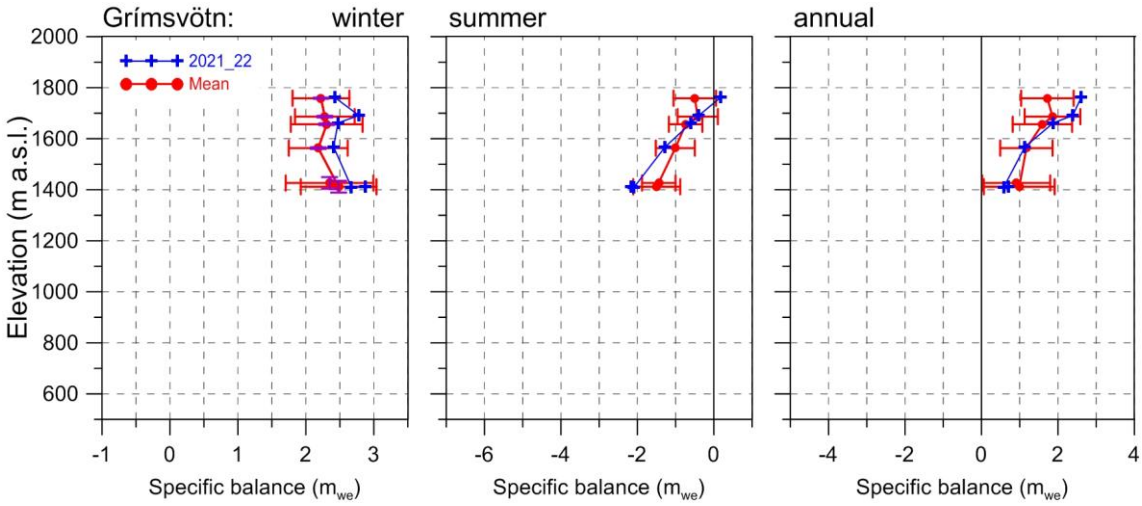

Figure 13. Mass balance at a flow line towards Grímsvötn 2021_22 and average mass balance 1991_92 to 2020_21.

3.2.6 Grímsvötn-Gjálp

Area = 174 km^2
B_w = 0.45 km^3_{we}; b_w = 2.64 m_{we}
B_s = -0.15 km^3_{we}; b_s = -0.89 m_{we}
B_n = 0.30 km^3_{we}; b_n= 1.75 m_{we}

Variation of mass balance at sites close to a flow line from Bárðarbunga towards Grímsvötn center is shown in Fig. 13. Snow accumulation was almost 1/2 std. more than average at all survey sites, and total winter accumulation 13% over the average. Summer mass loss varied from far over average at the lowest sites to far less than average at the top site; total summer mass loss was 10% over the average. Net balance was positive as always (except 2010), now 15% more than average.

In addition to surface mass loss in summer, geothermal melt in the Grímsvötn catchment area is on the order of 0.2 km^3 annually, this is not accounted for here.

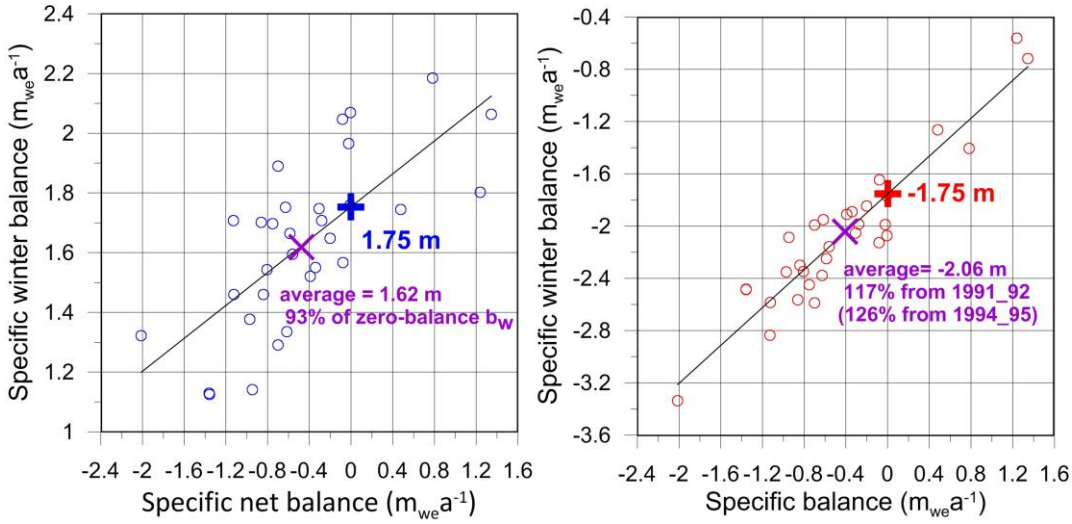

Figure 14. Vatnajökull winter (left)and summer (right) mass balance plotted against net mass balance for the survey period 1991_92 to 2021_22.

3.3 Vatnajökull: mass balance record

From the digital mb maps (Fig. 4) the glacier wide volumes of winter, summer and net balances for Vatnajökull have been calculated by integration and are as follows:

Area = 7656 km^2
B_w = 15.65 km$^3_{we}$; b_w = 2.05 m_{we}
B_s = -16.27 km$^3_{we}$; b_s = -2.13 m_{we}
B_n = -0.62 km$^3_{we}$; b_n = -0.08 m_{we}
AAR = 60%;
(balance values as a function of elevation are tabulated in appendix D)

The weather in the autumn and first winter months 2021_22, was wet and rather warm, but in December 2021 and the first week of January 2022 almost no snow was accumulated in Grímsvötn (data from snow elevation meter), an extremely dry period for most of Vatnajökull, and another dry period from mid-January till late February. In Grímsvötn snow accumulation started again at a steady rate till late April, then a dry period again to the end of May. Distribution of the winter snow was not typical (see fig. 5). In general, there was less snow than average in the lower ablation zones of the icecap, by far less in the west and south, but more than average in the mid elevation and upper ranges.
The total winter balance was ~27% over the average (over the observation period from 1991_92). This
The summer months were cloudy and relatively cold in East Iceland, resulting in under average melt. However, the warm autumn contributed markedly to the total melt. An event of dust blown from south over the SW outlets in early July greatly enhanced melt there, especially in the accumulation areas of those outlets (see fig. 5). The total summer mass loss was almost at the average of the survey period).
The zero-mass balance mass turnover for Vatnajökull (current topography) is estimated from the zero net balance crossover of the linear trend of bw plotted against b_n and equivalently b_s against b_n (see fig 14.) and found to be close to 1.75 m_{we} (13.4 km$^3_{we}$). The winter balance 2021_22 is ~17% over the estimated zero-mass balance turnover (0-mbt), while the average b_w of the survey period is close 93% of the 0-mbt. The summer balance of 2022 is -0.38 m (or 22%) more negative than 0-mbt. On average the summer mass loss has been 17% (average of summers 1992-2022) higher than 0-mbt, 26% for the period of 1995-2022.
This clearly shows that the high mass loss of the past 3 decades is governed by too much mass loss during summer rather than too little snow accumulation during winter.
The net balance of 2021_22 is only slightly negative (8 cm_{we}), or zero if method uncertainties are considered.
Since 2010, after the 15-year period of high mass loss, the summer and net balance have been highly variable, even one year with positive mass balance in 2014_15 and close to zero in 2010_11, 2016_17, 2017_18 and now in 2021_22.
During the period of high net mass loss since 1994_95, the northern outlets have had several years of close to zero and positive mass balance. After 2010 both winter and summer balance are highly variable, much more so than the 15 prior years of high mass loss, this is seen for all the mb records presented in figure 15. The variability of the winter balance is by far more prominent for the outlets closest to sea. That part of the glacier receives precipitation from all south and east wind directions, and thus has high snow accumulation in

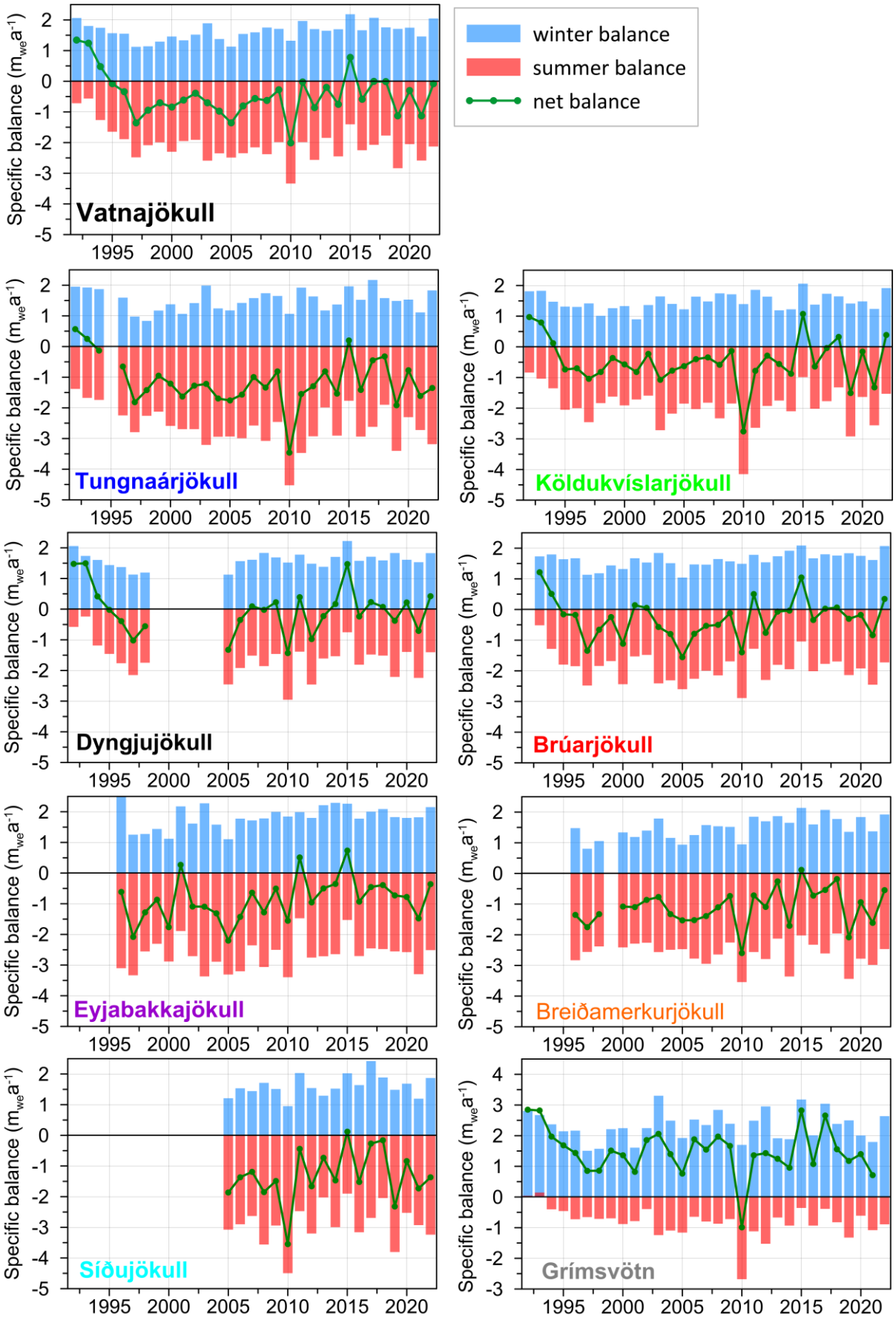

Figure 15. Specific mass balance record for Vatnajökull (top), and selected Vatnajökull outlets 1991_92-2021_22.

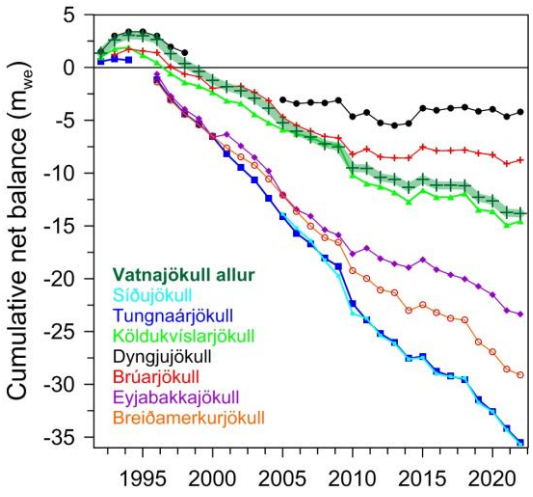

Figure 16. Cumulative specific surface mass balance Vatnajökull and selected Vatnajökull outlets 1991_92 – 2021_22.

winters when the paths of the North Atlantic low-pressure systems are just south and east of Iceland.

The cumulative net balance curves for the outlets of Vatnajökull in Fig. 17 show that all outlets have been lost mass since 1994_95. During the period of high mass loss, the mass loss speed is about -0.5 - -0.6 $m_{we}a^{-1}$ for the northern outlets but -1.1 - -1.5 $m_{we}a^{-1}$ for the south and western outlets. After 2010 there is a distinct difference between the north inland (Dyngju-jökull and Brúarjökull) and the south and west coastal (Breiðamerkurjökull, Tungnaárjökull and Síðujökull) outlets in that there is sudden change in the mass balance trend for the northern. The trend changes from -0.5ma^{-1} to about zero for the northern while there is little change for the others. The east outlet Eyjabakkajökull behaves like the coastal and is in fact close to sea, while Köldukvíslarjökull in the NV is more like the northern.

The cumulative mb for Vatnajökull is very similar to Köldukvíslarjökull, with a slope of -0.75 ma^{-1} in the period of high mass loss, but -0.35 ma^{-1} after 2010.

During the survey period starting 1991_92 Vatnajökull lost ~123 km^3 of ice or thinned ~15 m due to surface mass loss (summing from the start of high mass loss in 1994_95 yields 150 km^3 or 19 m thinning). Non-surface mass balance is estimated (calving, geothermal melt, internal friction, eruptions) ~0.2 m_{we} for Vatnajökull in a paper by Tómas Jóhannesson and others (Jóhannesson, T., Pálmason, B., Hjartarson, Á., Jarosch, A., Magnússon, E., Belart,J., et al. (2020). Non-surface mass balance of glaciers in Iceland. J. Glaciol. 66, 685–697. doi:10.1017/jog.2020.37) which amounts to a loss of ~57 km^3 or 7.5 m average thinning since 1994_95.

In Fig. 17 the relation of the annual net

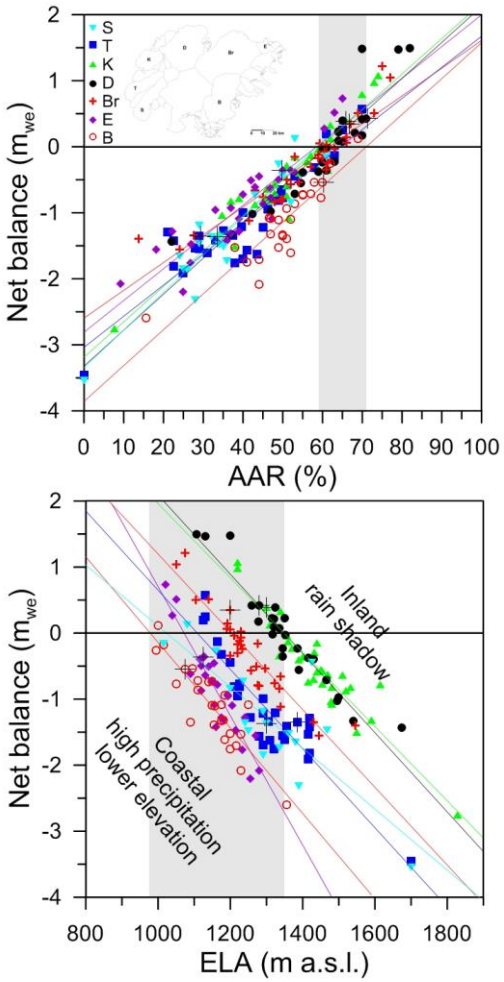

Figure 17. The relation between net annual balance (b_n) and accumulation area ratio (AAR) (upper) and b_n and equilibrium line altitude (ELA), for Vatnajökull outlets during the survey period. (This year's points are marked with a black +).

balance to the accumulation area ratio (AAR) and equilibrium line altitude (ELA) is shown for different outlets over the survey period. The b_n-AAR gradient is similar for all outlets, about 0.5 m_{we} for 10% change in AAR. The zero-balance AAR varies for different outlets in the range 60-65%, similar for all outlets except for the southern outlet Breiðamerkurjökull. Breiða-merkurjökull is far from equilibrium, the ablation area is too large. A large part of the outlet has carved 200-300 m deep valley into the former sediment bed, and the surface and bed elevation has lowered accordingly. Similarly, the zero-balance ELA varies from about 1000-1100 m a.s.l. for the southern outlets to 1400 m a.s.l. for the NW outlets. The bn-ELA slope is similar for all outlets -0.6 m_{we} per 100 m, except Eyjabakkajökull with a slope of -1.0 m_{we} per 100 m and Síðujökull with a slope of -.45 m_{we} per 100 m (for Síðujökull possibly due to outliers in the data set).

4. SURFACE VELOCITY MEASUREMENTS

The average summer surface velocity of the glacier surface at the survey was calculated fast static or kinematic GPS (accuracy about ~10 cm) positioning of the ablation stakes/wires. In 2022 all sites were surveyed in spring and autumn and many in June. At a few sites stakes from previous years were found and resurveyed, making it possible to calculate surface velocity over a year or longer time span. The average summer surface velocity is shown in Figure 18.

At sites close to the glacier terminus very small horizontal movement is measured. This indicates that the

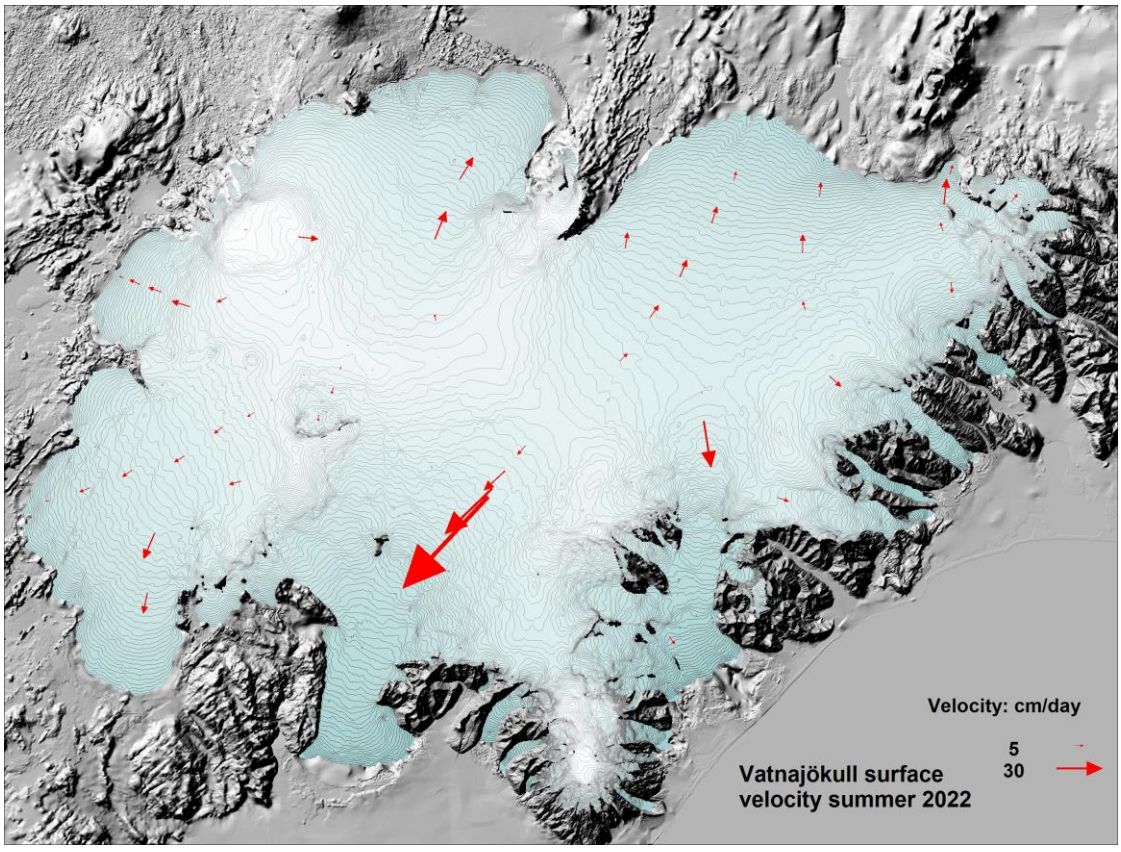

Figure 18. Average summer surface velocity at survey sites in 2022.

glacier snouts are almost stagnant. In the centre areas of some of the outlets especially close to the equilibrium line, there is an increase in velocity during summer compared to winter. The summer velocity is typically in the order of two-fold the winter velocity. This suggests that basal sliding is increased in the melting season and is of often at the same magnitude as the deformation velocity.

To better understand the variable velocity continuous GPS has been run during summer at several sites.

From previous velocity measurements, surging of outlets has been predicted. Currently the increase in velocity at sites D05 and D07 (Fig. 19.) persists and suggests that Dyngjujökull may surge within a few years. The velocity at sites D07 and D05 is now similar that in 1997 prior to the surge in 1998-2000 and the accumulation zone has thickened. To monitor velocity changes leading up to a surge GPS instruments were set up in spring to continuously monitor movement at sites D05 and D06.

The data collected allows for post-processing to acquire more accuracy (~dm instead of ~m), but the processing has not been finished when this report is written.

A figure similar Fig 20. Showing the average summer velocity and elevation change record at the survey sites on Eyjabakkajökull. There is an increase in velocity at sites E01 (many-fold) and E02 (1.5-fold). This may be caused by the rapid recession of the glacier snout, and thus steeper surface slopes, but may also be signs of a starting surge.

Images of velocity and elevation records for other survey sites are displayed in Appendix F.

Most vehicles used in the survey are equipped with survey type GPS that collect data while driving. These are post-processed, to yield surface profiles with an accuracy of ~dm in horizontal and vertical. Location of all profiles surveyed in 2022 is shown in image 21. The profiles have proved of high importance to increase accuracy of remote sensing-based surface DEMs.

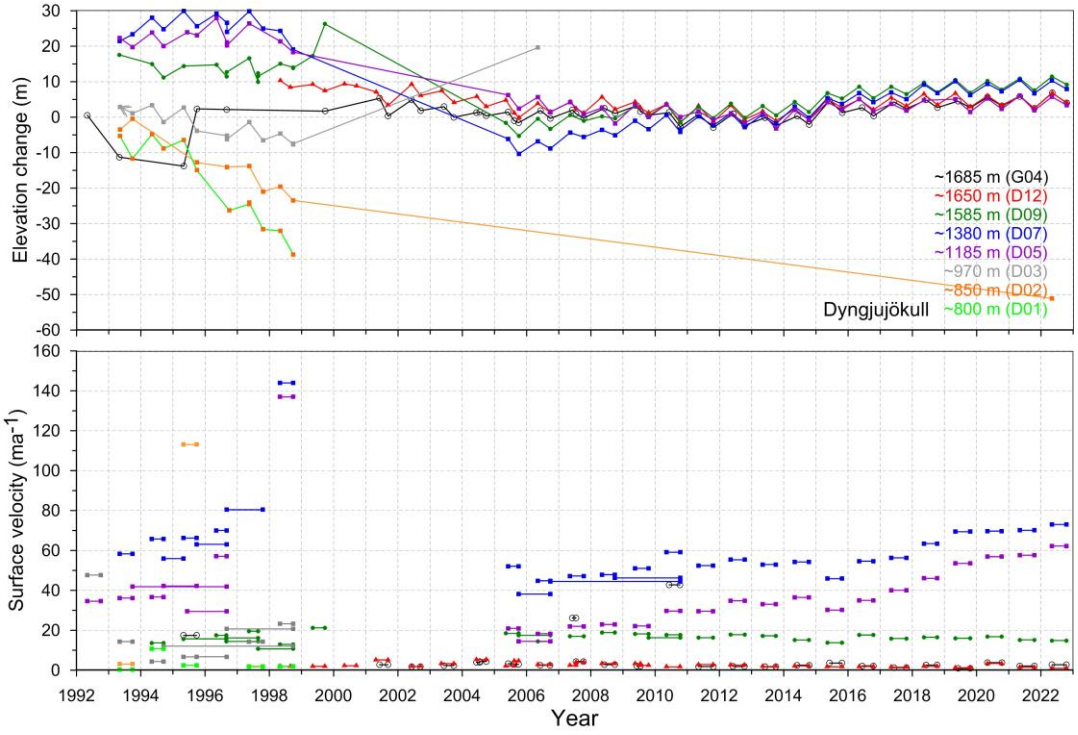

Figure 19. Surface elevation change relative to spring 2010 (upper panel) and average surface velocity (lower panel) at mb sites on Dyngjujökull in 1992 to 2022.

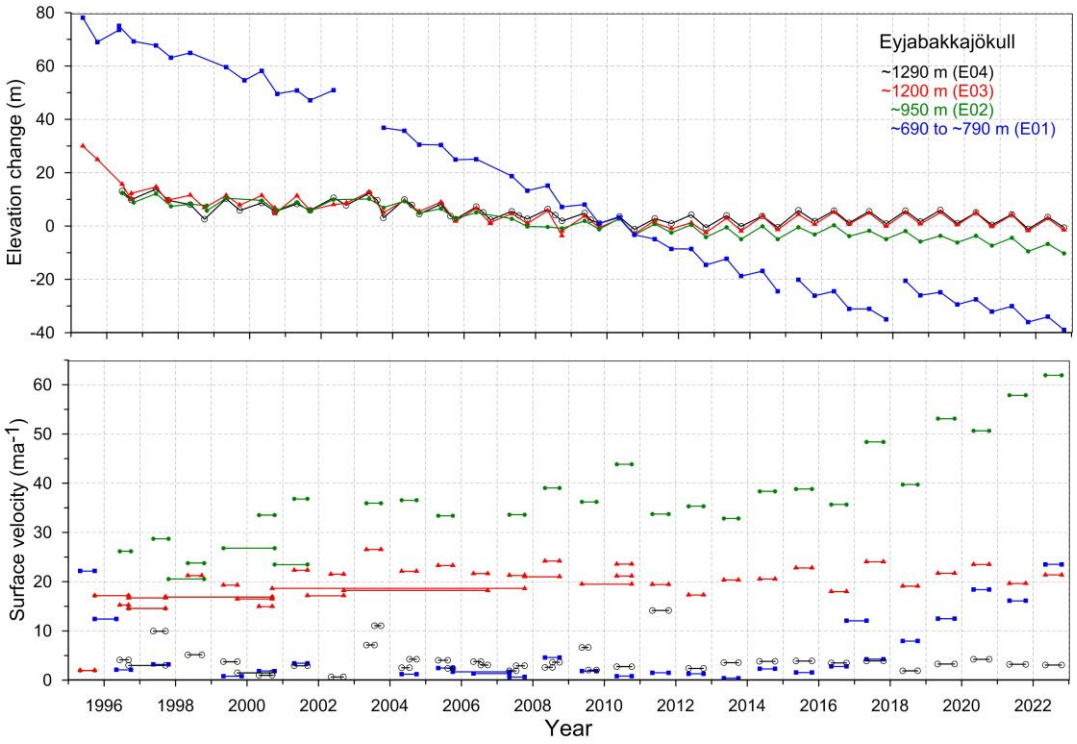

Figure 20. Surface elevation change relative to spring 2010 (upper panel) and average surface velocity (lower panel) at mb sites on Eyjabakkajökull in 1995 to 2022.

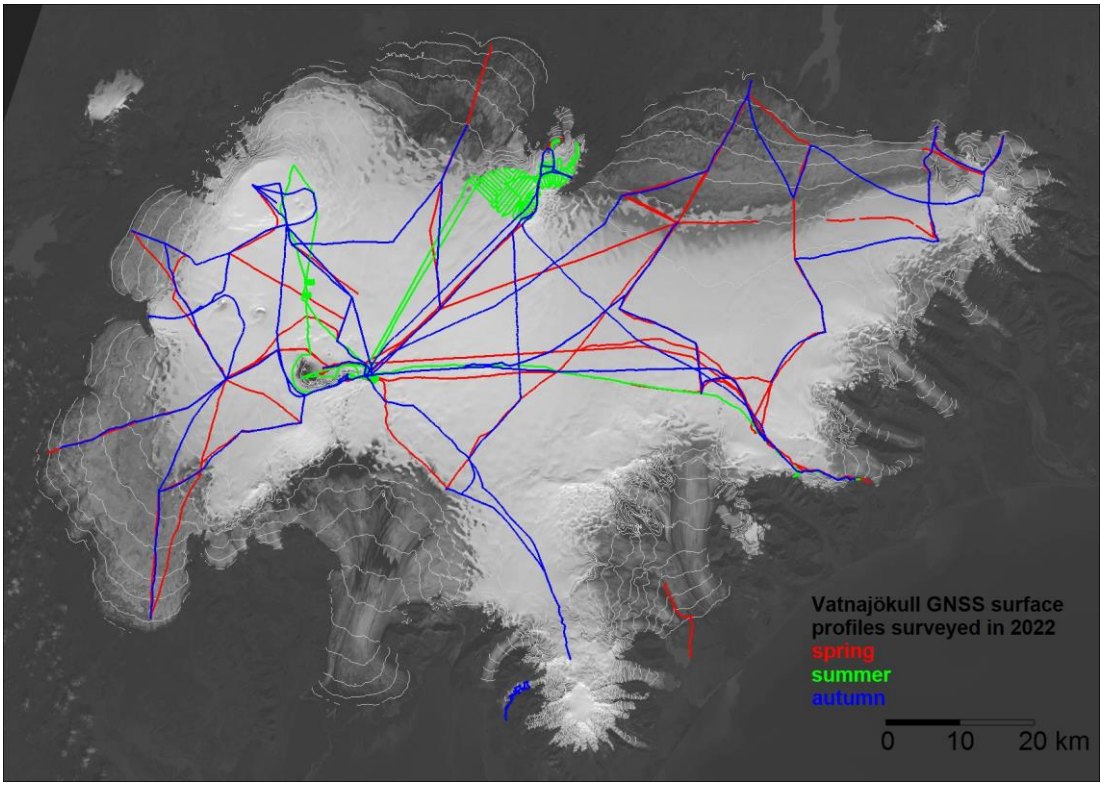

Figure 21. Location of surface elevation profiles surveyed in field trips on Vatnajökull in 2022. Survey in spring is shown in red, June in green and autumn survey in blue.

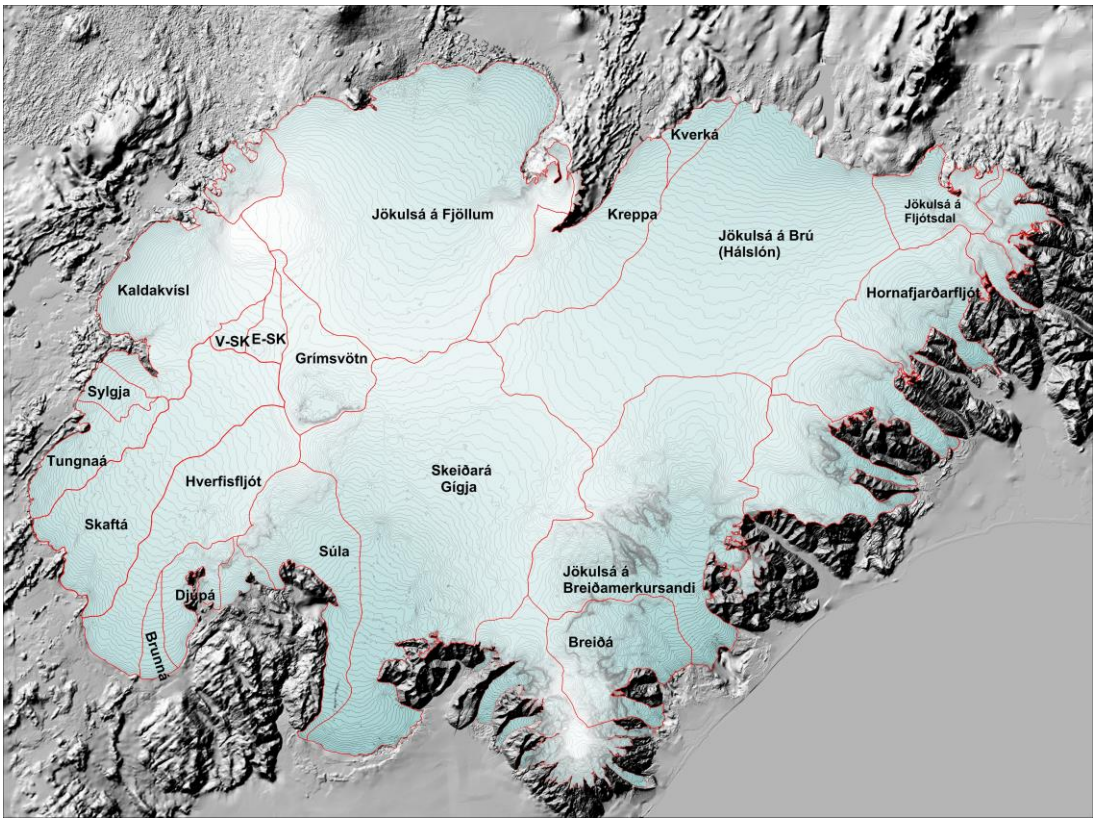

Figure 22. Water divides and drainage basins of selected rivers draining water from Vatnajökull, Súla is since summer 2016 diverted to Gígja.

5. Melt water runoff.

Water divides and drainage basins for rivers draining water from Vatnajökull have been defined from water pressure potential maps. The potential maps were produced from surface (year 2010) and bedrock DEMs.

Figure 22. shows the water divides and drainage areas for selected rivers draining melt water from Vatnajökull. The summer balance over the water basin is an estimate of meltwater contribution to rivers and groundwater storage. This estimate, however, does not include precipitation that falls as rain on the glacier, or snow that falls and melts during the summer. The meltwater contribution can be compared with river runoff at stream flow gauges closest to the glacier. For this comparison, we define the glaciological year from the start of October to the end of September and the period draining meltwater from the glacier during the summer from June through September. It would be misleading to include May in the summer period because runoff from the glacier melt in May is delayed due

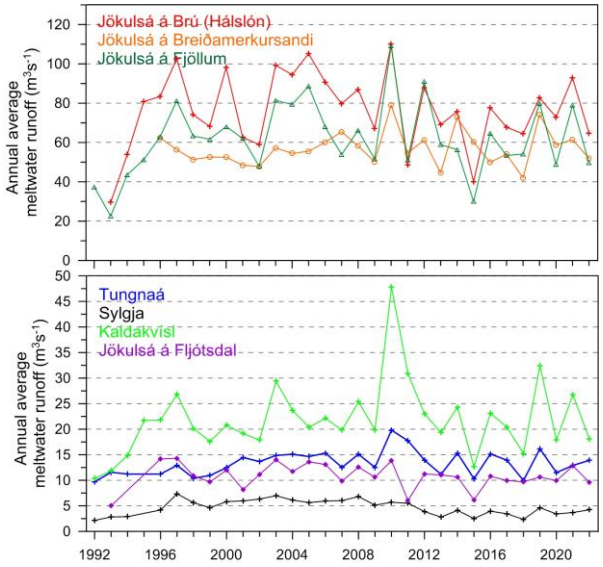

Figure 23. The temporal variation of average annual meltwater runoff to selected river catchments.

Table I. Melt water drainage to selected rivers in summer 2022.

Water Catchment:	Area (km^2)	ΣQ_s ($10^6 m^3$)	Q_s ($m^3 s^{-1}$)	Q_a ($m^3 s^{-1}$)	q_s ($ls^{-1}km^{-2}$)
Vatnajökull	7641	16697	1584,0	529,5	69,3
Tungnaá	110	439	41,6	13,9	126,6
Sylgja	39	133	12,7	4,2	109,3
Kaldakvísl	334	570	54,1	18,1	54,1
Jökulsá á Fjöllum	1116	1568	148,8	49,7	44,6
Kreppa	284	395	37,5	12,5	44,1
Kverka	37	165	15,7	5,2	142,4
Hálslón	1195	2043	193,8	64,8	54,2
Jökulsá á Fljótsdal	125	303	28,7	9,6	77,0
Jökulsá í Lóni	97	217	20,5	6,9	70,5
Hornafjarðarfljót	233	535	50,7	17,0	72,7
Jökulsá á Breiðamerkursandi	708	1638	155,4	51,9	73,3
Breiðá-Fjallsá	220	841	79,7	26,7	121,2
Skeiðará-Gígja	1394	3308	313,8	104,9	75,2
Brunná	32	154	14,6	4,9	154,0
Djúpá	74	290	27,5	9,2	124,4
Hverfisfljót	310	872	82,7	27,7	89,3
Skaftá	384	1188	112,7	37,7	98,1
Grímsvötn	170	155	14,7	4,9	28,8
Eystri Skaftárketill	34	15	1,5	0,5	14,3
Vestari Skaftárketill	25	14	1,3	0,5	17,9
Hólmsá	161	392	37,2	12,4	77,3
Heinabergsvötn	224	592	56,2	18,8	83,9
Skjálfandafljót	96	102	9,6	3,2	33,5

ΣQ_s: total summer melt water; Q_s: average runoff (averaged over summer, 4 months, June – September)
Q_a: average runoff (averaged over a whole year); q_s: average runoff per km^2 (averaged over a whole year)

to refreezing during elimination of the cold wave and because of the contribution of the spring snow melt from the highlands to the runoff. Some melting also occurs during winter, especially in the terminus regions of the southern outlets.

Average melt water runoff to different rivers is given in Table I, and temporal variation of the average meltwater runoff in Fig. 24. The average specific runoff (q_s) differs from basin to basin from ~20 to ~170 $ls^{-1}km^{-2}$. This is mainly due to different elevation distributions, for example, the water drainage basins for Tungnaá and Kverká are within the ablation area, while that of Grímsvötn and Skaftárkatlar are high in the accumulation zone.

Runoff as function of elevation, estimated from summer balance, is tabulated for individual water catchments in Appendix E.

6. Conclusions

In the glaciological year 2021_22 the winter balance for Vatnajökull was 27% more than average, over the observation period from 1991_92. Only the winters of 2014_15, 2016_17 and 1991_92 had slightly higher winter accumulation.
The total summer surface mass loss was 97% of average since 1995 (3% more than average since 1991_92), so a summer of average surface mass loss. The net balance was slightly negative, or zero within the error limits of the survey method.
Since 2010, after the 15-year period of high mass loss, the summer and net balance have been highly variable, even one year with positive mass balance in 2014_15 and close to zero in 2010_11, 2016_17, 2017_18 and now in 2021_22. In contrast 2018_19 and 2020_21 are both among years with highest surface mass loss of the survey period.
The total mass loss due to surface mass balance over the 31-year survey period is ice volume of ~123 km^3, (average thinning of ~14 m) since 1991_92. This volume loss since 1991_92 amounts to ~4% of total ice volume.
In addition to surface melt, mass is lost due to calving, geothermal melting at the glacier bed and melt from frictional energy due to ice deformation and sliding. This is estimated to be close to 0.21 $m_{we}a^{-1}$ for Vatnajökull and amounts to ~57 km^3 of ice in the survey period, leading to an estimation of the (Jóhannesson, T., Pálmason, B., Hjartarson, Á., Jarosch, A., Magnússon, E., Belart,J., et al. (2020). Non-surface mass balance of glaciers in Iceland. J. Glaciol. 66, 685–697. doi:10.1017/jog.2020.37).

Glacier surface meltwater runoff in summer 2021 (estimated from summer surface balance only, summer rain and snow that falls and melts during summer, calving and geothermal and internal melting, is not included):
to Tungnaá 104% of the average, 90% of the average to Kaldakvísl, 84% of the average to Jökulsá á Fjöllum, 91% of the average to Hálslón, 93% to Jökulsá í Fljótsdal and 96% to Jökulsá á Breiðamerkursandi.
(Averages refer to the survey period of each outlet.)
Surface velocity measurements suggest that Dyngjujökull is in the first phase of a surge and may complete a surge cycle within the next few years.

Surface mass balance summary 2021_22:

B_w = 15.65 km^3_{we}
B_s = -16.27 km^3_{we}
B_n = -0.62 km^3_{we}
AAR = 60%

Specific Values:

b_w = 2.05 m_{we}
b_s = -2.13 m_{we}
b_n = -0.08 m_{we}

Appendix A: Surface mass balance at measurement sites 2021_22.

b_w: specific winter balance, **b_s**: specific summer balance, **b_n**: specific net balance,
l_a: new snow in autumn (all in water equivalent).

Site	Position				Elevation	Date	Date	b_w	b_s	b_n	la
	Latitude		Longite		(m a.s.l.)	in spring	in autumn	(m)	(m)	(m)	(m)
B09-22	64	44,6433	16	6,1125	721,2	20220503	20221017	0,090	-5,022	-4,932	0,007
B10-22	64	43,6831	16	6,7045	763,8	20220504	20221017	0,575	-5,300	-4,725	0,018
B11-22	64	40,9448	16	10,4791	946,3	20220503	20221017	1,090	-3,565	-2,475	0,147
B12-22	64	38,2696	16	14,1619	1078,1	20220503	20221017	1,469	-2,666	-1,197	0,193
B13-22	64	34,5757	16	19,6327	1222,1	20220503	20221017	1,757	-1,553	0,204	0,200
B14-22	64	31,6458	16	24,7058	1323,1	20220503	20221017	2,131	-1,117	1,014	0,144
B15-22	64	28,5072	16	30,0320	1405,4	20220503	20221017	2,864	-1,016	1,848	0,133
B16-22	64	24,1244	16	40,8961	1529,6	20220505	20221017	2,915	-0,161	2,754	0,060
B17-22	64	36,7343	16	28,7875	1217,1	20220503	20221017	1,602	-1,488	0,114	0,235
Br1-22	64	5,9599	16	19,8222	89,0	20220501	20221017	-1,450	-7,280	-8,730	0,000
Br2-22	64	6,3568	16	22,5289	164,1	20220330		-1,060			
Br3-22	64	8,4240	16	23,9858	357,8	20220330		-0,620			
Br7-22	64	22,1447	16	16,9173	1246,2	20220503	20221017	2,670	-1,212	1,458	0,147
B07-22	64	25,7932	16	17,4763	1359,1	20220503	20221017	2,256	-1,182	1,074	0,196
BB0-22	64	22,7047	16	5,0558	1518,4	20220503	20221017	3,375	-1,460	1,915	0,133
Bru-22	64	39,7478	15	56,5425	892,9	20220503	20221017	1,378	-3,502	-2,124	0,035
Bud-22	64	35,9889	15	59,8736	1137,6	20220503	20221017	1,762	-1,789	-0,027	0,224
B18-22	64	31,5680	16	0,1202	1316,2	20220503	20221017	2,428	-0,676	1,752	0,263
B19-22	64	27,9925	15	55,9770	1439,8	20220503	20221017	3,290	-0,392	2,898	0,200
D01-22	64	48,0778	16	50,1525	820,7	20220505	20220000	0,075			0,000
D05-22	64	42,2267	16	54,6804	1205,8	20220505	20221018	1,428	-1,770	-0,342	0,196
D07-22	64	38,2848	16	59,2567	1378,7	20220505	20221018	1,902	-1,452	0,450	0,263
D09-22	64	31,7835	17	0,6030	1589,1	20220505	20221018	2,230	-0,502	1,728	0,280
D12-22	64	28,9709	17	0,1827	1651,3	20220506	20221018	2,553	-0,429	2,124	0,203
E01-22	64	40,6437	15	34,8284	754,9	20220504	20221017	1,020	-5,673	-4,653	0,018
E02-22	64	39,1235	15	36,0032	949,7	20220504	20221017	1,096	-4,255	-3,159	0,070
E03-22	64	36,6526	15	36,9110	1188,4	20220504	20221017	2,789	-1,655	1,134	0,165
E04-22	64	34,9573	15	37,1404	1288,2	20220504	20221017	2,977	-0,877	2,100	0,196
K01-22	64	35,1734	17	51,8649	1040,1	20220507	20221018	1,003	-4,054	-3,051	0,046
K02-22	64	34,8076	17	49,6942	1168,5	20220507	20221018	1,425	-2,766	-1,341	0,063
K03-22	64	34,2400	17	46,4038	1292,5	20220507	20221018	1,833	-1,896	-0,063	0,133
K04-22	64	33,2148	17	42,2512	1487,2	20220507	20221018	2,048	-1,202	0,846	0,175
K05-22	64	33,4399	17	35,4737	1679,2	20220506	20221018	2,368	-0,208	2,160	0,175
K06-22	64	38,3496	17	31,3011	1946,2	20220506	20221018	2,773	0,107	2,880	0,350
K07-22	64	29,1150	17	42,0247	1532,8	20220507	20221018	2,136	-1,128	1,008	0,133
S01-22	64	7,0017	17	49,9702	704,1	20220507	20221018	0,607	-5,152	-4,545	0,000
S02-22	64	12,1619	17	48,9804	1001,4	20220507	20221018	1,972	-3,709	-1,737	0,000
S04-22	64	16,1786	17	48,1880	1158,4	20220507	20221018	1,994	-3,065	-1,071	0,063
S05-22	64	20,5148	17	33,9957	1453,0	20220507	20221018	2,845	-1,760	1,085	0,154
Haab-22	64	20,9606	17	24,1195	1731,9	20220507	20221018	2,856	-0,060	2,796	0,168
T01-22	64	19,1575	18	6,5226	769,0	20220507	20221027	0,692	-6,272	-5,580	0,000
T02-22	64	19,4778	18	4,5409	886,2	20220507	20221018	0,651	-4,962	-4,311	0,000
T03-22	64	20,2047	17	58,5797	1065,6	20220507	20221018	1,071	-3,681	-2,610	0,000

T04-22	64	21,331	17	51,515	1222	20220507	20221018	2,304	-2,943	-0,639	0,05
T05-22	64	22,269	17	43,007	1347	20220507	20221018	2,38	-2,667	-0,287	0,12
T06-22	64	24,26	17	36,514	1470	20220507	20221018	2,664	-2,04	0,624	0,12
T07-22	64	25,294	17	31,213	1565	20220508	20221018	2,56	-1,444	1,116	0,18
T08-22	64	26,296	17	27,756	1638	20220508	20221018	2,736	-1,068	1,668	0,12
Bor-22	64	24,942	17	20,156	1411	20220527	20221019	2,878	-2,17	0,708	0,16
Borth-22	64	24,996	17	19,194	1410	20220506	20221019	2,67	-2,088	0,582	0,16
G02-22	64	26,858	17	17,73	1568	20220506	20221018	2,408	-1,274	1,134	0,14
G03-22	64	28,44	17	16,329	1662	20220506	20221018	2,472	-0,594	1,878	0,14
G04-22	64	30,02	17	15,039	1691	20220506	20221018	2,78	-0,392	2,388	0,18
G01-22	64	33,96	17	24,936	1762	20220506	20221018	2,426	0,178	2,604	0,19
Skf00-22	64	15,459	15	54,065	949,4	20220502		3,524			0,25
Hof01-22	64	32,342	15	35,817	1143	20220504	20221017	2,824	-0,394	2,43	0,11
Skf01-22	64	18,017	16	5,0216	1285	20220502	20221017	3,621	-1,464	2,157	0,12
Fl01-22	64	26,161	15	55,623	1348	20220503	20221017	3,312	-0,594	2,718	0,15
Ske02-22	64	15,912	17	0,0631	1181	20220505	20221019	2,828	-2,42	0,408	0,04
Ske03-22	64	18,058	16	56,158	1301	20220505	20221019	2,431	-1,321	1,11	0,14
Ske04-22	64	20,147	16	51,805	1402	20220505	20221019	3,01	-1,276	1,734	0,14
Ske05-22	64	22,237	16	47,232	1474	20220505	20221019	2,679	-0,873	1,806	0,15
Oer01-22	64	59,861	16	39,002	1828	20220604		6,9			
E08-22	64	39,717	15	23,847	951,1	20220504	20221017	1,709	-3,365	-1,656	0,04
E07-22	64	38,411	15	24,693	1071	20220504	20221017	2,21	-3,227	-1,017	0,19
Herm-22	64	7,008	16	41,997	1299	20220604	20221020	3,32	-2	1,32	0,12
Kværk-22	64	38,653	16	40,526	1823	20220602	20221020	2,25	0,066	2,316	0,49

Appendix B: Surface mass balance distribution by elevation in 2021_22.

ΔS : area in elevation range, ∑ΔS: cumulative area above given elevation, b_w: specific winter balance, b_s: specific summer balance. b_n: specific winter balance, ΔB_w : winter balance at a given elevation range, $\sum\Delta B_w$: cumulative winter balance above given elevation, ΔB_s summer balance at a given elevation range, $\sum\Delta B_s$: cumulative summer balance above given elevation, ΔB_n: net annual balance in a given elevation range, $\sum B_n$: cumulative net annual balance above given elevation.

Vatnajökull

Elevation (m a.s.l.)			ΔS (km^2)	∑ΔS (km^2)	b_w (mm)	b_s (mm)	b_n (mm)	ΔB_w ($10^6 m^3$)	$\sum\Delta B_w$ ($10^6 m^3$)	ΔB_s ($10^6 m^3$)	$\sum\Delta B_s$ ($10^6 m^3$)	ΔB_n ($10^6 m^3$)	$\sum B_n$ ($10^6 m^3$)
2000	2050	2025	0,3	0,3	6809	554	7364	2,4	2,4	0,2	0,2	2,6	2,6
1950	2000	1975	7,0	7,3	3523	252	3775	24,6	27,0	1,8	2,0	26,4	29,0
1900	1950	1925	41,4	48,7	2894	247	3141	120,0	146,9	10,2	12,2	130,2	159,1
1850	1900	1875	43,9	92,6	3171	210	3382	139,3	286,2	9,2	21,4	148,5	307,6
1800	1850	1825	45,6	138,2	3542	155	3698	161,4	447,7	7,1	28,5	168,5	476,2
1750	1800	1775	54,3	192,5	3101	63	3164	168,5	616,2	3,4	32,0	171,9	648,2
1700	1750	1725	113,3	305,8	2790	-104	2685	316,0	932,3	-11,8	20,1	304,2	952,4
1650	1700	1675	215,9	521,7	2735	-409	2325	590,6	1522,9	-88,5	-68,4	502,1	1454,5
1600	1650	1625	370,9	892,6	2655	-512	2143	984,9	2507,8	-190,0	-258,4	794,9	2249,4
1550	1600	1575	357,2	1249,8	2638	-627	2011	942,4	3450,2	-224,1	-482,5	718,3	2967,7
1500	1550	1525	422,0	1671,8	2654	-772	1881	1120,3	4570,5	-326,1	-808,6	794,2	3761,9
1450	1500	1475	453,2	2125,0	2706	-1029	1676	1226,4	5796,9	-466,5	-1275,1	759,9	4521,8
1400	1450	1425	504,6	2629,6	2776	-1153	1622	1401,1	7198,0	-582,2	-1857,3	818,9	5340,7
1350	1400	1375	544,4	3174,0	2681	-1240	1440	1459,7	8657,7	-675,4	-2532,7	784,3	6125,0
1300	1350	1325	535,3	3709,3	2566	-1383	1183	1374,1	10031,8	-740,6	-3273,3	633,5	6758,5
1250	1300	1275	501,3	4210,6	2468	-1548	920	1237,5	11269,3	-776,4	-4049,7	461,1	7219,6
1200	1250	1225	440,4	4651,0	2278	-1863	415	1003,6	12273,0	-820,8	-4870,4	182,8	7402,6
1150	1200	1175	391,2	5042,2	2066	-2195	-128	808,4	13081,4	-858,8	-5729,2	-50,4	7352,2
1100	1150	1125	347,9	5390,1	1874	-2547	-673	652,0	13733,4	-886,2	-6615,5	-234,2	7117,9
1050	1100	1075	300,4	5690,5	1683	-2917	-1233	505,7	14239,0	-876,2	-7491,7	-370,5	6747,3
1000	1050	1025	281,7	5972,2	1495	-3251	-1756	421,2	14660,2	-915,9	-8407,6	-494,7	6252,6
950	1000	975	252,6	6224,8	1358	-3531	-2173	343,2	15003,4	-892,2	-9299,8	-549,0	5703,6
900	950	925	216,6	6441,4	1208	-3840	-2632	261,8	15265,3	-832,0	-10131,8	-570,2	5133,5
850	900	875	188,6	6630,0	1044	-4156	-3111	197,1	15462,3	-784,0	-10915,8	-586,9	4546,5
800	850	825	171,6	6801,6	901	-4457	-3556	154,7	15617,0	-765,0	-11680,8	-610,3	3936,2
750	800	775	150,0	6951,6	767	-4688	-3921	115,0	15732,1	-703,1	-12383,9	-588,1	3348,2
700	750	725	120,6	7072,2	637	-4862	-4224	76,9	15809,0	-586,2	-12970,1	-509,3	2838,9
650	700	675	100,4	7172,6	517	-4905	-4388	52,0	15860,9	-492,7	-13462,8	-440,7	2398,1
600	650	625	60,0	7232,6	404	-4881	-4476	24,3	15885,2	-292,8	-13755,5	-268,5	2129,7
550	600	575	58,4	7291,0	194	-5006	-4812	11,3	15896,6	-292,5	-14048,0	-281,2	1848,6
500	550	525	46,9	7337,9	13	-5236	-5222	0,6	15897,2	-245,6	-14293,7	-245,0	1603,5
450	500	475	36,1	7374,0	-153	-5498	-5651	-5,6	15891,7	-198,8	-14492,4	-204,4	1399,3
400	450	425	40,4	7414,4	-356	-5752	-6109	-14,4	15877,2	-232,5	-14725,0	-246,9	1152,2
350	400	375	38,3	7452,7	-558	-6068	-6626	-21,4	15855,8	-232,4	-14957,4	-253,8	898,4
300	350	325	34,3	7487,0	-765	-6356	-7122	-26,2	15829,6	-217,9	-15175,3	-244,1	654,3
250	300	275	32,5	7519,5	-912	-6569	-7481	-29,7	15799,9	-213,8	-15389,1	-243,5	410,8
200	250	225	30,7	7550,2	-1038	-6786	-7825	-31,9	15768,0	-208,2	-15597,2	-240,1	170,8
150	200	175	30,7	7580,9	-1163	-7070	-8233	-35,8	15732,3	-217,3	-15814,5	-253,1	-82,2
100	150	125	25,9	7606,8	-1312	-7391	-8704	-34,0	15698,3	-191,1	-16005,6	-225,1	-307,3
50	100	75	18,0	7624,8	-1450	-7609	-9059	-26,1	15672,2	-137,1	-16142,7	-163,2	-470,5
0	50	25	16,3	7641,1	-1636	-7797	-9433	-26,6	15645,6	-126,8	-16269,5	-153,4	-623,9

Tungnaárjökull

Elevation (m a.s.l.)			ΔS (km^2)	∑ΔS (km^2)	b_w (mm)	b_s (mm)	b_n (mm)	ΔB_w ($10^6 m^3$)	$\sum\Delta B_w$ ($10^6 m^3$)	ΔB_s ($10^6 m^3$)	$\sum\Delta B_s$ ($10^6 m^3$)	ΔB_n ($10^6 m^3$)	$\sum B_n$ ($10^6 m^3$)
1650	1700	1675	1,7	1,7	2751	-918	1833	4,6	4,6	-1,5	-1,5	3,0	3,0
1600	1650	1625	12,2	13,9	2734	-1070	1664	33,3	37,8	-13,0	-14,6	20,3	23,3
1550	1600	1575	16,4	30,3	2671	-1298	1373	43,7	81,6	-21,2	-35,8	22,5	45,8
1500	1550	1525	15,9	46,2	2627	-1611	1015	41,8	123,3	-25,6	-61,4	16,1	61,9
1450	1500	1475	18,4	64,6	2572	-1915	657	47,3	170,6	-35,2	-96,6	12,1	74,0
1400	1450	1425	23,2	87,8	2543	-2242	300	58,9	229,5	-51,9	-148,6	7,0	81,0
1350	1400	1375	21,2	109,0	2466	-2488	-21	52,3	281,8	-52,7	-201,3	-0,5	80,5
1300	1350	1325	27,2	136,2	2396	-2669	-272	65,2	347,0	-72,6	-273,9	-7,4	73,1
1250	1300	1275	20,7	156,9	2352	-2791	-438	48,6	395,6	-57,7	-331,6	-9,1	64,0
1200	1250	1225	22,6	179,5	2196	-2947	-751	49,5	445,1	-66,5	-398,0	-16,9	47,1
1150	1200	1175	20,8	200,3	1837	-3161	-1324	38,3	483,4	-65,9	-463,9	-27,6	19,5
1100	1150	1125	18,0	218,3	1403	-3435	-2032	25,2	508,6	-61,7	-525,6	-36,5	-17,0
1050	1100	1075	17,3	235,6	1083	-3716	-2632	18,7	527,3	-64,2	-589,8	-45,5	-62,5
1000	1050	1025	16,7	252,3	901	-4032	-3131	15,1	542,4	-67,4	-657,3	-52,4	-114,9
950	1000	975	16,1	268,4	829	-4374	-3544	13,4	555,8	-70,5	-727,8	-57,1	-172,0
900	950	925	16,3	284,7	792	-4731	-3939	12,9	568,7	-77,2	-805,0	-64,3	-236,2
850	900	875	12,4	297,1	763	-5119	-4356	9,5	578,2	-63,6	-868,6	-54,1	-290,4
800	850	825	12,8	309,9	741	-5490	-4748	9,5	587,7	-70,2	-938,8	-60,7	-351,1
750	800	775	9,8	319,7	704	-5853	-5149	6,9	594,6	-57,5	-996,4	-50,6	-401,8
700	750	725	6,3	326,0	643	-6049	-5406	4,1	598,7	-38,2	-1034,6	-34,2	-435,9
650	700	675	1,4	327,4	586	-6148	-5561	0,8	599,5	-8,4	-1043,0	-7,6	-443,5

Sylgjujökull

Elevation (m a.s.l.)			ΔS (km^2)	∑ΔS (km^2)	b_w (mm)	b_s (mm)	b_n (mm)	ΔB_w ($10^6 m^3$)	$\sum\Delta B_w$ ($10^6 m^3$)	ΔB_s ($10^6 m^3$)	$\sum\Delta B_s$ ($10^6 m^3$)	ΔB_n ($10^6 m^3$)	$\sum B_n$ ($10^6 m^3$)
1600	1650	1625	1,4	1,4	2509	-867	1641	3,4	3,4	-1,2	-1,2	2,2	2,2
1550	1600	1575	5,0	6,4	2471	-1057	1413	12,4	15,8	-5,3	-6,5	7,1	9,3
1500	1550	1525	18,7	25,1	2279	-1212	1066	42,6	58,4	-22,7	-29,1	19,9	29,3
1450	1500	1475	13,7	38,8	2243	-1425	817	30,7	89,1	-19,5	-48,7	11,2	40,5
1400	1450	1425	8,2	47,0	2290	-1900	390	18,9	108,0	-15,7	-64,3	3,2	43,7
1350	1400	1375	5,6	52,6	2312	-2268	44	13,0	121,0	-12,7	-77,1	0,2	43,9
1300	1350	1325	5,2	57,8	2290	-2579	-289	11,8	132,8	-13,3	-90,4	-1,5	42,4
1250	1300	1275	9,8	67,6	2201	-2771	-569	21,5	154,3	-27,0	-117,4	-5,6	36,9
1200	1250	1225	11,6	79,2	2010	-2935	-925	23,4	177,7	-34,2	-151,6	-10,8	26,1
1150	1200	1175	13,1	92,3	1702	-3151	-1449	22,3	200,0	-41,3	-192,9	-19,0	7,1
1100	1150	1125	12,3	104,6	1345	-3432	-2086	16,5	216,5	-42,1	-235,0	-25,6	-18,5
1050	1100	1075	11,4	116,0	1095	-3736	-2640	12,5	229,0	-42,6	-277,6	-30,1	-48,6
1000	1050	1025	10,3	126,3	877	-4187	-3309	9,0	238,0	-43,1	-320,7	-34,1	-82,7
950	1000	975	3,2	129,5	749	-4350	-3600	2,4	240,4	-14,0	-334,7	-11,6	-94,2
900	950	925	1,2	130,7	678	-4512	-3834	0,8	241,3	-5,5	-340,2	-4,7	-98,9

Köldukvíslarjökul

Elevation (m a.s.l.)			ΔS (km^2)	∑ΔS (km^2)	b_w (mm)	b_s (mm)	b_n (mm)	ΔB_w ($10^6 m^3$)	$\sum\Delta B_w$ ($10^6 m^3$)	ΔB_s ($10^6 m^3$)	$\sum\Delta B_s$ ($10^6 m^3$)	ΔB_n ($10^6 m^3$)	$\sum B_n$ ($10^6 m^3$)
1950	2000	1975	0,7	0,7	2678	190	2868	1,8	1,8	0,1	0,1	1,9	1,9
1900	1950	1925	13,8	14,5	2616	269	2885	36,2	37,9	3,7	3,9	39,9	41,8
1850	1900	1875	6,5	21,0	2508	217	2726	16,4	54,3	1,4	5,3	17,8	59,6
1800	1850	1825	6,1	27,1	2459	131	2591	15,0	69,3	0,8	6,1	15,8	75,4
1750	1800	1775	10,1	37,2	2468	101	2569	24,8	94,1	1,0	7,1	25,8	101,2
1700	1750	1725	17,2	54,4	2414	-70	2344	41,6	135,6	-1,2	5,9	40,3	141,5
1650	1700	1675	16,0	70,4	2337	-320	2017	37,4	173,0	-5,1	0,8	32,3	173,8
1600	1650	1625	14,2	84,6	2258	-588	1669	32,0	205,1	-8,3	-7,6	23,7	197,5
1550	1600	1575	18,6	103,2	2182	-850	1331	40,5	245,6	-15,8	-23,4	24,7	222,2
1500	1550	1525	19,9	123,1	2094	-1090	1004	41,7	287,3	-21,7	-45,1	20,0	242,2
1450	1500	1475	19,3	142,4	2047	-1216	830	39,5	326,8	-23,5	-68,5	16,0	258,2
1400	1450	1425	15,0	157,4	1991	-1337	654	29,8	356,5	-20,0	-88,5	9,8	268,0
1350	1400	1375	14,8	172,2	1920	-1478	442	28,5	385,0	-21,9	-110,5	6,6	274,6
1300	1350	1325	16,5	188,7	1841	-1673	168	30,4	415,5	-27,7	-138,1	2,8	277,3
1250	1300	1275	17,5	206,2	1730	-1979	-249	30,3	445,8	-34,7	-172,8	-4,4	273,0
1200	1250	1225	16,8	223,0	1575	-2416	-841	26,5	472,3	-40,7	-213,5	-14,2	258,8
1150	1200	1175	16,1	239,1	1417	-2884	-1467	22,8	495,1	-46,5	-260,0	-23,6	235,2
1100	1150	1125	14,3	253,4	1275	-3324	-2048	18,2	513,4	-47,5	-307,4	-29,3	205,9
1050	1100	1075	12,9	266,3	1163	-3707	-2543	15,0	528,3	-47,6	-355,1	-32,7	173,2
1000	1050	1025	10,3	276,6	1070	-4065	-2994	11,0	539,4	-41,9	-397,0	-30,9	142,4
950	1000	975	7,7	284,3	964	-4359	-3395	7,4	546,8	-33,6	-430,6	-26,1	116,2
900	950	925	1,5	285,8	808	-4538	-3730	1,3	548,0	-7,0	-437,6	-5,8	110,4

Dyngjujökull

Elevation (m a.s.l.)			ΔS (km^2)	∑ΔS (km^2)	b_w (mm)	b_s (mm)	b_n (mm)	ΔB_w ($10^6 m^3$)	$\sum\Delta B_w$ ($10^6 m^3$)	ΔB_s ($10^6 m^3$)	$\sum\Delta B_s$ ($10^6 m^3$)	ΔB_n ($10^6 m^3$)	$\sum B_n$ ($10^6 m^3$)
1950	2000	1975	2,4	2,4	2600	163	2763	6,2	6,2	0,4	0,4	6,6	6,6
1900	1950	1925	17,7	20,1	2671	224	2896	47,4	53,6	4,0	4,4	51,4	57,9
1850	1900	1875	21,7	41,8	2614	183	2797	56,6	110,2	4,0	8,4	60,6	118,6
1800	1850	1825	13,2	55,0	2554	85	2639	33,6	143,8	1,1	9,5	34,8	153,3
1750	1800	1775	15,5	70,5	2537	18	2556	39,2	183,1	0,3	9,8	39,5	192,8
1700	1750	1725	32,4	102,9	2565	-107	2457	83,2	266,3	-3,5	6,3	79,7	272,6
1650	1700	1675	73,9	176,8	2611	-322	2288	193,0	459,3	-23,8	-17,5	169,2	441,8
1600	1650	1625	120,2	297,0	2425	-421	2003	291,6	750,9	-50,7	-68,3	240,9	682,7
1550	1600	1575	95,9	392,9	2227	-540	1687	213,6	964,6	-51,8	-120,1	161,8	844,5
1500	1550	1525	87,5	480,4	2133	-747	1385	186,7	1151,3	-65,4	-185,5	121,3	965,8
1450	1500	1475	73,0	553,4	2076	-1006	1070	151,6	1302,9	-73,5	-259,0	78,1	1043,9
1400	1450	1425	60,5	613,9	2022	-1266	755	122,3	1425,2	-76,6	-335,6	45,7	1089,6
1350	1400	1375	48,0	661,9	1929	-1431	497	92,7	1517,9	-68,8	-404,4	23,9	1113,5
1300	1350	1325	36,5	698,4	1811	-1497	314	66,1	1584,1	-54,7	-459,1	11,5	1125,0
1250	1300	1275	39,6	738,0	1677	-1553	123	66,4	1650,5	-61,5	-520,6	4,9	1129,9
1200	1250	1225	44,0	782,0	1494	-1682	-187	65,8	1716,3	-74,1	-594,7	-8,3	1121,6
1150	1200	1175	44,4	826,4	1271	-2015	-744	56,4	1772,7	-89,5	-684,2	-33,0	1088,6
1100	1150	1125	42,3	868,7	1053	-2467	-1413	44,5	1817,3	-104,3	-788,4	-59,7	1028,9
1050	1100	1075	30,6	899,3	816	-2991	-2175	25,0	1842,3	-91,5	-880,0	-66,6	962,3
1000	1050	1025	30,9	930,2	616	-3476	-2859	19,0	1861,3	-107,3	-987,3	-88,3	874,0
950	1000	975	28,8	959,0	451	-3906	-3455	13,0	1874,3	-112,5	-1099,8	-99,5	774,5
900	950	925	24,2	983,2	323	-4257	-3933	7,8	1882,1	-103,0	-1202,7	-95,1	679,4
850	900	875	20,9	1004,1	218	-4629	-4410	4,6	1886,7	-96,8	-1299,5	-92,2	587,1
800	850	825	18,0	1022,1	128	-5000	-4872	2,3	1889,0	-89,8	-1389,4	-87,5	499,6
750	800	775	10,6	1032,7	64	-5264	-5200	0,7	1889,7	-56,0	-1445,3	-55,3	444,3
700	750	725	1,5	1034,2	33	-5371	-5338	0,0	1889,7	-8,2	-1453,5	-8,2	436,2

Brúarjökull

Elevation (m a.s.l.)			ΔS (km^2)	∑ΔS (km^2)	b_w (mm)	b_s (mm)	b_n (mm)	ΔB_w ($10^6 m^3$)	$\sum\Delta B_w$ ($10^6 m^3$)	ΔB_s ($10^6 m^3$)	$\sum\Delta B_s$ ($10^6 m^3$)	ΔB_n ($10^6 m^3$)	$\sum B_n$ ($10^6 m^3$)
1900	1950	1925	0,0	0,0	2532	-23	2508	0,0	0,0	0,0	0,0	0,0	0,0
1850	1900	1875	1,2	1,2	2513	7	2521	3,0	3,0	0,0	0,0	3,0	3,1
1800	1850	1825	4,4	5,6	2430	33	2463	10,7	13,8	0,1	0,2	10,9	13,9
1750	1800	1775	2,8	8,4	2522	-82	2439	7,2	21,0	-0,2	0,0	7,0	20,9
1700	1750	1725	3,9	12,3	2582	-202	2379	10,0	31,0	-0,8	-0,9	9,3	30,2
1650	1700	1675	5,5	17,8	2605	-282	2322	14,3	45,3	-1,5	-2,4	12,7	42,9
1600	1650	1625	51,0	68,8	2657	-433	2224	135,7	180,9	-22,1	-24,5	113,5	156,4
1550	1600	1575	47,4	116,2	2843	-399	2443	134,7	315,6	-18,9	-43,4	115,7	272,2
1500	1550	1525	73,6	189,8	2923	-359	2564	215,3	530,8	-26,5	-69,9	188,8	460,9
1450	1500	1475	80,3	270,1	2938	-642	2296	235,9	766,7	-51,6	-121,5	184,3	645,3
1400	1450	1425	113,9	384,0	2944	-800	2144	335,3	1102,0	-91,1	-212,6	244,1	889,4
1350	1400	1375	158,6	542,6	2630	-931	1698	417,2	1519,2	-147,7	-360,3	269,5	1158,8
1300	1350	1325	148,4	691,0	2347	-1012	1334	348,4	1867,5	-150,3	-510,6	198,1	1357,0
1250	1300	1275	139,1	830,1	2201	-1190	1010	306,1	2173,7	-165,6	-676,2	140,5	1497,5
1200	1250	1225	117,3	947,4	1988	-1464	524	233,2	2406,9	-171,8	-848,0	61,5	1558,9
1150	1200	1175	100,0	1047,4	1793	-1773	20	179,3	2586,3	-177,3	-1025,3	2,0	1561,0
1100	1150	1125	80,4	1127,8	1624	-2175	-550	130,7	2717,0	-175,0	-1200,3	-44,3	1516,7
1050	1100	1075	65,6	1193,4	1470	-2584	-1114	96,5	2813,4	-169,6	-1369,9	-73,1	1443,6
1000	1050	1025	57,9	1251,3	1314	-2944	-1630	76,1	2889,5	-170,5	-1540,4	-94,4	1349,2
950	1000	975	52,6	1303,9	1163	-3320	-2157	61,2	2950,7	-174,6	-1715,0	-113,4	1235,7
900	950	925	44,2	1348,1	1029	-3771	-2741	45,5	2996,2	-166,6	-1881,5	-121,1	1114,6
850	900	875	39,3	1387,4	902	-4253	-3351	35,5	3031,7	-167,2	-2048,8	-131,7	982,9
800	850	825	35,0	1422,4	786	-4687	-3900	27,5	3059,2	-163,9	-2212,7	-136,4	846,5
750	800	775	32,1	1454,5	597	-5070	-4473	19,2	3078,4	-162,8	-2375,5	-143,6	702,9
700	750	725	25,6	1480,1	297	-5318	-5021	7,6	3086,0	-135,9	-2511,4	-128,3	574,6
650	700	675	11,0	1491,1	110	-5520	-5410	1,2	3087,2	-60,8	-2572,2	-59,6	515,0
600	650	625	0,3	1491,4	10	-5610	-5599	0,0	3087,2	-1,9	-2574,0	-1,8	513,1

Eyjabakkajökull

Elevation (m a.s.l.)			ΔS (km^2)	∑ΔS (km^2)	b_w (mm)	b_s (mm)	b_n (mm)	ΔB_w ($10^6 m^3$)	$\sum\Delta B_w$ ($10^6 m^3$)	ΔB_s ($10^6 m^3$)	$\sum\Delta B_s$ ($10^6 m^3$)	ΔB_n ($10^6 m^3$)	$\sum B_n$ ($10^6 m^3$)
1550	1600	1575	0,0	0,0	3351	-436	2914	0,1	0,1	0,0	0,0	0,0	0,0
1500	1550	1525	0,0	0,0	3335	-442	2892	0,3	0,4	0,0	0,0	0,3	0,3
1450	1500	1475	1,1	1,1	3322	-471	2851	3,8	4,2	-0,5	-0,6	3,3	3,6
1400	1450	1425	2,0	3,1	3299	-531	2767	6,7	10,9	-1,1	-1,7	5,6	9,2
1350	1400	1375	2,5	5,6	3263	-645	2617	8,3	19,2	-1,6	-3,3	6,6	15,9
1300	1350	1325	4,3	9,9	3232	-815	2416	13,8	33,0	-3,5	-6,8	10,3	26,2
1250	1300	1275	13,5	23,4	3059	-1112	1946	41,2	74,2	-15,0	-21,8	26,2	52,4
1200	1250	1225	12,9	36,3	2938	-1476	1462	37,8	112,0	-19,0	-40,8	18,8	71,2
1150	1200	1175	14,0	50,3	2555	-1861	694	35,7	147,7	-26,0	-66,8	9,7	80,9
1100	1150	1125	11,5	61,8	2020	-2306	-285	23,3	171,0	-26,6	-93,4	-3,3	77,6
1050	1100	1075	10,0	71,8	1547	-2868	-1321	15,4	186,4	-28,6	-121,9	-13,2	64,5
1000	1050	1025	9,3	81,1	1340	-3400	-2060	12,5	198,9	-31,7	-153,6	-19,2	45,3
950	1000	975	7,5	88,6	1207	-3869	-2662	9,1	207,9	-29,0	-182,6	-20,0	25,3
900	950	925	5,0	93,6	1125	-4317	-3192	5,6	213,6	-21,5	-204,2	-15,9	9,4
850	900	875	3,8	97,4	1084	-4658	-3574	4,2	217,7	-17,8	-222,0	-13,7	-4,3
800	850	825	2,9	100,3	1071	-5033	-3961	3,1	220,8	-14,5	-236,5	-11,5	-15,7
750	800	775	1,9	102,2	1048	-5616	-4568	2,0	222,8	-10,7	-247,3	-8,7	-24,5
700	750	725	1,7	103,9	964	-6175	-5211	1,6	224,4	-10,5	-257,8	-8,9	-33,3
650	700	675	0,7	104,6	841	-6685	-5844	0,6	225,1	-4,9	-262,7	-4,3	-37,6

Hoffellsjökull

Elevation (m a.s.l.)			ΔS (km^2)	∑ΔS (km^2)	b_w (mm)	b_s (mm)	b_n (mm)	ΔB_w ($10^6 m^3$)	$\sum\Delta B_w$ ($10^6 m^3$)	ΔB_s ($10^6 m^3$)	$\sum\Delta B_s$ ($10^6 m^3$)	ΔB_n ($10^6 m^3$)	$\sum B_n$ ($10^6 m^3$)
1450	1500	1475	1,2	1,2	3332	-441	2890	3,9	3,9	-0,5	-0,5	3,4	3,4
1400	1450	1425	7,2	8,4	3332	-465	2867	24,1	28,0	-3,4	-3,9	20,7	24,1
1350	1400	1375	10,0	18,4	3273	-564	2708	32,8	60,8	-5,7	-9,5	27,2	51,2
1300	1350	1325	16,3	34,7	3203	-762	2440	52,2	113,0	-12,4	-22,0	39,8	91,0
1250	1300	1275	34,9	69,6	3073	-1113	1959	107,2	220,2	-38,8	-60,8	68,3	159,3
1200	1250	1225	25,6	95,2	3026	-1449	1577	77,4	297,5	-37,0	-97,9	40,3	199,7
1150	1200	1175	17,9	113,1	2906	-1875	1031	52,0	349,5	-33,6	-131,4	18,4	218,1
1100	1150	1125	16,7	129,8	2700	-2300	400	45,1	394,6	-38,4	-169,8	6,7	224,8
1050	1100	1075	12,5	142,3	2403	-2704	-300	30,0	424,6	-33,8	-203,6	-3,8	221,0
1000	1050	1025	9,6	151,9	2159	-2943	-783	20,8	445,4	-28,3	-231,9	-7,5	213,5
950	1000	975	8,6	160,5	1907	-3133	-1225	16,4	461,8	-26,9	-258,8	-10,5	203,0
900	950	925	6,4	166,9	1624	-3327	-1703	10,3	472,1	-21,1	-279,9	-10,8	192,2
850	900	875	4,2	171,1	1362	-3539	-2176	5,8	477,9	-14,9	-294,9	-9,2	183,0
800	850	825	3,2	174,3	1220	-3672	-2452	4,0	481,8	-11,9	-306,8	-7,9	175,0
750	800	775	3,3	177,6	1089	-3791	-2701	3,6	485,4	-12,4	-319,1	-8,8	166,2
700	750	725	3,0	180,6	844	-4129	-3285	2,5	487,9	-12,3	-331,5	-9,8	156,4
650	700	675	3,3	183,9	600	-4443	-3842	2,0	489,9	-14,5	-346,0	-12,6	143,8
600	650	625	2,4	186,3	377	-4654	-4276	0,9	490,8	-11,0	-357,0	-10,1	133,7
550	600	575	1,6	187,9	221	-4815	-4593	0,4	491,1	-7,7	-364,7	-7,3	126,4
500	550	525	1,5	189,4	58	-5009	-4950	0,0	491,2	-7,3	-372,0	-7,2	119,2
450	500	475	0,9	190,3	-152	-5270	-5423	-0,1	491,1	-4,8	-376,8	-4,9	114,2
400	450	425	0,7	191,0	-337	-5547	-5885	-0,2	490,8	-4,1	-380,9	-4,4	109,9
350	400	375	0,7	191,7	-473	-5888	-6362	-0,3	490,5	-3,9	-384,9	-4,3	105,6
300	350	325	0,5	192,2	-585	-6155	-6740	-0,3	490,2	-3,1	-388,0	-3,4	102,2
250	300	275	0,7	192,9	-679	-6359	-7038	-0,5	489,7	-4,7	-392,7	-5,2	97,0
200	250	225	1,5	194,4	-784	-6582	-7367	-1,2	488,5	-10,0	-402,7	-11,2	85,8
150	200	175	2,3	196,7	-936	-6838	-7775	-2,2	486,3	-15,8	-418,5	-18,0	67,8
100	150	125	2,5	199,2	-1211	-7074	-8285	-3,0	483,3	-17,6	-436,1	-20,6	47,2
50	100	75	1,8	201,0	-1419	-7267	-8687	-2,6	480,7	-13,3	-449,4	-15,9	31,3
0	50	25	1,9	202,9	-1610	-7594	-9205	-3,0	477,7	-14,2	-463,6	-17,2	14,1

Breiðamerkurjökull

Elevation (m a.s.l.)			ΔS (km^2)	∑ΔS (km^2)	b_w (mm)	b_s (mm)	b_n (mm)	ΔB_w ($10^6 m^3$)	$\sum\Delta B_w$ ($10^6 m^3$)	ΔB_s ($10^6 m^3$)	$\sum\Delta B_s$ ($10^6 m^3$)	ΔB_n ($10^6 m^3$)	$\sum B_n$ ($10^6 m^3$)
1900	1950	1925	0,0	0,0	6713	504	7218	0,3	0,3	0,0	0,0	0,4	0,4
1850	1900	1875	0,4	0,4	6688	434	7123	2,5	2,9	0,2	0,2	2,7	3,1
1800	1850	1825	0,5	0,9	6572	321	6894	3,0	5,9	0,1	0,3	3,2	6,2
1750	1800	1775	0,9	1,8	6354	143	6498	5,7	11,6	0,1	0,5	5,8	12,0
1700	1750	1725	2,6	4,4	4796	-20	4776	12,7	24,3	0,0	0,4	12,7	24,7
1650	1700	1675	6,2	10,6	3708	-70	3637	22,8	47,1	-0,4	0,0	22,4	47,1
1600	1650	1625	17,6	28,2	3252	-75	3176	57,3	104,4	-1,3	-1,4	56,0	103,1
1550	1600	1575	26,2	54,4	3090	-216	2874	80,9	185,3	-5,7	-7,0	75,2	178,3
1500	1550	1525	31,9	86,3	3041	-507	2534	97,1	282,5	-16,2	-23,2	80,9	259,2
1450	1500	1475	46,3	132,6	3022	-744	2278	139,9	422,3	-34,4	-57,6	105,4	364,7
1400	1450	1425	57,9	190,5	2952	-964	1987	170,9	593,2	-55,8	-113,5	115,0	479,7
1350	1400	1375	88,5	279,0	2801	-1163	1638	248,0	841,2	-102,9	-216,4	145,0	624,7
1300	1350	1325	94,9	373,9	2753	-1337	1415	261,3	1102,5	-127,0	-343,4	134,3	759,1
1250	1300	1275	56,9	430,8	2694	-1473	1221	153,2	1255,7	-83,8	-427,1	69,5	828,5
1200	1250	1225	38,8	469,6	2583	-1639	943	100,3	1356,0	-63,7	-490,8	36,7	865,2
1150	1200	1175	30,7	500,3	2431	-1844	587	74,6	1430,6	-56,6	-547,4	18,0	883,2
1100	1150	1125	25,6	525,9	2272	-2059	213	58,2	1488,7	-52,7	-600,1	5,5	888,7
1050	1100	1075	21,4	547,3	2133	-2277	-144	45,7	1534,4	-48,8	-648,8	-3,1	885,6
1000	1050	1025	19,3	566,6	2011	-2500	-489	38,9	1573,3	-48,3	-697,2	-9,5	876,1
950	1000	975	21,0	587,6	1892	-2817	-924	39,7	1613,0	-59,1	-756,3	-19,4	856,7
900	950	925	22,4	610,0	1654	-3212	-1557	37,1	1650,1	-71,9	-828,2	-34,9	821,8
850	900	875	19,7	629,7	1329	-3559	-2229	26,1	1676,2	-70,0	-898,2	-43,8	778,0
800	850	825	20,4	650,1	1127	-3825	-2698	22,9	1699,1	-77,9	-976,1	-54,9	723,1
750	800	775	22,3	672,4	900	-4073	-3172	20,1	1719,2	-90,9	-1067,0	-70,8	652,3
700	750	725	17,4	689,8	706	-4214	-3508	12,3	1731,5	-73,2	-1140,2	-60,9	591,3
650	700	675	27,1	716,9	527	-4336	-3809	14,3	1745,8	-117,6	-1257,8	-103,3	488,0
600	650	625	23,9	740,8	385	-4569	-4183	9,2	1755,0	-109,0	-1366,8	-99,8	388,2
550	600	575	24,7	765,5	197	-4808	-4610	4,9	1759,9	-118,7	-1485,5	-113,8	274,4
500	550	525	15,9	781,4	3	-5063	-5060	0,0	1760,0	-80,3	-1565,9	-80,3	194,1
450	500	475	12,7	794,1	-163	-5326	-5489	-2,1	1757,9	-67,8	-1633,7	-69,9	124,2
400	450	425	16,3	810,4	-338	-5562	-5901	-5,5	1752,4	-90,7	-1724,3	-96,2	28,0
350	400	375	12,7	823,1	-519	-5819	-6338	-6,6	1745,8	-73,6	-1798,0	-80,2	-52,2
300	350	325	10,6	833,7	-673	-6073	-6746	-7,1	1738,7	-64,3	-1862,2	-71,4	-123,5
250	300	275	10,6	844,3	-843	-6340	-7184	-9,0	1729,7	-67,3	-1929,6	-76,3	-199,8
200	250	225	9,2	853,5	-1022	-6607	-7629	-9,4	1720,3	-60,5	-1990,1	-69,9	-269,7
150	200	175	9,7	863,2	-1193	-6887	-8080	-11,6	1708,7	-66,9	-2057,0	-78,5	-348,3
100	150	125	8,0	871,2	-1390	-7172	-8563	-11,1	1697,6	-57,4	-2114,4	-68,5	-416,8
50	100	75	5,3	876,5	-1547	-7415	-8963	-8,2	1689,4	-39,4	-2153,8	-47,6	-464,4
0	50	25	1,5	878,0	-1669	-7684	-9353	-2,4	1687,0	-11,2	-2165,0	-13,7	-478,0

Síðujökull

Elevation (m a.s.l.)			ΔS (km^2)	∑ΔS (km^2)	b_w (mm)	b_s (mm)	b_n (mm)	ΔB_w ($10^6 m^3$)	$\sum\Delta B_w$ ($10^6 m^3$)	ΔB_s ($10^6 m^3$)	$\sum\Delta B_s$ ($10^6 m^3$)	ΔB_n ($10^6 m^3$)	$\sum B_n$ ($10^6 m^3$)
1700	1750	1725	0,9	0,9	2835	-372	2463	2,5	2,5	-0,3	-0,3	2,2	2,2
1650	1700	1675	5,9	6,8	2825	-795	2030	16,7	19,2	-4,7	-5,0	12,0	14,2
1600	1650	1625	11,2	18,0	2822	-1023	1799	31,6	50,8	-11,4	-16,5	20,1	34,3
1550	1600	1575	11,5	29,5	2819	-1197	1621	32,4	83,2	-13,8	-30,2	18,6	52,9
1500	1550	1525	21,3	50,8	2829	-1358	1471	60,4	143,6	-29,0	-59,2	31,4	84,3
1450	1500	1475	38,2	89,0	2833	-1695	1137	108,2	251,8	-64,8	-124,0	43,4	127,8
1400	1450	1425	24,9	113,9	2761	-2069	691	68,7	320,5	-51,5	-175,5	17,2	145,0
1350	1400	1375	21,1	135,0	2640	-2410	229	55,8	376,3	-51,0	-226,4	4,9	149,9
1300	1350	1325	17,2	152,2	2533	-2638	-105	43,6	419,9	-45,5	-271,9	-1,8	148,0
1250	1300	1275	15,5	167,7	2421	-2777	-355	37,6	457,5	-43,1	-315,0	-5,5	142,5
1200	1250	1225	21,1	188,8	2306	-2886	-580	48,7	506,2	-60,9	-375,9	-12,2	130,3
1150	1200	1175	17,9	206,7	2089	-3027	-938	37,4	543,5	-54,1	-430,0	-16,8	113,5
1100	1150	1125	17,0	223,7	1878	-3181	-1303	31,8	575,4	-53,9	-484,0	-22,1	91,4
1050	1100	1075	15,4	239,1	1705	-3379	-1674	26,3	601,7	-52,2	-536,2	-25,8	65,6
1000	1050	1025	19,3	258,4	1560	-3627	-2066	30,2	631,9	-70,1	-606,3	-39,9	25,6
950	1000	975	19,8	278,2	1357	-3960	-2602	26,9	658,8	-78,4	-684,7	-51,5	-25,9
900	950	925	20,3	298,5	1099	-4282	-3183	22,3	681,1	-86,9	-771,6	-64,6	-90,5
850	900	875	19,0	317,5	929	-4505	-3575	17,6	698,7	-85,5	-857,1	-67,8	-158,4
800	850	825	18,8	336,3	830	-4702	-3872	15,6	714,4	-88,5	-945,6	-72,9	-231,3
750	800	775	21,4	357,7	745	-4932	-4187	15,9	730,3	-105,5	-1051,1	-89,6	-320,8
700	750	725	21,3	379,0	660	-5228	-4568	14,1	744,4	-111,5	-1162,7	-97,4	-418,3
650	700	675	19,8	398,8	567	-5609	-5041	11,2	755,6	-110,8	-1273,5	-99,6	-517,9
600	650	625	7,0	405,8	499	-5855	-5355	3,5	759,1	-40,9	-1314,4	-37,4	-555,3

Skaftárjökull

Elevation (m a.s.l.)			ΔS (km^2)	∑ΔS (km^2)	b_w (mm)	b_s (mm)	b_n (mm)	ΔB_w ($10^6 m^3$)	$\sum\Delta B_w$ ($10^6 m^3$)	ΔB_s ($10^6 m^3$)	$\sum\Delta B_s$ ($10^6 m^3$)	ΔB_n ($10^6 m^3$)	$\sum B_n$ ($10^6 m^3$)
1400	1450	1425	0,0	0,0	2635	-2347	287	0,0	0,0	0,0	0,0	0,0	0,0
1350	1400	1375	2,5	2,5	2549	-2501	48	6,3	6,3	-6,2	-6,2	0,1	0,1
1300	1350	1325	5,3	7,8	2452	-2668	-216	13,0	19,3	-14,1	-20,3	-1,1	-1,0
1250	1300	1275	4,0	11,8	2366	-2800	-433	9,5	28,9	-11,3	-31,6	-1,7	-2,8
1200	1250	1225	6,4	18,2	2203	-2944	-741	14,0	42,9	-18,8	-50,4	-4,7	-7,5
1150	1200	1175	7,6	25,8	1952	-3104	-1152	14,8	57,7	-23,6	-74,0	-8,7	-16,2
1100	1150	1125	10,9	36,7	1622	-3299	-1676	17,6	75,3	-35,8	-109,8	-18,2	-34,4
1050	1100	1075	12,1	48,8	1314	-3546	-2231	15,9	91,3	-43,0	-152,8	-27,1	-61,5
1000	1050	1025	12,8	61,6	1104	-3838	-2733	14,1	105,4	-49,1	-201,8	-34,9	-96,4
950	1000	975	8,7	70,3	953	-4227	-3274	8,3	113,7	-36,8	-238,6	-28,5	-124,9
900	950	925	5,6	75,9	883	-4574	-3691	5,0	118,7	-25,7	-264,4	-20,7	-145,7
850	900	875	4,9	80,8	830	-4878	-4048	4,0	122,7	-23,8	-288,1	-19,7	-165,4
800	850	825	4,9	85,7	789	-5135	-4345	3,9	126,6	-25,2	-313,3	-21,3	-186,7
750	800	775	4,5	90,2	748	-5347	-4598	3,4	130,0	-24,2	-337,5	-20,8	-207,5
700	750	725	4,1	94,3	696	-5583	-4887	2,8	132,8	-22,8	-360,3	-20,0	-227,5
650	700	675	2,6	96,9	620	-5768	-5148	1,6	134,4	-15,1	-375,4	-13,4	-241,0
600	650	625	0,3	97,2	580	-5832	-5252	0,2	134,6	-1,9	-377,3	-1,7	-242,7

Vestari Skaftárketill

Elevation (m a.s.l.)			ΔS (km^2)	∑ΔS (km^2)	b_w (mm)	b_s (mm)	b_n (mm)	ΔB_w ($10^6 m^3$)	$\sum\Delta B_w$ ($10^6 m^3$)	ΔB_s ($10^6 m^3$)	$\sum\Delta B_s$ ($10^6 m^3$)	ΔB_n ($10^6 m^3$)	$\sum B_n$ ($10^6 m^3$)
1900	1950	1925	0,6	0,6	2634	263	2897	1,5	1,5	0,1	0,1	1,6	1,6
1850	1900	1875	0,6	1,2	2618	248	2867	1,6	3,1	0,2	0,3	1,8	3,4
1800	1850	1825	0,8	2,0	2592	235	2828	2,0	5,1	0,2	0,5	2,2	5,6
1750	1800	1775	2,5	4,5	2541	180	2721	6,3	11,5	0,4	0,9	6,8	12,4
1700	1750	1725	5,4	9,9	2484	-20	2464	13,5	24,9	-0,1	0,8	13,4	25,8
1650	1700	1675	6,5	16,4	2435	-328	2106	15,8	40,7	-2,1	-1,3	13,6	39,4
1600	1650	1625	7,2	23,6	2418	-606	1811	17,4	58,1	-4,4	-5,7	13,0	52,4
1550	1600	1575	5,0	28,6	2375	-821	1553	11,9	70,0	-4,1	-9,8	7,8	60,2
1500	1550	1525	2,7	31,3	2334	-917	1416	6,3	76,2	-2,5	-12,2	3,8	64,0
1450	1500	1475	0,0	31,3	2351	-857	1494	0,0	76,3	0,0	-12,3	0,0	64,1

Eystri Skaftárketill

Elevation (m a.s.l.)			ΔS (km^2)	∑ΔS (km^2)	b_w (mm)	b_s (mm)	b_n (mm)	ΔB_w ($10^6 m^3$)	$\sum\Delta B_w$ ($10^6 m^3$)	ΔB_s ($10^6 m^3$)	$\sum\Delta B_s$ ($10^6 m^3$)	ΔB_n ($10^6 m^3$)	$\sum B_n$ ($10^6 m^3$)
1750	1800	1775	1,1	1,1	2543	157	2700	2,8	2,8	0,2	0,2	3,0	3,0
1700	1750	1725	9,8	10,9	2556	-80	2475	25,1	27,9	-0,8	-0,6	24,3	27,3
1650	1700	1675	15,5	26,4	2627	-404	2223	40,6	68,5	-6,2	-6,9	34,4	61,7
1600	1650	1625	9,3	35,7	2607	-620	1986	24,1	92,6	-5,7	-12,6	18,4	80,0
1550	1600	1575	4,3	40,0	2596	-731	1865	11,0	103,7	-3,1	-15,7	7,9	88,0

Gjálp

Elevation (m a.s.l.)			ΔS (km^2)	∑ΔS (km^2)	b_w (mm)	b_s (mm)	b_n (mm)	ΔB_w ($10^6 m^3$)	$\sum\Delta B_w$ ($10^6 m^3$)	ΔB_s ($10^6 m^3$)	$\sum\Delta B_s$ ($10^6 m^3$)	ΔB_n ($10^6 m^3$)	$\sum B_n$ ($10^6 m^3$)
1900	1950	1925	0,3	0,3	2645	261	2907	0,9	0,9	0,0	0,0	1,0	1,0
1850	1900	1875	0,7	1,0	2622	235	2857	1,9	2,9	0,2	0,3	2,1	3,1
1800	1850	1825	1,2	2,2	2590	212	2803	3,0	5,9	0,2	0,5	3,3	6,4
1750	1800	1775	5,5	7,7	2563	164	2727	14,1	20,0	0,9	1,4	15,0	21,4
1700	1750	1725	23,5	31,2	2691	-114	2577	63,3	83,2	-2,7	-1,3	60,6	82,0
1650	1700	1675	8,1	39,3	2773	-309	2463	22,5	105,7	-2,5	-3,8	20,0	101,9

Grímsvötn

Elevation (m a.s.l.)			ΔS (km^2)	∑ΔS (km^2)	b_w (mm)	b_s (mm)	b_n (mm)	ΔB_w ($10^6 m^3$)	$\sum\Delta B_w$ ($10^6 m^3$)	ΔB_s ($10^6 m^3$)	$\sum\Delta B_s$ ($10^6 m^3$)	ΔB_n ($10^6 m^3$)	$\sum B_n$ ($10^6 m^3$)
1700	1750	1725	1,3	1,3	2750	-404	2346	3,6	3,6	-0,5	-0,5	3,1	3,1
1650	1700	1675	40,7	42,0	2671	-614	2057	108,7	112,3	-25,0	-25,5	83,7	86,8
1600	1650	1625	30,6	72,6	2594	-941	1653	79,3	191,6	-28,8	-54,3	50,5	137,3
1550	1600	1575	19,6	92,2	2506	-1189	1317	49,2	240,8	-23,3	-77,6	25,8	163,1
1500	1550	1525	16,4	108,6	2559	-1485	1074	42,0	282,8	-24,4	-102,0	17,6	180,8
1450	1500	1475	9,4	118,0	2611	-1780	830	24,6	307,4	-16,8	-118,8	7,8	188,6
1400	1450	1425	13,7	131,7	2752	-2069	682	37,6	345,0	-28,3	-147,1	9,3	197,9
1350	1400	1375	1,5	133,2	2832	-1897	935	4,2	349,2	-2,8	-149,9	1,4	199,3

Appendix C: Coordinates of the velocity measurement stakes in 2022.

Position of the velocity measurement stakes determined by GPS sub-metre differential (I), fast static (FS) and kinematic (K). (Accuracy of horizontal position 0.5 – 1.0 m, and vertical accuracy 1-2 m for DGPS, about 1cm for fast static, and 3 cm for kinematic).
The station Hofn in Höfn í Hornafirði is used as a stationary reference for all measurements, ÍSN93 datum, h_l is elevation above ellipsoid, dL antenna height, N estimated difference between ellipsoid and sea-level, H elevation in metres above sea level ($H= h_l+N+dL$). X and Y are ÍSN93 Lambert conformal conic projected coordinates. M is a quality marker.

Site	time	Date	Calender Day #	Year	Latitude		Longitude		h_l (m a. e.)	dL (m)	N (m)	H (m a. s. l.)	X	Y	M
B07-22	14,67	3	5	123	2022	64	25,7932	16	17,4763	1426,1	0	-67,1	1359,1	630458,1	439238,7	K
B07-22	13,235	17	10	290	2022	64	25,7924	16	17,4756	1422,3	0	-67,1	1355,3	630458,8	439237,3	K
B09-22	15,143	3	5	123	2022	64	44,6433	16	6,11253	787,85	0	-66,7	721,17	637968,6	474629,9	K
B09-22	17,518	17	10	290	2022	64	44,6435	16	6,1129	782,15	0	-66,7	715,47	637968,3	474630,3	K
B10-22	17,324	4	5	124	2022	64	43,6831	16	6,70448	830,53	0	-66,7	763,82	637580,7	472826,3	K
B10-22	17,157	17	10	290	2022	64	43,6831	16	6,70488	824,09	0	-66,7	757,38	637580,4	472826,1	K
B11-22	16,548	3	5	123	2022	64	40,9448	16	10,4791	1013,1	0	-66,8	946,25	634813,4	467608,2	K
B11-22	17,966	17	10	290	2022	64	40,95	16	10,4755	1009	0	-66,8	942,14	634815,8	467618	K
B12-22	11,985	4	5	124	2022	64	38,2696	16	14,1619	1145	0	-66,9	1078,1	632103,7	462513	K
B12-22	18,232	17	10	290	2022	64	38,2792	16	14,1536	1141,5	0	-66,9	1074,6	632109,6	462531,1	K
B13-22	18,855	3	5	123	2022	64	34,5757	16	19,6327	1289,1	0	-67	1222,1	628038,5	455468,4	K
B13-22	16,052	17	10	290	2022	64	34,5853	16	19,6223	1285,8	0	-67	1218,8	628046,1	455486,6	K
B13ror15	18,53	3	5	123	2022	64	34,6407	16	19,5892	1286,6	0	-67	1219,6	628068,1	455590,4	K
B13ror15	16,196	17	10	290	2022	64	34,65	16	19,5787	1286,5	0	-67	1219,5	628075,8	455608,1	K
B14-22	16,964	3	5	123	2022	64	31,6458	16	24,7058	1390,2	0	-67,1	1323,1	624213,2	449860,7	K
B14-22	14,779	17	10	290	2022	64	31,6532	16	24,6929	1386,9	0	-67,1	1319,8	624223	449874,8	K
B15-22	16,004	3	5	123	2022	64	28,5072	16	30,032	1472,6	0	-67,2	1405,4	620185,8	443862,3	K
B15-22	14,112	17	10	290	2022	64	28,5117	16	30,0208	1468,9	0	-67,2	1401,7	620194,4	443870,9	K
B16-22	11,19	5	5	125	2022	64	24,1244	16	40,8961	1597	0	-67,3	1529,6	611781,8	435392,7	K
B16-22	14,555	17	10	290	2022	64	24,1246	16	40,8961	1594,3	-0,38	-67,3	1526,6	611781,8	435393,1	K
B17-22	17,952	3	5	123	2022	64	36,7343	16	28,7875	1284,2	0	-67,1	1217,1	620573,4	459175,7	K
B17-22	18,689	17	10	290	2022	64	36,7437	16	28,7835	1281,5	0	-67,1	1214,3	620575,9	459193,3	K
B18-22	12,734	3	5	123	2022	64	31,568	16	0,12022	1383,1	0	-66,9	1316,2	643871,3	450585	K
B18-22	11,271	17	10	290	2022	64	31,5733	16	0,12315	1380	0	-66,9	1313,1	643868,5	450594,9	K
B19-22	11,8	3	5	123	2022	64	27,9925	15	55,977	1506,7	0	-66,9	1439,8	647504,7	444108,6	K
B19-22	10,903	17	10	290	2022	64	27,9928	15	55,9771	1502,9	0	-66,9	1436	647504,7	444109,1	K
BB0-22	11,056	3	5	123	2022	64	22,7047	16	5,05578	1585,3	0	-66,9	1518,4	640685,9	433949,9	K
BB0-22	10,455	17	10	290	2022	64	22,7046	16	5,05709	1581,3	0	-66,9	1514,4	640684,8	433949,7	K
BB-Hak	15,95	4	6	155	2022	64	37,6514	17	21,0336	1856,3	0	-67,8	1788,4	578881,1	459505	K
BB-Hak	18,059	18	10	291	2022	64	37,6501	17	21,0119	1853,8	0	-67,8	1786	578898,4	459503,1	K
Bor-22	19,75	27	5	147	2022	64	24,9422	17	20,1562	1476,5	2,08	-67,7	1410,9	580201,7	435917,9	K
Bor-22	13,785	19	10	292	2022	64	24,939	17	20,1567	1474,7	-1,55	-67,7	1405,5	580201,5	435911,9	K
Br1-21	13,499	30	3	89	2022	64	5,95986	16	19,8222	155,23	-0,35	-65,9	88,98	630131,9	402340,8	K
Br1-22	13,499	30	3	89	2022	64	5,95986	16	19,8222	155,23	-0,35	-65,9	88,98	630131,9	402340,8	K
Br2-21	15,298	30	3	89	2022	64	6,35684	16	22,5269	230,5	-0,35	-66	164,12	627905,2	402985,7	K
Br2-22	15,298	30	3	89	2022	64	6,35684	16	22,5289	230,5	-0,35	-66	164,12	627903,2	402985,7	K
Br3-21	17,397	30	3	89	2022	64	8,42401	16	23,9858	424,45	-0,35	-66,3	357,84	626563	406774,4	K
Br3-22	17,397	30	3	89	2022	64	8,42401	16	23,9858	424,45	-0,35	-66,3	357,84	626563	406774,4	K
Br7-22	13,448	3	5	123	2022	64	22,1447	16	16,9173	1313,2	0	-67	1246,2	631197,9	432485,4	K
Br7-22	12,497	17	10	290	2022	64	22,1171	16	16,9103	1308,2	0	-67	1241,1	631205,7	432434,5	K
Bru-22	14,509	3	5	123	2022	64	39,7478	15	56,5425	959,71	0	-66,8	892,92	645995,8	465902,5	K
Bru-22	15,832	17	10	290	2022	64	39,7558	15	56,5398	955,71	0	-66,8	888,93	645997,2	465917,4	K
Bud-22	13,742	3	5	123	2022	64	35,9889	15	59,8736	1204,5	0	-66,9	1137,6	643678,5	458799,2	K
Bud-22	16,508	17	10	290	2022	64	35,9994	15	59,8721	1201,2	0	-66,9	1134,3	643678,7	458818,8	K

D01-22	20,303	5	5	125	2022	64	48,0778	16	50,1525	887,74	0	-67	820,7	602823,2	479608,4	K
D05-22	17,742	5	5	125	2022	64	42,2267	16	54,6804	1273,2	0	-67,4	1205,8	599598,2	468622,3	K
D05-22	13,262	18	10	291	2022	64	42,2395	16	54,6609	1272,4	-2,32	-67,4	1202,7	599612,9	468646,5	K
D07-22	15,453	5	5	125	2022	64	38,2848	16	59,2567	1446,2	0	-67,5	1378,7	596195,5	461184	K
D07-22	12,128	18	10	291	2022	64	38,3012	16	59,2401	1444,4	-1,61	-67,5	1375,3	596207,7	461214,9	K
D09-22	13,828	5	5	125	2022	64	31,7835	17	0,60302	1656,6	0	-67,6	1589,1	595503,4	449076,7	K
D09-22	11,184	18	10	291	2022	64	31,7871	17	0,60416	1655,3	-1	-67,6	1586,7	595502,3	449083,4	K
D12-22	11,114	6	5	126	2022	64	28,9709	17	0,18267	1718,9	0	-67,6	1651,3	596004,6	443864	K
D12-22	10,739	18	10	291	2022	64	28,9711	17	0,18247	1717	-0,78	-67,6	1648,7	596004,7	443864,4	K
E01-22	15,086	4	5	124	2022	64	40,6437	15	34,8284	821,57	0	-66,7	754,85	663169,9	468449,8	K
E01-22	13,644	17	10	290	2022	64	40,6491	15	34,8237	815,96	0	-66,7	749,24	663173,1	468460	K
E02-22	14,409	4	5	124	2022	64	39,1235	15	36,0032	1016,4	0	-66,8	949,66	662388,4	465578,9	K
E02-22	13,404	17	10	290	2022	64	39,1384	15	35,9973	1011,4	0	-66,8	944,58	662391,6	465606,9	K
E03-22	13,497	4	5	124	2022	64	36,6526	15	36,911	1255,3	0	-66,9	1188,4	661912,1	460955,7	K
E03-22	13,137	17	10	290	2022	64	36,6576	15	36,9141	1250,6	0	-66,9	1183,7	661909,2	460965	K
E04-22	12,414	4	5	124	2022	64	34,9573	15	37,1404	1355,1	0	-66,8	1288,2	661897,8	457800,6	K
E04-22	12,911	17	10	290	2022	64	34,958	15	37,14	1351,1	0	-66,8	1284,3	661898,1	457802	K
E07-22	16,178	4	5	124	2022	64	38,411	15	24,6935	1137,6	0	-66,6	1071	671457	464754,8	K
E07-22	14,139	17	10	290	2022	64	38,4152	15	24,6846	1132,4	0	-66,6	1065,8	671463,7	464763,1	K
E08-22	17,028	4	5	124	2022	64	39,7167	15	23,847	1017,6	0	-66,6	951,09	671992,2	467215,2	K
E08-22	14,614	17	10	290	2022	64	39,7184	15	23,8465	1012,4	0	-66,6	945,8	671992,4	467218,5	K
Fl01-22	10,934	3	5	123	2022	64	26,1608	15	55,6231	1414,5	0	-66,8	1347,7	647953,5	440723	K
Fl01-22	10,708	17	10	290	2022	64	26,1541	15	55,6077	1409,8	0	-66,8	1342,9	647966,5	440711,3	K
G02-22	18,621	6	5	126	2022	64	26,8576	17	17,7304	1635,8	0	-67,7	1568,1	582053,9	439527,3	K
G02-22	18,399	18	10	291	2022	64	26,8536	17	17,7335	1631,9	0	-67,7	1564,2	582051,6	439519,8	K
G03-22	11,916	6	5	126	2022	64	28,4401	17	16,3287	1729,7	0	-67,7	1661,9	583097,9	442497	K
G03-22	18,201	18	10	291	2022	64	28,4382	17	16,3298	1726,4	0	-67,7	1658,7	583097,1	442493,6	K
G04-22	12,679	6	5	126	2022	64	30,0199	17	15,0394	1759	0	-67,7	1691,2	584049,8	445459,6	K
G04-22	18,047	18	10	291	2022	64	30,0204	17	15,0384	1756,1	0	-67,7	1688,4	584050,6	445460,5	K
G01-22	13,676	6	5	126	2022	64	33,9597	17	24,9365	1829,6	0	-67,8	1761,7	575942,8	452568,5	K
G01-22	16,197	18	10	291	2022	64	33,9583	17	24,9355	1828	-0,75	-67,8	1759,4	575943,7	452565,8	K
Haab-22	15,508	7	5	127	2022	64	20,9606	17	24,1195	1799,4	0	-67,5	1731,9	577205,8	428440,3	K
Haab-22	10,629	18	10	291	2022	64	20,9609	17	24,1194	1796,1	0	-67,5	1728,5	577205,9	428440,9	K
Herm-22	13,932	19	10	292	2022	64	7,01247	16	41,9852	1356,4	0	-66,9	1289,5	612063,7	403587,5	K
Hof01-22	11,429	4	5	124	2022	64	32,3422	15	35,8166	1209,7	0	-66,7	1143,1	663214,8	453005,5	K
Hof01-22	12,439	17	10	290	2022	64	32,3357	15	35,8163	1205,2	0	-66,7	1138,5	663215,6	452993,4	K
K01-22	13,141	7	5	127	2022	64	35,1734	17	51,8649	1107,7	0	-67,6	1040,1	554392,9	454360,4	K
K01-22	16,15	18	10	291	2022	64	35,1748	17	51,8706	1103,2	0	-67,6	1035,7	554388,3	454362,8	K
K02-21	15,95	18	10	291	2022	64	34,8171	17	49,7274	1230,9	0	-67,6	1163,3	556111,4	453729,6	K
K02-22	12,582	7	5	127	2022	64	34,8076	17	49,6942	1236,1	0	-67,6	1168,5	556138,2	453712,4	K
K02-22	15,778	18	10	291	2022	64	34,8104	17	49,7081	1232,1	0	-67,6	1164,4	556127,1	453717,3	K
K03-22	12,046	7	5	127	2022	64	34,24	17	46,4038	1360,1	0	-67,7	1292,5	558785,7	452707,9	K
K03-22	15,565	18	10	291	2022	64	34,2429	17	46,4211	1356,3	0	-67,7	1288,6	558771,8	452712,9	K
K04-22	11,494	7	5	127	2022	64	33,2148	17	42,2512	1554,9	0	-67,7	1487,2	562141,2	450869,6	K
K04-22	16,528	18	10	291	2022	64	33,2181	17	42,2752	1550,6	0	-67,7	1482,8	562121,9	450875,4	K
K05-22	16,984	6	5	126	2022	64	33,4399	17	35,4737	1747	0	-67,8	1679,2	567548	451403,6	K
K05-22	16,761	18	10	291	2022	64	33,4371	17	35,4872	1744,1	0	-67,8	1676,3	567537,4	451398,2	K
K06-22	15,783	6	5	126	2022	64	38,3496	17	31,3011	2014	0	-67,9	1946,2	570668,6	460599,4	K
K06-22	17,275	18	10	291	2022	64	38,3494	17	31,2982	2014,2	-1,9	-67,9	1944,4	570670,9	460599,1	K
K07-22	10,78	7	5	127	2022	64	29,115	17	42,0247	1600,5	0	-67,7	1532,8	562478,8	443257,6	K
K07-22	15,155	18	10	291	2022	64	29,1151	17	42,026	1596,9	0	-67,7	1529,2	562477,8	443257,8	K
Kve01-22	13,155	20	10	293	2022	64	38,6566	16	40,5325	1889,6	0	-67,4	1822,3	611081,3	462386	K
S01-22	18,64	7	5	127	2022	64	7,0017	17	49,9702	770,93	0	-66,8	704,09	556871,7	402053,5	K
S01-22	12,487	18	10	291	2022	64	7,00159	17	49,9713	764,94	0	-66,8	698,1	556870,8	402053,3	K
S02-22	17,875	7	5	127	2022	64	12,1619	17	48,9804	1068,5	0	-67,1	1001,4	557495,9	411654,7	K
S02-22	11,846	18	10	291	2022	64	12,1499	17	48,9863	1063,3	0	-67	996,25	557491,5	411632,2	K
S04-22	17,461	7	5	127	2022	64	16,1786	17	48,188	1225,6	0	-67,2	1158,4	557996,1	419128,4	K
S04-22	11,437	18	10	291	2022	64	16,1637	17	48,203	1220,2	0	-67,2	1153	557984,5	419100,6	K
S05-22	16,351	7	5	127	2022	64	20,5148	17	33,9957	1520,5	0	-67,5	1453	569273,4	427421,4	K
S05-22	10,991	18	10	291	2022	64	20,513	17	34,0115	1515,2	0	-67,5	1447,7	569260,8	427417,9	K

Ske02-22	15,6	5	5	125	2022	64	15,9123	17	0,06314	1247,7	0	-67,1	1180,6	596867,4	419616,3	K
Ske02-22	15,771	19	10	292	2022	64	15,8604	17	0,18372	1239,2	0	-67,1	1172,1	596773,1	419516,8	K
Ske03-22	14,862	5	5	125	2022	64	18,058	16	56,1577	1368,3	0	-67,2	1301,1	599890,4	423702,3	K
Ske03-22	16,229	19	10	292	2022	64	18,032	16	56,2244	1361,1	0	-67,2	1293,9	599838,2	423652,2	K
Ske04-22	13,144	5	5	125	2022	64	20,1473	16	51,8055	1468,9	0	-67,3	1401,6	603268,4	427698,6	K
Ske04-22	13,2	19	10	292	2022	64	20,1363	16	51,8348	1464,1	0	-67,3	1396,8	603245,5	427677,3	K
Ske05-22	12,386	5	5	125	2022	64	22,2367	16	47,2318	1541,8	0	-67,4	1474,5	606815,4	431705	K
Ske05-22	13,044	19	10	292	2022	64	22,2316	16	47,2427	1537,5	0	-67,4	1470,2	606807	431695,2	K
Skf00-22	20,465	2	5	122	2022	64	15,4587	15	54,0647	1015,4	0	-66	949,37	650177,4	420923,4	K
Skf01-22	21,739	2	5	122	2022	64	18,0173	16	5,02164	1351,4	0	-66,6	1284,7	641114,9	425251,2	K
Skf01-22	11,122	17	10	290	2022	64	18,0147	16	5,0063	1345,8	0	-66,6	1279,2	641127,5	425246,9	K
T01-22	15,818	7	5	127	2022	64	19,1575	18	6,52262	836,24	0	-67,3	768,99	543111,9	424418,2	K
T02-22	15,44	7	5	127	2022	64	19,4778	18	4,54091	953,47	0	-67,3	886,21	544700,7	425036,2	K
T02-22	13,735	18	10	291	2022	64	19,478	18	4,54606	947,25	0	-67,3	879,99	544696,6	425036,5	K
T03-22	13,419	7	5	127	2022	64	20,2047	17	58,5797	1132,9	0	-67,3	1065,6	549483,3	426460,6	K
T03-22	12,158	18	10	291	2022	64	20,2028	17	58,5921	1128,2	0	-67,3	1060,9	549473,4	426456,8	K
T04-22	11,793	7	5	127	2022	64	21,3314	17	51,515	1289,2	0	-67,4	1221,9	555136,6	428651,2	K
T04-22	11,825	18	10	291	2022	64	21,3276	17	51,5285	1284	0	-67,4	1216,7	555125,8	428643,9	K
T05-22	11,034	7	5	127	2022	64	22,2689	17	43,0075	1414,7	0	-67,5	1347,2	561949,6	430524	K
T05-22	11,429	18	10	291	2022	64	22,2655	17	43,0207	1408,7	0	-67,5	1341,3	561939,1	430517,4	K
t05rorh	11,538	18	10	291	2022	64	22,2324	17	43,2169	1406	0	-67,5	1338,5	561782,6	430452,8	K
T06-22	19,919	7	5	127	2022	64	24,2595	17	36,5145	1537,5	0	-67,6	1469,9	567091,8	434332,2	K
T06-22	14,471	18	10	291	2022	64	24,2556	17	36,5258	1532,2	0	-67,6	1464,6	567082,9	434324,8	K
T07-22	10,328	8	5	128	2022	64	25,2943	17	31,2127	1632,9	0	-67,7	1565,2	571306,8	436351,1	K
T07-22	10,929	18	10	291	2022	64	25,292	17	31,221	1628,2	0	-67,7	1560,5	571300,2	436346,7	K
T08-22	10,946	8	5	128	2022	64	26,2959	17	27,7562	1705,4	0	-67,8	1637,6	574037	438277,7	K
T08-22	10,712	18	10	291	2022	64	26,2956	17	27,758	1701,8	0	-67,8	1634	574035,5	438277,2	K

Appendix D: Measured surface velocity at marked sites on Vatnajökull in 2022.

Site	Calendar day date	#	Calendar day date	#	# of days	translation (m)	(°)	velocity (cm/day)	(m/annum)
B07-22	220503	123	221017	290	167	1,57	157	0,94	3,43
B09-22	220503	123	221017	290	167	0,49	323	0,29	1,06
B10-22	220504	124	221017	290	166	0,34	248	0,21	0,75
B11-22	220503	123	221017	290	167	10,04	16	6,01	21,94
B12-22	220504	124	221017	290	166	18,99	21	11,44	41,74
B13-22	220503	123	221017	290	167	19,65	25	11,77	42,95
B13ror15	211016	289	220503	123	199	5,37	32	2,70	9,85
B13ror15	220503	123	221017	290	167	19,24	26	11,52	42,05
B14-22	220503	123	221017	290	167	17,09	37	10,24	37,36
B15-22	220503	123	221017	290	167	12,22	47	7,32	26,71
B16-22	220505	125	221017	290	165	0,37	358	0,22	0,82
B17-22	220503	123	221017	290	167	17,72	10	10,61	38,72
B18-22	220503	123	221017	290	167	10,22	347	6,12	22,33
B19-22	220503	123	221017	290	167	0,48	359	0,29	1,05
BB0-22	220503	123	221017	290	167	1,06	262	0,64	2,33
BB-Hak	220604	155	221018	291	136	17,40	98	12,80	46,70
Bor-22	220527	147	221019	292	145	5,99	183	4,13	15,09
Br1-21	210413	103	220330	89	351	0,98	184	0,28	1,02
Br2-21	210413	103	220330	89	351	3,62	146	1,03	3,77
Br3-21	210413	103	220330	89	351	22,14	146	6,31	23,02
Br7-22	220503	123	221017	290	167	51,37	174	30,76	112,28
Bru-22	220503	123	221017	290	167	14,95	8	8,95	32,68
Bud-22	220503	123	221017	290	167	19,56	4	11,71	42,74
D05-22	220505	125	221018	291	166	28,24	33	17,01	62,08
D07-22	220505	125	221018	291	166	33,12	23	19,95	72,82
D09-22	220505	125	221018	291	166	6,73	352	4,05	14,80
D12-22	220506	126	221018	291	165	0,44	21	0,27	0,97
E01-22	220504	124	221017	290	166	10,68	20	6,43	23,48
E02-22	220504	124	221017	290	166	28,09	10	16,92	61,77
E03-22	220504	124	221017	290	166	9,69	345	5,84	21,31
E04-22	220504	124	221017	290	166	1,39	14	0,84	3,06
E07-22	220504	124	221017	290	166	10,59	42	6,38	23,29
E08-22	220504	124	221017	290	166	3,23	8	1,95	7,11
Fl01-22	220503	123	221017	290	167	17,47	135	10,46	38,19
G02-22	220506	126	221018	291	165	7,79	199	4,72	17,24
G03-22	220506	126	221018	291	165	3,51	195	2,13	7,76
G04-22	220506	126	221018	291	165	1,23	42	0,74	2,71
G01-22	220506	126	221018	291	165	2,75	163	1,67	6,08
Haab-22	220507	127	221018	291	164	0,58	9	0,35	1,29
Hof01-22	220504	124	221017	290	166	12,00	179	7,23	26,39
K01-22	220507	127	221018	291	164	5,19	299	3,16	11,55
K02-21	210505	125	221018	291	531	34,01	296	6,40	23,38
K02-22	220507	127	221018	291	164	12,22	295	7,45	27,19
K03-22	220507	127	221018	291	164	14,81	291	9,03	32,96
K04-22	220507	127	221018	291	164	20,15	288	12,29	44,85
K05-22	220506	126	221018	291	165	11,94	245	7,24	26,42
K06-22	220506	126	221018	291	165	2,39	98	1,45	5,28
K07-22	220507	127	221018	291	164	1,08	282	0,66	2,40

S01-22	220507	127	221018	291	164	0,96	258	0,59	2,14
S02-22	220507	127	221018	291	164	22,83	192	13,92	50,81
S04-22	220507	127	221018	291	164	30,06	204	18,33	66,89
S05-22	220507	127	221018	291	164	13,13	256	8,01	29,22
Ske02-22	220505	125	221019	292	167	136,87	225	81,96	299,14
Ske03-22	220505	125	221019	292	167	72,24	228	43,26	157,89
Ske04-22	220505	125	221019	292	167	31,19	229	18,68	68,18
Ske05-22	220505	125	221019	292	167	12,86	223	7,70	28,10
Skf01-22	220502	122	221017	290	168	13,29	111	7,91	28,88
T02-22	220507	127	221018	291	164	4,17	275	2,54	9,28
T03-22	220507	127	221018	291	164	10,62	250	6,47	23,63
T04-22	220507	127	221018	291	164	12,97	237	7,91	28,86
T05-22	220507	127	221018	291	164	12,41	239	7,57	27,63
T06-22	220507	127	221018	291	164	11,61	232	7,08	25,84
T07-22	220508	128	221018	291	163	7,88	238	4,84	17,65
T08-22	220508	128	221018	291	163	1,53	250	0,94	3,44

Appendix E: Melt water runoff to selected rivers in summer 2022, derived from summer surface balance.

ΔS: area in each elevation range where summer balance is negative, **∑ΔS**: cumulative area above a given elevation, **ΔQ_s**: melt water runoff from a given elevation range, **$\sum \Delta Q_s$**: cumulative melt water runoff from an area above given elevation.

Tungnaá water drainage basin

Elevation (m a. s. l.)		ΔS km^2	∑ΔS km^2	ΔQ_s ($10^6 m^3$)	$\sum \Delta Q_s$ ($10^6 m^3$)
1350	1400	0,3	0,3	0,8	0,8
1300	1350	6,0	6,4	15,9	16,7
1250	1300	10,0	16,3	27,9	44,6
1200	1250	10,9	27,2	32,3	76,9
1150	1200	9,5	36,7	30,8	107,7
1100	1150	11,4	48,1	40,2	148,0
1050	1100	10,8	58,9	41,0	189,0
1000	1050	9,5	68,4	38,6	227,6
950	1000	9,1	77,5	39,7	267,3
900	950	8,8	86,2	41,1	308,4
850	900	6,6	92,9	34,2	342,5
800	850	6,8	99,6	37,8	380,3
750	800	5,7	105,4	32,7	413,1
700	750	3,7	109,1	21,3	434,4
650	700	0,8	109,9	4,4	438,7

Sylgja water drainage basin

Elevation (m a. s. l.)		ΔS km^2	∑ΔS km^2	ΔQ_s ($10^6 m^3$)	$\sum \Delta Q_s$ ($10^6 m^3$)
1300	1350	1,1	1,1	3,0	3,0
1250	1300	3,4	4,5	9,6	12,6
1200	1250	5,5	10,0	16,1	28,7
1150	1200	8,2	18,2	25,7	54,4
1100	1150	5,8	24,0	19,9	74,3
1050	1100	6,2	30,2	23,2	97,5
1000	1050	5,8	36,0	24,2	121,7
950	1000	1,9	37,9	8,2	130,0
900	950	0,8	38,7	3,3	133,2
850	900	0,0	38,7	0,1	133,4

Western Skaftá cauldron water drainage basin

Elevation (m a. s. l.)		ΔS km^2	∑ΔS km^2	ΔQ_s ($10^6 m^3$)	$\sum \Delta Q_s$ ($10^6 m^3$)
1700	1750	2,2	2,2	0,3	0,3
1650	1700	7,2	9,4	2,2	2,5
1600	1650	7,9	17,3	5,1	7,6
1550	1600	5,1	22,4	4,2	11,8
1500	1550	2,6	25,1	2,4	14,2
1450	1500	0,0	25,1	0,0	14,2

Eastern Skaftár cauldron water drainage basin

Elevation (m a. s. l.)		ΔS km²	∑ΔS km²	ΔQs ($10^6 m^3$)	∑ΔQs ($10^6 m^3$)
1800	1850	0,0	0,0	0,0	0,0
1750	1800	0,0	0,0	0,0	0,0
1700	1750	6,7	6,7	0,8	0,8
1650	1700	13,7	20,4	5,7	6,5
1600	1650	9,4	29,9	5,8	12,3
1550	1600	4,1	34,0	3,0	15,3

Grímsvötn water drainage basin

Elevation (m a. s. l.)		ΔS km²	∑ΔS km²	ΔQs ($10^6 m^3$)	∑ΔQs ($10^6 m^3$)
1900	1950	0,0	0,0	0,0	0,0
1850	1900	0,0	0,0	0,0	0,0
1800	1850	0,0	0,0	0,0	0,0
1750	1800	0,0	0,0	0,0	0,0
1700	1750	19,4	19,4	3,3	3,3
1650	1700	48,2	67,5	26,9	30,3
1600	1650	30,6	98,1	28,8	59,0
1550	1600	19,7	117,7	23,3	82,4
1500	1550	16,3	134,0	24,2	106,6
1450	1500	9,7	143,8	16,8	123,4
1400	1450	13,8	157,6	28,3	151,7
1350	1400	1,5	159,1	2,8	154,5

Kaldakvísl water drainage basin

Elevation (m a. s. l.)		ΔS km²	∑ΔS km²	ΔQs ($10^6 m^3$)	∑ΔQs ($10^6 m^3$)
1950	2000	0,0	0,0	0,0	0,0
1900	1950	0,0	0,0	0,0	0,0
1850	1900	0,0	0,0	0,0	0,0
1800	1850	0,4	0,4	0,0	0,0
1750	1800	1,9	2,3	0,2	0,2
1700	1750	14,0	16,3	1,5	1,8
1650	1700	16,8	33,1	5,4	7,2
1600	1650	14,3	47,5	8,4	15,6
1550	1600	18,5	66,0	15,7	31,3
1500	1550	24,0	90,0	26,7	58,0
1450	1500	28,0	117,9	35,1	93,1
1400	1450	22,4	140,3	34,0	127,1
1350	1400	20,8	161,1	35,2	162,3
1300	1350	20,2	181,3	35,7	198,0
1250	1300	21,1	202,4	43,8	241,8
1200	1250	20,4	222,8	50,8	292,6
1150	1200	19,3	242,1	56,3	349,0
1100	1150	17,3	259,4	57,2	406,2
1050	1100	16,1	275,4	59,2	465,4
1000	1050	14,1	289,6	56,7	522,1
950	1000	9,2	298,8	37,6	559,7
900	950	2,6	301,4	10,0	569,8

Jökulsá á Fjöllum water drainage basin

Elevation (m a. s. l.)		ΔS km^2	∑ΔS km^2	ΔQ_s ($10^6 m^3$)	$\sum\Delta Q_s$ ($10^6 m^3$)
1950	2000	0,0	0,0	0,0	0,0
1900	1950	0,0	0,0	0,0	0,0
1800	1850	0,9	0,9	0,0	0,0
1750	1800	12,0	12,9	0,9	0,9
1700	1750	32,9	45,9	4,6	5,6
1650	1700	80,3	126,2	26,0	31,5
1600	1650	122,0	248,2	50,8	82,4
1550	1600	100,5	348,7	53,8	136,2
1500	1550	93,2	441,9	69,6	205,8
1450	1500	80,0	521,9	80,4	286,1
1400	1450	69,0	590,9	87,1	373,2
1350	1400	54,7	645,6	77,6	450,8
1300	1350	43,2	688,8	64,2	515,0
1250	1300	46,8	735,5	72,6	587,6
1200	1250	49,8	785,4	84,0	671,6
1150	1200	49,6	835,0	100,2	771,9
1100	1150	43,8	878,8	108,3	880,1
1050	1100	31,3	910,1	93,6	973,7
1000	1050	31,4	941,5	109,0	1082,7
950	1000	29,1	970,6	113,6	1196,3
900	950	24,4	995,1	104,0	1300,3
850	900	21,1	1016,1	97,4	1397,6
800	850	18,7	1034,8	92,4	1490,0
750	800	12,3	1047,1	61,9	1551,9
700	750	3,7	1050,8	16,4	1568,4

Kreppa and Kverká water drainage basin

Elevation (m a. s. l.)		ΔS km²	∑ΔS km²	ΔQs ($10^6 m^3$)	∑ΔQs ($10^6 m^3$)
1900	1950	0,0	0,0	0,0	0,0
1850	1900	0,6	0,6	0,0	0,0
1800	1850	0,6	1,2	0,0	0,0
1750	1800	2,5	3,7	0,2	0,2
1700	1750	3,8	7,5	0,8	1,0
1650	1700	5,2	12,7	1,4	2,4
1600	1650	41,4	54,1	17,9	20,3
1550	1600	20,5	74,6	9,3	29,6
1500	1550	13,4	88,0	6,5	36,1
1450	1500	16,4	104,4	10,7	46,8
1400	1450	20,0	124,4	19,0	65,8
1350	1400	26,2	150,6	29,5	95,3
1300	1350	20,4	171,0	24,7	120,0
1250	1300	15,5	186,5	20,4	140,4
1200	1250	18,1	204,6	27,1	167,5
1150	1200	17,4	222,0	32,1	199,6
1100	1150	16,0	238,0	37,1	236,7
1050	1100	10,5	248,5	29,2	265,9
1000	1050	12,1	260,6	37,1	303,0
950	1000	13,3	273,9	45,7	348,7
900	950	12,6	286,5	49,7	398,4
850	900	12,6	299,1	55,6	454,0
800	850	10,4	309,5	48,7	502,7
750	800	7,3	316,8	36,7	539,4
700	750	3,5	320,3	18,5	557,9
650	700	0,4	320,7	2,4	560,3

Hálslón water drainage basin

Elevation (m a. s. l.)		ΔS km²	∑ΔS km²	ΔQs ($10^6 m^3$)	∑ΔQs ($10^6 m^3$)
1600	1650	10,3	10,3	4,7	4,7
1550	1600	32,9	43,2	11,3	16,0
1500	1550	65,3	108,6	22,2	38,3
1450	1500	70,0	178,6	45,2	83,5
1400	1450	99,0	277,5	76,0	159,4
1350	1400	133,7	411,3	119,3	278,8
1300	1350	130,3	541,6	127,2	405,9
1250	1300	123,4	665,0	144,8	550,7
1200	1250	98,2	763,2	143,2	693,9
1150	1200	82,2	845,5	144,6	838,5
1100	1150	64,5	909,9	137,8	976,4
1050	1100	55,1	965,0	140,6	1117,0
1000	1050	46,1	1011,1	134,1	1251,1
950	1000	39,4	1050,5	129,4	1380,5
900	950	31,6	1082,1	117,1	1497,6
850	900	26,8	1108,9	112,0	1609,6
800	850	25,1	1134,0	116,9	1726,5
750	800	25,2	1159,2	127,4	1853,9
700	750	22,4	1181,6	118,9	1972,8
650	700	12,1	1193,6	64,6	2037,4
600	650	1,1	1194,8	5,3	2042,7

Jökulsá á Fljótsdal water drainage basin

Elevation (m a. s. l.)		ΔS km^2	∑ΔS km^2	ΔQ_s ($10^6 m^3$)	$\sum \Delta Q_s$ ($10^6 m^3$)
1550	1600	0,0	0,0	0,0	0,0
1500	1550	0,0	0,1	0,0	0,0
1450	1500	1,1	1,2	0,5	0,6
1400	1450	2,1	3,4	1,1	1,7
1350	1400	3,1	6,5	2,1	3,8
1300	1350	5,9	12,4	5,2	9,0
1250	1300	16,1	28,5	18,3	27,3
1200	1250	15,8	44,3	23,3	50,6
1150	1200	17,0	61,3	31,1	81,7
1100	1150	14,3	75,6	32,6	114,3
1050	1100	11,9	87,6	33,8	148,1
1000	1050	11,1	98,6	36,9	185,0
950	1000	8,7	107,3	32,8	217,8
900	950	5,5	112,8	23,4	241,2
850	900	4,2	117,0	19,0	260,2
800	850	3,1	120,0	15,2	275,4
750	800	1,9	122,0	10,8	286,2
700	750	1,7	123,7	10,7	296,9
650	700	1,0	124,8	6,1	303,0

Hornafjarðarfljót water drainage basin

Elevation (m a. s. l.)		ΔS km^2	∑ΔS km^2	ΔQ_s ($10^6 m^3$)	$\sum\Delta Q_s$ ($10^6 m^3$)
1450	1500	1,2	1,2	0,5	0,5
1400	1450	8,2	9,4	3,9	4,5
1350	1400	12,7	22,2	7,4	11,9
1300	1350	19,2	41,4	15,0	26,9
1250	1300	37,9	79,3	42,4	69,3
1200	1250	28,8	108,1	42,0	111,3
1150	1200	20,3	128,4	38,7	150,1
1100	1150	18,9	147,3	43,8	193,9
1050	1100	14,2	161,5	38,2	232,1
1000	1050	11,1	172,5	32,4	264,5
950	1000	10,4	182,9	32,3	296,8
900	950	8,1	191,0	26,7	323,6
850	900	5,4	196,3	19,0	342,6
800	850	4,5	200,8	16,4	359,0
750	800	4,1	204,9	15,5	374,6
700	750	3,4	208,4	14,1	388,7
650	700	3,6	212,0	15,9	404,5
600	650	2,6	214,5	12,0	416,5
550	600	1,8	216,4	8,7	425,3
500	550	1,7	218,1	8,7	434,0
450	500	1,2	219,3	6,3	440,3
400	450	1,1	220,4	6,1	446,4
350	400	0,8	221,3	4,9	451,3
300	350	0,6	221,9	3,7	455,0
250	300	0,8	222,7	5,2	460,2
200	250	1,6	224,3	10,3	470,5
150	200	2,3	226,6	16,1	486,6
100	150	2,5	229,1	17,8	504,4
50	100	1,9	231,0	13,9	518,3
0	50	2,2	233,2	16,6	534,9

Jökulsá á Breiðamerkursandi water drainage basin

Elevation (m a. s. l.)		ΔS km^2	∑ΔS km^2	ΔQ_s ($10^6 m^3$)	$\sum\Delta Q_s$ ($10^6 m^3$)
1700	1750	0,0	0,0	0,0	0,0
1650	1700	0,8	0,8	0,2	0,2
1600	1650	2,8	3,6	0,6	0,9
1550	1600	16,2	19,8	2,9	3,8
1500	1550	22,9	42,6	10,6	14,4
1450	1500	36,1	78,7	26,1	40,5
1400	1450	51,2	130,0	48,5	89,0
1350	1400	83,5	213,5	95,7	184,7
1300	1350	83,4	296,8	107,4	292,0
1250	1300	51,7	348,5	74,1	366,1
1200	1250	34,7	383,2	55,9	422,1
1150	1200	28,3	411,5	51,8	473,9
1100	1150	23,8	435,3	48,6	522,5
1050	1100	20,4	455,6	46,0	568,6
1000	1050	17,5	473,2	43,6	612,1
950	1000	19,2	492,4	52,8	664,9
900	950	19,8	512,2	60,9	725,8
850	900	18,5	530,7	62,3	788,1
800	850	18,7	549,4	66,8	854,9
750	800	19,9	569,3	76,1	931,0
700	750	16,7	586,0	67,1	998,1
650	700	27,3	613,3	115,8	1113,9
600	650	19,3	632,5	86,3	1200,3
550	600	19,0	651,6	90,0	1290,3
500	550	10,3	661,8	51,2	1341,5
450	500	5,1	666,9	26,8	1368,3
400	450	7,1	674,0	40,1	1408,4
350	400	5,0	679,0	29,5	1437,9
300	350	4,5	683,5	27,6	1465,5
250	300	5,3	688,8	34,1	1499,6
200	250	4,4	693,2	29,4	1529,0
150	200	5,0	698,2	34,5	1563,5
100	150	4,6	702,8	33,1	1596,6
50	100	3,8	706,7	28,4	1625,1
0	50	1,7	708,4	12,7	1637,7

Breiðárlón/Fjallsárlón water drainage basin

Elevation (m a. s. l.)		ΔS km^2	∑ΔS km^2	ΔQ_s ($10^6 m^3$)	$\sum\Delta Q_s$ ($10^6 m^3$)
2000	2050	0,0	0,0	0,0	0,0
1950	2000	0,0	0,0	0,0	0,0
1900	1950	0,0	0,0	0,0	0,0
1850	1900	0,0	0,0	0,0	0,0
1800	1850	0,0	0,0	0,0	0,0
1750	1800	0,0	0,0	0,0	0,0
1700	1750	1,7	1,7	0,2	0,2
1650	1700	3,0	4,7	0,8	1,0
1600	1650	4,1	8,9	2,0	3,0
1550	1600	4,3	13,2	3,0	6,1
1500	1550	5,8	19,0	5,1	11,1
1450	1500	5,0	24,0	5,1	16,2
1400	1450	5,3	29,3	6,2	22,4
1350	1400	6,4	35,7	8,5	30,9
1300	1350	12,9	48,5	21,2	52,1
1250	1300	6,2	54,7	11,1	63,2
1200	1250	5,8	60,5	10,6	73,8
1150	1200	4,8	65,3	9,4	83,2
1100	1150	4,5	69,7	9,8	93,0
1050	1100	5,0	74,7	11,8	104,8
1000	1050	6,1	80,8	15,5	120,3
950	1000	6,7	87,5	19,6	139,9
900	950	7,9	95,4	26,4	166,2
850	900	6,2	101,6	23,3	189,5
800	850	7,6	109,2	30,7	220,2
750	800	8,6	117,7	36,6	256,8
700	750	6,6	124,3	28,8	285,6
650	700	6,2	130,5	28,5	314,1
600	650	7,3	137,9	34,9	349,0
550	600	8,2	146,0	40,4	389,4
500	550	8,3	154,3	42,2	431,6
450	500	8,8	163,1	46,8	478,5
400	450	10,4	173,4	57,2	535,7
350	400	8,7	182,2	50,5	586,2
300	350	7,0	189,2	42,1	628,3
250	300	6,4	195,6	40,4	668,7
200	250	6,0	201,6	39,8	708,5
150	200	6,0	207,6	41,3	749,9
100	150	4,5	212,1	32,3	782,2
50	100	3,7	215,8	27,3	809,4
0	50	4,1	219,9	31,2	840,6

Skeiðarársandur (Gígja) water drainage basin

Elevation (m a. s. l.)		ΔS km^2	∑ΔS km^2	ΔQ_s ($10^6 m^3$)	$\sum\Delta Q_s$ ($10^6 m^3$)
1700	1750	1,0	1,0	0,5	0,5
1650	1700	17,9	18,9	12,3	12,8
1600	1650	68,3	87,2	39,0	51,8
1550	1600	85,0	172,2	50,5	102,2
1500	1550	110,8	283,0	75,5	177,7
1450	1500	106,5	389,5	107,5	285,3
1400	1450	104,2	493,7	127,8	413,1
1350	1400	91,4	585,1	122,8	535,9
1300	1350	77,9	663,0	109,7	645,6
1250	1300	69,6	732,6	112,2	757,8
1200	1250	60,5	793,1	119,3	877,1
1150	1200	54,6	847,7	129,7	1006,8
1100	1150	51,4	899,1	136,0	1142,8
1050	1100	46,3	945,4	134,8	1277,6
1000	1050	41,5	986,9	129,8	1407,4
950	1000	40,3	1027,3	135,1	1542,5
900	950	37,2	1064,5	133,1	1675,6
850	900	38,6	1103,2	146,5	1822,1
800	850	32,6	1135,8	131,6	1953,7
750	800	27,3	1163,1	117,1	2070,8
700	750	25,2	1188,3	113,9	2184,6
650	700	20,2	1208,5	97,3	2282,0
600	650	15,5	1224,0	78,9	2360,8
550	600	23,3	1247,3	122,9	2483,8
500	550	20,5	1267,8	111,7	2595,5
450	500	13,5	1281,4	76,9	2672,4
400	450	12,0	1293,4	72,2	2744,6
350	400	13,0	1306,4	81,8	2826,4
300	350	14,1	1320,5	92,3	2918,7
250	300	12,2	1332,7	82,5	3001,2
200	250	12,1	1344,8	83,6	3084,8
150	200	11,2	1356,0	81,8	3166,6
100	150	9,8	1365,8	74,9	3241,5
50	100	6,0	1371,8	47,3	3288,8
0	50	2,4	1374,2	18,6	3307,5

Djúpá water drainage basin

Elevation (m a. s. l.)		ΔS km^2	∑ΔS km^2	ΔQ_s ($10^6 m^3$)	$\sum\Delta Q_s$ ($10^6 m^3$)
1450	1500	0,1	0,1	0,3	0,3
1400	1450	0,3	0,4	0,7	1,0
1350	1400	0,7	1,1	1,7	2,7
1300	1350	3,5	4,6	8,9	11,6
1250	1300	3,3	7,9	8,7	20,3
1200	1250	2,9	10,8	8,2	28,5
1150	1200	3,3	14,2	9,7	38,2
1100	1150	5,3	19,5	16,1	54,3
1050	1100	5,5	24,9	18,0	72,3
1000	1050	8,8	33,7	31,3	103,6
950	1000	7,4	41,1	29,4	133,0
900	950	7,4	48,5	32,4	165,4
850	900	6,3	54,8	28,9	194,4
800	850	6,6	61,4	31,4	225,8
750	800	6,0	67,4	29,7	255,5
700	750	3,5	70,9	18,8	274,3
650	700	2,5	73,4	13,2	287,5
600	650	0,6	74,0	2,8	290,3

Brunná water drainage basin

Elevation (m a. s. l.)		ΔS km^2	∑ΔS km^2	ΔQ_s ($10^6 m^3$)	$\sum\Delta Q_s$ ($10^6 m^3$)
1000	1050	0,8	0,8	3,0	3,0
950	1000	2,1	3,0	8,5	11,5
900	950	4,0	7,0	17,1	28,6
850	900	4,0	10,9	17,8	46,4
800	850	3,7	14,7	17,5	63,9
750	800	4,1	18,8	20,1	84,0
700	750	5,0	23,8	25,6	109,6
650	700	5,2	29,0	29,3	139,0
600	650	2,8	31,8	15,4	154,4

Hverfisfljót water drainage basin

Elevation (m a. s. l.)		ΔS km^2	∑ΔS km^2	ΔQ_s ($10^6 m^3$)	$\sum\Delta Q_s$ ($10^6 m^3$)
1700	1750	0,9	0,9	0,4	0,4
1650	1700	5,9	6,8	4,7	5,0
1600	1650	9,1	15,9	9,2	14,2
1550	1600	10,4	26,3	12,3	26,5
1500	1550	20,8	47,1	28,0	54,4
1450	1500	40,3	87,4	67,4	121,8
1400	1450	26,6	114,0	55,4	177,3
1350	1400	24,2	138,2	58,5	235,7
1300	1350	22,7	160,9	60,0	295,7
1250	1300	17,6	178,5	48,9	344,6
1200	1250	20,3	198,8	58,5	403,1
1150	1200	14,4	213,2	43,5	446,6
1100	1150	10,9	224,1	34,8	481,4
1050	1100	9,3	233,4	31,7	513,0
1000	1050	8,7	242,0	31,6	544,6
950	1000	8,6	250,6	34,2	578,8
900	950	7,9	258,5	33,6	612,4
850	900	7,8	266,3	35,0	647,4
800	850	6,8	273,1	31,7	679,1
750	800	8,5	281,6	41,3	720,4
700	750	10,7	292,2	55,4	775,8
650	700	11,2	303,4	62,3	838,2
600	650	6,0	309,4	33,0	871,2
550	600	0,2	309,6	0,8	872,0

Skaftá water drainage basin

Elevation (m a. s. l.)		ΔS km^2	∑ΔS km^2	ΔQ_s ($10^6 m^3$)	$\sum\Delta Q_s$ ($10^6 m^3$)
1650	1700	1,9	1,9	1,7	1,7
1600	1650	14,8	16,7	15,8	17,6
1550	1600	22,8	39,5	28,4	45,9
1500	1550	31,7	71,1	45,1	91,0
1450	1500	24,9	96,0	45,6	136,7
1400	1450	22,5	118,4	50,2	186,9
1350	1400	20,5	138,9	51,1	238,0
1300	1350	22,2	161,1	59,3	297,3
1250	1300	15,1	176,2	42,2	339,6
1200	1250	20,5	196,7	60,1	399,6
1150	1200	22,3	219,0	69,5	469,1
1100	1150	23,3	242,3	77,5	546,7
1050	1100	22,7	264,9	81,0	627,6
1000	1050	25,2	290,1	97,3	725,0
950	1000	20,2	310,3	85,8	810,7
900	950	16,8	327,1	77,4	888,1
850	900	13,5	340,6	66,0	954,1
800	850	14,2	354,8	73,1	1027,1
750	800	12,4	367,2	67,2	1094,3
700	750	9,9	377,1	55,6	1149,9
650	700	6,3	383,4	34,2	1184,1
600	650	0,8	384,2	4,2	1188,3

Appendix F: Records of surface elevation change a surface velocity at mass balance survey sties on Vatnajökull.

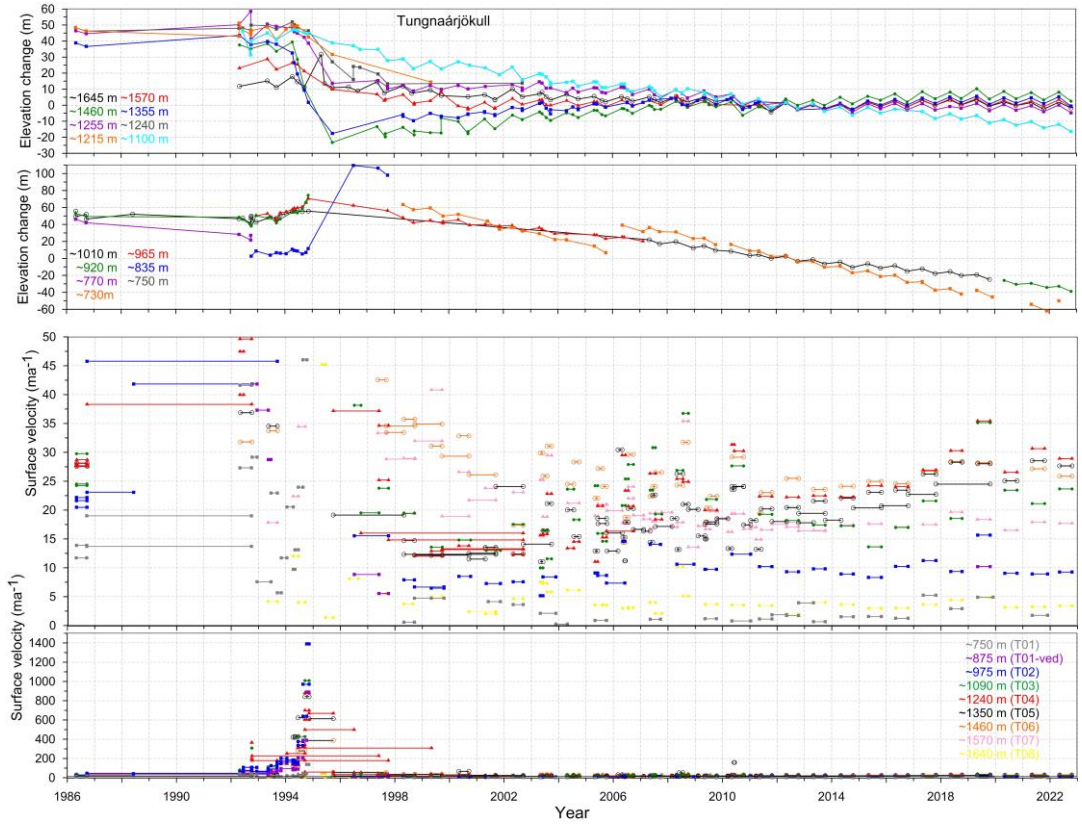

Surface elevation change relative to spring 2010 (upper panel) and average surface velocity (lower panel) at mb sites on Tungnaárjökull in 1986 to 2022.

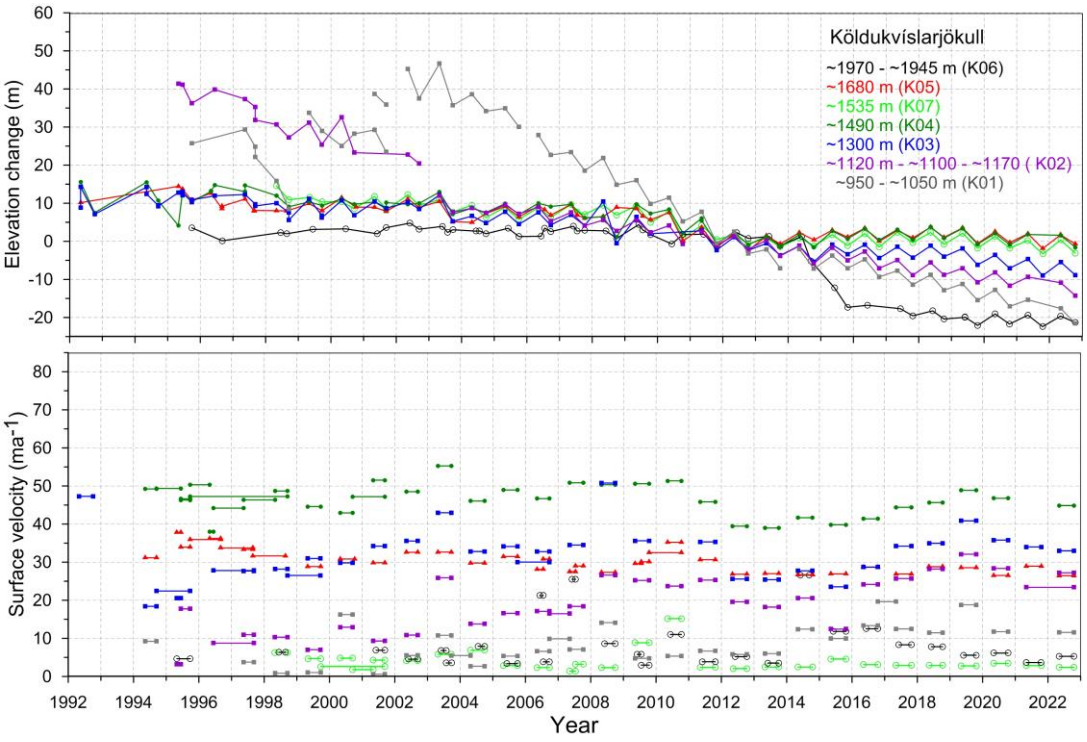

Surface elevation change relative to spring 2010 (upper panel) and average surface velocity (lower panel) at mb sites on Köldukvíslarjökull in 1992 to 2022.

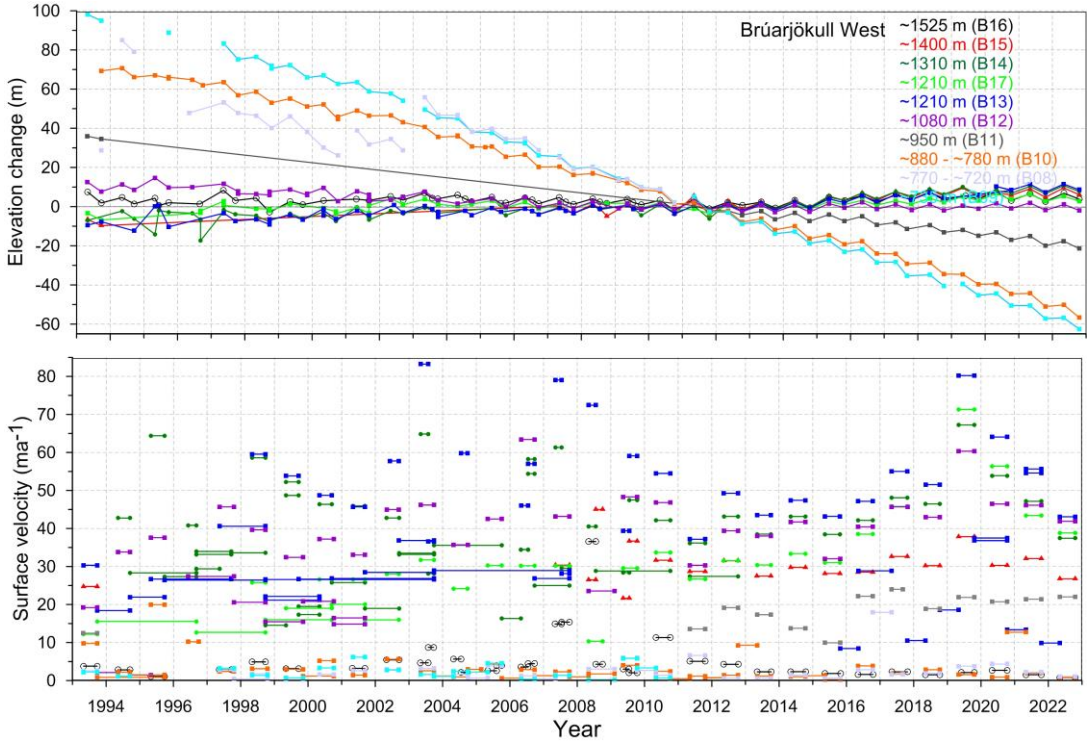

Surface elevation change relative to spring 2010 (upper panel) and average surface velocity at mb sites (lower panel) on W-Brúarjökull in 1993 to 2022.

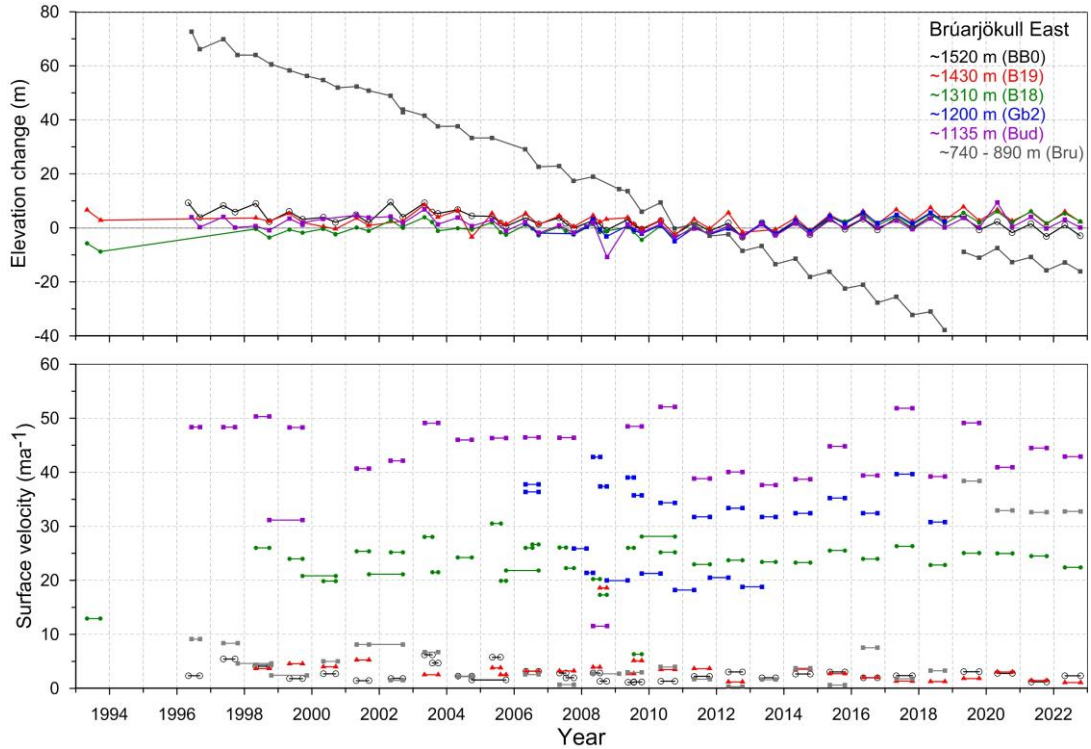

Surface elevation change relative to spring 2010 (upper panel) and average surface velocity at mb sites (lower panel) on E-Brúarjökull in 1993 to 2022.

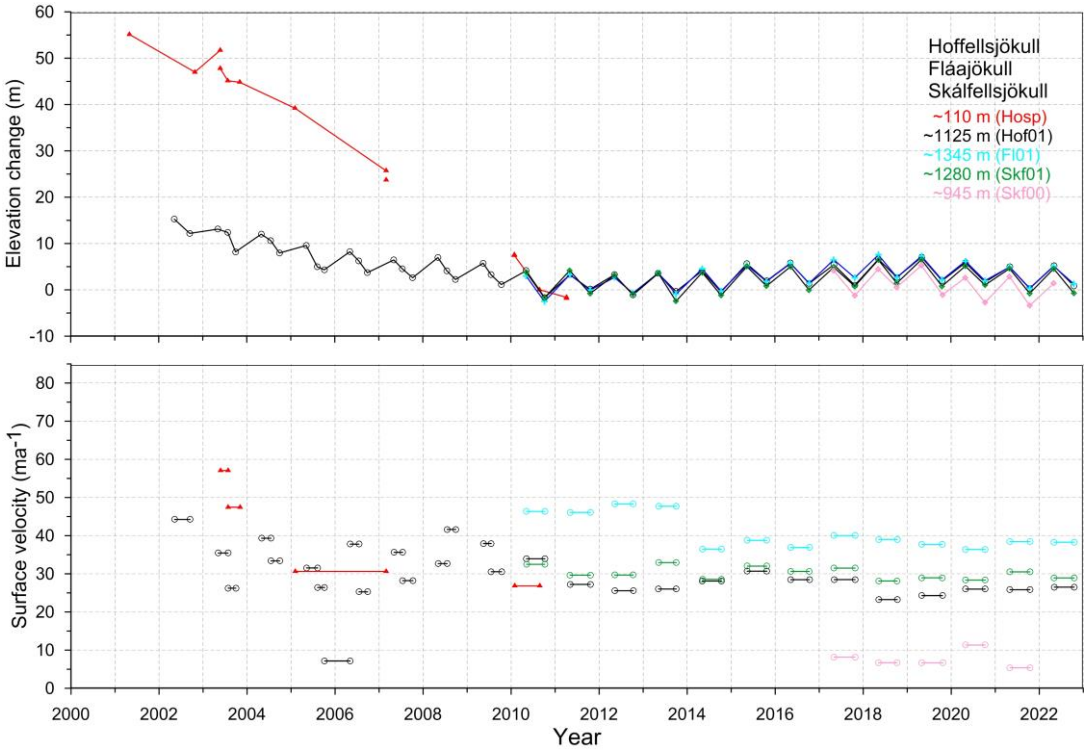

Surface elevation change relative to spring 2010 (upper panel) and average surface velocity) at mb sites (lower panel) on SE-Vatnajökull outlets in 2000 to 2022.

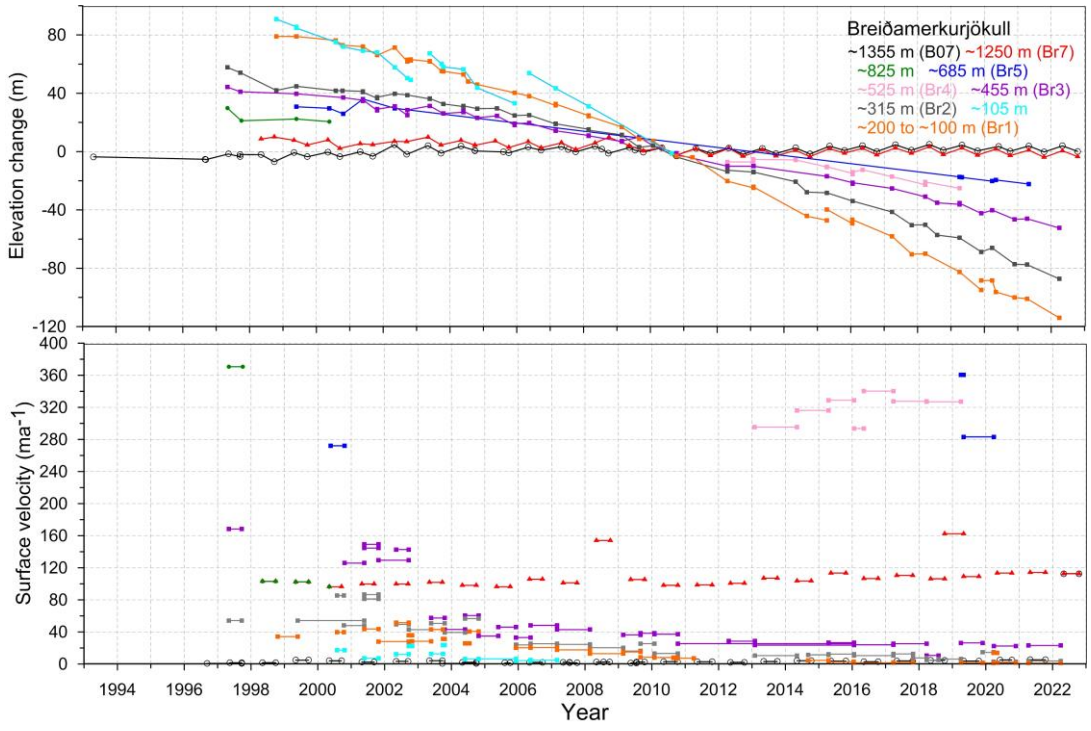

Surface elevation change relative to spring 2010 (upper panel) and average surface velocity at mb sites (lower panel) on Breiðamerkurjökull in 1993 to 2022.

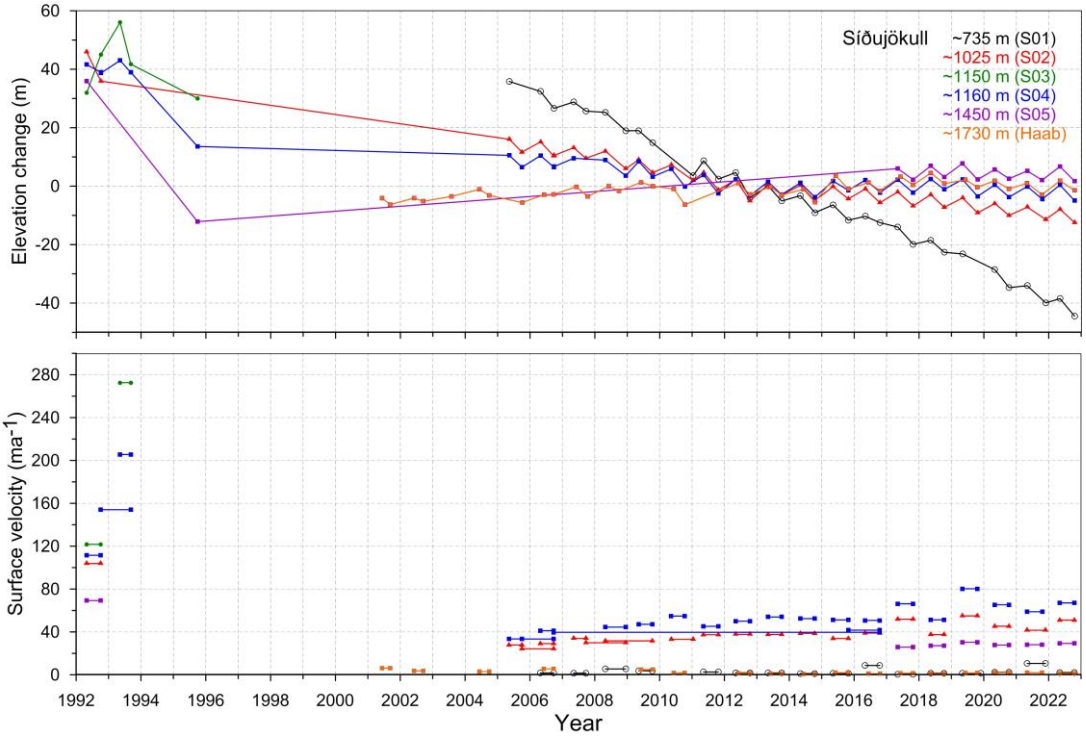

Surface elevation change relative to spring 2010 (upper panel) and average surface velocity at mb sites (lower panel) on Síðujökull in 1992 to 2022.

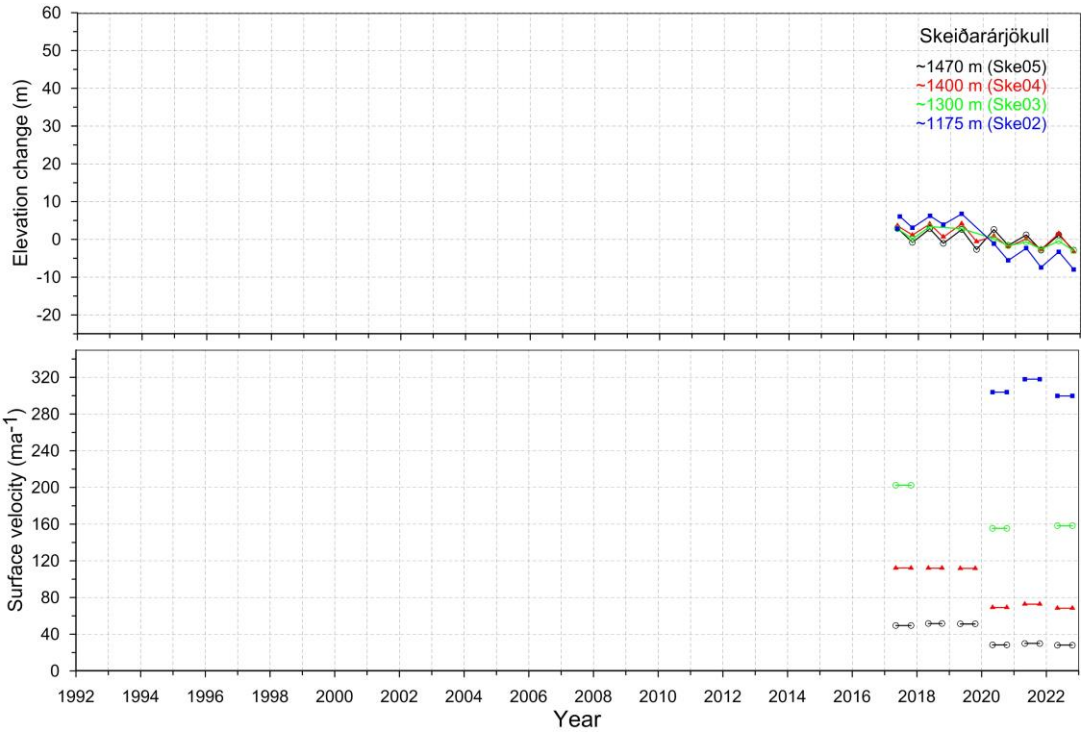

Surface elevation change relative to spring 2010 (upper panel) and average surface velocity at mb sites (lower panel) on Skeiðarárjökull in 2017 to 2022.

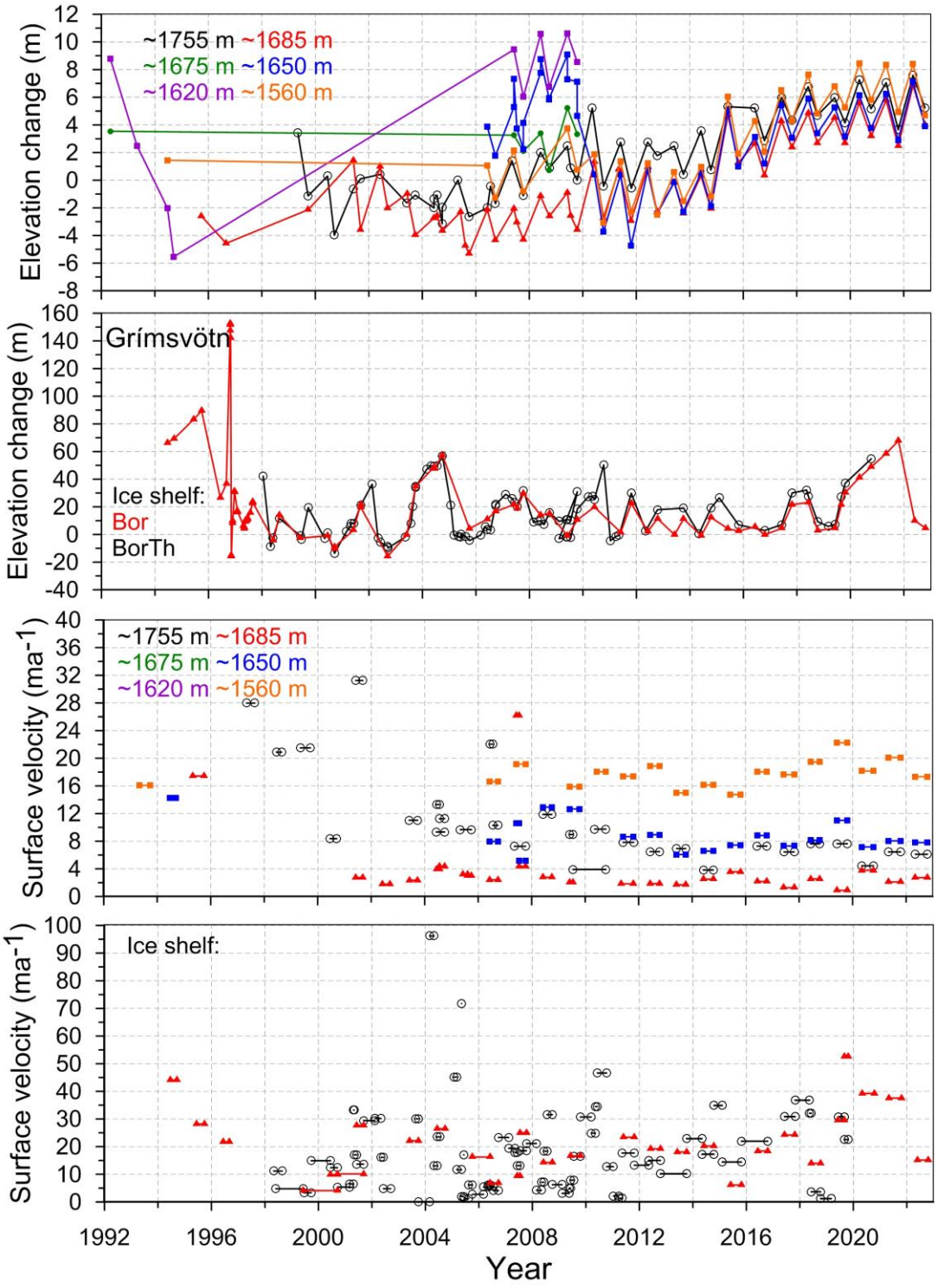

Surface elevation change relative to spring 2010 (upper panel) and average surface velocity at mb sites (lower panel) in Grímsvötn ice catchment in 1993 to 2022.